

**New insights into the N-end Rule Pathway: from the  
substrate recognition to its selective inhibition**

by

Luana Couto Assis Leitao

A thesis submitted in partial fulfillment of the requirements for the degree  
of

Doctor of Philosophy

Department of Biochemistry  
University of Alberta

© Luana Couto Assis Leitao, 2019

## ABSTRACT

The N-end rule represents a crucial proteolytic pathway which regulates in vivo half-life of a protein by the identity of its N-terminal residues. As such, the instability of the substrate is conferred by the ability of the cellular machinery to recognize the N-terminal amino acid and target the protein for cellular degradation. In mammals, the recognition of the destabilizing N-terminal is mediated by the redundant E3 ubiquitin ligases UBR1/UBR2 which have two key recognition domains: UBR box domain and the N-domain. These recognition domains bind to type I primary residues (Arg, Lys, and His) and type II amino acids (Trp, Tyr, Ile, Phe, and Leu).

In the first part of this study, we demonstrated that, in addition to the recognition of the N-termini by the E3 ubiquitin ligase, an N-end Rule substrate, the PKC $\delta$  has an extended half-life by the phosphorylation of Ser331, the second position residue of the cleaved fragment. Using the ubiquitin fusion method, it was shown that the PKC $\delta$  fragment was stable despite the unstable N-terminal, Asn. The findings appear to be related to the hydrophilic aspect of the phosphorylated Ser331 that disrupts the substrate binding to the NTAN1, inhibiting the ubiquitination of the fragment and subsequent protein degradation. The data presented in this study reveals that the mutation of the second position residue into an amino acid with no hydrophilic characteristics, enable the binding affinity to be reestablished.

In the second part, the study is directed towards the identification of a novel inhibitor of the N-end rule pathway. Substrates of the N-end Rule Pathway have been related to several pathogeneses, such as malignant cell growth, but only a few nonselective inhibitory compounds were discovered. We have identified through half-life assays, using different reporter proteins, a novel chemical inhibitor that

stabilizes type I N-terminal amino acid proteins. The selective inhibition of this proteolytic pathway could be used to suppress the degradation of specific substrates, such as pro-apoptotic protein fragments (e.g., Asp-BCL(XL), Arg-BID, and Arg-BIM(EL)). This research is the first in the field to demonstrate the selective inhibition of the Arg/N-end Rule Pathway. The PPCP and Analogs (I and II), demonstrated high specificity in the inhibition of type I N-termini with an EC50 of 3.8  $\mu$ M, 1.1  $\mu$ M, and 0.8  $\mu$ M, respectively. Additionally, these small molecules demonstrated low cellular toxicity when used alone, appearing as great candidates for drug development. The discovery of these novel N-terminal inhibitors expands the understanding of the degradation pathway and could have a valuable therapeutic implication towards distinct malignancies.

## PREFACE

This thesis is an original work by Luana Couto Assis Leitao (LCAL) and is written to fulfill the requirement of Doctor of Philosophy Degree in Biochemistry at the University of Alberta. The experiments conducted as part of my research investigation along with the results presented here are a complete work of the author, LCAL unless otherwise indicated. I joined Dr. Fahlman's lab in September 2014 after completing my Master of Science in Public Health and my Pharmacy degree both from the University State of Paraiba, Brazil. Dr. Fahlman has thoughtfully mentored me and attentively taught techniques in Molecular Biology and Proteomics that have widely extend my knowledge and appreciation for scientific research.

Much of Dr. Fahlman's research focuses on cellular processes that regulate the cellular proteome. Upon beginning my journey into the lab, I started to investigate the protein degradation by the N-End rule pathway. With a lengthy record of publications in the field, I had a solid base to develop meaningful investigation on the regulation of the protein degradation. To mention, one of the publications is the study developed by a former Ph.D. student, Dr. Mohamed Eldeeb, that revealed a novel N-end rule substrate, the cleaved BMX, and an important interplay between the substrate phosphorylation and N-end rule degradation, revealing an increasingly complex regulatory network of apoptotic proteolytic signalling cascades. In my investigation, I sought to identify additional aspects of the interplay between the phosphorylation and substrate recognition by the N-end rule pathway. On an additional note, in a different branch of my study, I was able to identify a novel inhibitor for the protein degradation pathway with prospective applicability towards pharmacological use.

The thesis consists of five chapters. **Chapter 1** presents an introduction to the N-end rule. Part of this chapter has been published as Eldeeb MA, Leitao LCA,

and Fahlman RP (2017) Emerging branches of the N-end rule pathways are revealing the sequence complexities of N-termini dependent protein. *Biochem. Cell Biol.* 00: 1–6 (0000) [dx.doi.org/10.1139/bcb-2017-0274](https://doi.org/10.1139/bcb-2017-0274). **Chapter 2** illustrates the materials and methods used to achieve the research goals in this thesis. **Chapter 3** elucidates an important role of the phosphorylation of Ser331 of the PKC $\delta$  on the N-end rule pathway regulation. **Chapter 4** outlines the pharmacological modulation of the N-end Rule Pathway through the selective inhibition of UBR1/UBR2 E3 Ligase. **Chapter 5** provides the overall summary of the projects and remarks for future research.

"Two roads diverged in a wood, and I – I took the one less traveled by, and  
that has made all the difference"  
-- Robert Frost

## DEDICATION

This study is wholeheartedly dedicated to my beloved sons, who have been my source of inspiration and gave me strength especially on the toughest days.

## ACKNOWLEDGEMENTS

I want to thank my supervisor, Dr. Richard Fahlman, for the incredible support he gave to me throughout my graduate studies. I sincerely appreciate his wise mentorship, brilliant scientific insights, and the thoughtfulness he demonstrates to all his students.

To my collaborators Dr. Jack Tuszynski and Dr. Michael Weinfeld, both from the Department of Oncology at the Faculty of Medicine and Dentistry, University of Alberta and who provided me with important complementary data. To my supervisory committee Dr. Nicolas Touret and Dr. Gopinath Sutendra, who have provided me with insightful inputs throughout the development of my thesis. To my internal examiner, Dr. Mark Glover, and my external examiner, Dr. Eriq Lukong from the University of Saskatchewan. To Dr. David Stuart and the Graduate Student Advisor, Lisa Dublin and Kelsey Robertson, for supporting throughout my program to fulfill the graduation requirements. A special thanks to the Science Without Borders for their scholarship support.

I would like to express my sincere thanks for the Fahlman's lab group, present and former members, Dr. Mohamed Eldeeb, Dr. David Krammer, Dr. Faraz Hussain, Dr. Angela Fung, Dr. Roxane Payoe, Guru, John Trethart, Prarthna, Julian (in memory), Alaa, and Wenbin, for all the collaborative work, enlightening scientific discussions and for all the funny moments that made graduate studies memorable. Special thanks to the summer/499/498 students that I have supervised, who have contributed to parts of this research. Thanks to Jack from IBD for the support with proteomics analysis. It is my greatest pleasure to have worked with these wonderful and fun people.



To my great friend Swai Mon Kaing, from Touret's lab, for always being there for me. To my friends who have supported me throughout my graduate study, especially Lucy, Erik, Katie, Darpan, Nada, Claudia, Adekunle, Sara, Charnpal, Razieh, Kim, Jasdeep, Vrajesh and Dr. John Githaka. To the Biochemistry Graduate Student Association (BCGSA) members who I had the pleasure to work with, Ghazaleh, Cameron, Vineet, Gareth, Qian, Jessi, Rabih, and Sayed.

A very special thanks to my family, for their encouragement and support. To my father and sisters for understanding the distance and not being physically present during important moments of their lives. To my grandmother, Anedite, who I was apart on her last moments, but always reassured me to be strong and fight for my dreams. To my husband, for supporting me and for all the sacrifices he made. Thank you for supporting me to grow and to be a better person. A sweet thanks for my sons, Rogerio, Joao Pedro, and Miguel, for being patient at times I could not be with you, and for your unconditional love and understanding. I love you more than words can say.

# TABLE OF CONTENTS

Abstract .....	ii
Preface.....	iv
Dedication .....	vii
Acknowledgements .....	viii
List of Tables.....	xiv
List of Figures .....	xv
List of Abbreviations .....	xvii
<b>Chapter 1 . Introduction .....</b>	<b>1</b>
1. Protein degradation pathways .....	2
1.1 Implications of the N-Termini Dependent Degradation.....	2
1.2 Characteristics of the N-End-Rule Pathway .....	6
1.2.1 UBR box structure .....	11
2. Sequence specificity in N-terminal dependent protein degradation .....	13
3. Pharmacological inhibition of N-end Rule Pathway .....	15
3.1 Dipeptide Ligands.....	16
3.2. Heterovalent Ligands .....	17
3.3 Monomeric inhibitors .....	19
3.4. Upstream inhibitors .....	20
4. N-end Rule implication on apoptosis regulation .....	21
References.....	23
<b>Chapter 2 . Materials and Methods.....</b>	<b>35</b>

1.	Materials .....	36
1.1	Cell Culture .....	36
1.2	DNA plasmids and Stable Expression of Constructs .....	36
1.3	Antibodies .....	36
1.4	Cell culture of Escherichia coli .....	37
2.	Methods .....	37
2.1	Cell Transfections .....	37
2.2	Protein Half-life Determination .....	37
2.3	Western Blot Analysis .....	38
2.4	Protein expression and purification .....	39
2.5	Site-directed Mutagenesis .....	40
2.6	Cell Cycle Analysis .....	41
2.7	Acridine Orange/ Ethidium Bromide (AO/EB) staining .....	41
2.8	Metabolic activity .....	42
2.9	Thermal Shift Assays .....	43
3.	Statistical Analysis.....	43
3.1	Effective Half Life Concentration .....	43
3.2	Data representation .....	44
	References.....	45

**Chapter 3 . Phosphorylation of Ser331 and its role in the N-end rule pathway regulation..... 47**

1.	Introduction to the PKC family .....	48
----	--------------------------------------	----

1.1	Overall view of the PKC enzymatic activation .....	49
1.2	The PKC $\delta$ isoform specificities .....	50
1.2.1	PKC $\delta$ Physiological Roles .....	52
1.3	The PKC $\delta$ fragment as an N-end rule substrate .....	55
1.3.1	PKC $\delta$ phosphorylation and its implication on protein degradation .....	60
2.	The second residue and the implication on N-termini recognition .....	62
2.1	The phosphorylation of internal tyrosine .....	63
<b>Chapter 4 . Selective inhibition of UBR1/UBR2 E3 Ligase by a small molecule .....</b>		<b>77</b>
1.	The identification of a selective N-end rule inhibitor .....	78
1.1	Chemical compounds with binding affinity with UBR-box domain .....	80
1.2	Small molecule affects type I N-terminal protein stability .....	82
1.3	The link between cellular stress response and protein degradation .....	85
1.4	Cell proliferation is affected by the selective inhibition of the N-end Rule pathway .....	87
1.5	PPCP influences the programmed cell death .....	90
2.	Analysis of PPCP analogs enlighten the understanding of its inhibitory activity .....	92
2.1	Aromatic groups are essential to the inhibitory activity .....	95
2.1.1	Binding affinity to UBR box domain .....	96
2.2	Marine compound demonstrates higher efficacy on protein stability ...	97
	References .....	101
<b>Chapter 5 . Final considerations .....</b>		<b>109</b>

1.	The N-end rule pathway and its growing level of complexity .....	110
2.	Second position amino acid pivotal role in N-termini recognition.....	110
3.	The regulation of the protein degradation through the UBR box inhibition 111	
4.	Future directions .....	114
	References.....	115
	<b>Bibliography .....</b>	<b>119</b>
	<b>Appendix .....</b>	<b>146</b>

## List of Tables

Table 1-1. Physiological cleaved fragments and implications of the mammalian Arg/N-end Rule Pathway.....	4
Table 4-1. Chemical compounds selected through in silico docking.....	81
Table 4-2. PPCP and analogs chemical characteristics.....	99
Table A - 1 Cell counting after Gy irradiation 1-hour post inhibitor treatment. .....	148
Table A - 2. Trypan Blue cell viability test in Jurkat cell line.....	149

## LIST OF FIGURES

Figure 1-1. Destabilizing N-Terminal Amino Acids. ....	7
Figure 1-2. Diagram illustrating the poly-ubiquitination in mammalian cells. ....	9
Figure 1-3. Crystal structure of the UBR-box domain in complex with type I residue .....	12
Figure 1-4. Summary of the penultimate amino acid effects. ....	14
Figure 2-1. Schematic of Protein Stability .....	38
Figure 2-2. Cell viability assay through double staining.....	42
Figure 3-1. Schematic of PKC $\delta$ structure.....	51
Figure 3-2. Diagram of Ubiquitin Fusion Technique. ....	56
Figure 3-3. PKC $\delta$ expression and C-terminal fragment stability.....	57
Figure 3-4. Stability of $\Delta$ N-PKC $\delta$ fragment after serial mutation.....	59
Figure 3-5. $\Delta$ N-PKC $\delta$ Stability after Tyr334 mutation.....	63
Figure 4-1. Molecular docking workflow and the quantification of degradation rate after drug treatment. ....	83
Figure 4-2. Selective inhibition of the N-end Rule Pathway.....	84
Figure 4-3. Protein stability after cell stress after PPCP treatment. ....	86
Figure 4-4. Proliferation assay after PPCP treatment. ....	89
Figure 4-5. Representative histograms for cells stained with PI after DMSO and PPCP treatment. ....	90
Figure 4-6. Cell Viability after UBR-box inhibition.....	93

Figure 4-7. Quantification of the combination index for PPCP and PAC1 drug interaction. ....	94
Figure 4-8. Protein Stability after PPCP and analogs treatment .....	98
Figure 4-9. Comparison of protein stability after PPCP and analogs inhibition. ....	100
Figure 5-1. Schematic of the E3 ligase inhibitor activity. ....	113
Figure A - 1. Docking result of top scoring Analogs .....	147



## LIST OF ABBREVIATIONS

<b>α</b>	Greek small letter Alpha
<b>β</b>	Greek small letter Beta
<b>γ</b>	Greek small letter Gamma
<b>δ</b>	Greek small letter Delta
<b>ε</b>	Greek small letter Epison
<b>θ</b>	Greek small letter Theta
<b>η</b>	Greek small letter Eta
<b>ζ</b>	Greek small letter Zeta
<b>ι</b>	Greek small letter Iota
<b>Δ</b>	Greek capital letter Delta
<b>Ala</b>	Alanine (A)
<b>An</b>	Analog
<b>AO</b>	Acridine Orange
<b>Arg</b>	Arginine (R)
<b>Asn</b>	Asparagine (N)
<b>Asp</b>	Aspartic acid (D)
<b>ATE1</b>	Arginyl transferase
<b>BMX</b>	Tyrosine protein kinase
<b>BSA</b>	Bovine Serum Albumin
<b>BTZ</b>	Bortezomib
<b>CFZ</b>	Carfilzomib
<b>CHX</b>	Cycloheximide
<b>CI</b>	Combination Index
<b>Cys</b>	Cysteine (C)

<b>DAG</b>	Diacylglycerol
<b>DMEM</b>	Dulbecco's Modified Eagle's medium
<b>DMSO</b>	Dimetilsulfóxido ou sulfóxido de dimetilo
<b>E1</b>	Ubiquitin-activating enzyme
<b>E2</b>	Ubiquitin-conjugating enzyme
<b>E3</b>	Ubiquitin ligase
<b>EB</b>	Ethidium Bromide
<b>EC50</b>	Half maximal effective concentration
<b>ER</b>	Endoplasmic Reticulum
<b>FBS</b>	Fetal Bovine Serum
<b>Gln</b>	Glutamine (Q)
<b>Glu</b>	Glutamic acid (E)
<b>Gly</b>	Glycine (G)
<b>GST</b>	Glutathione S-transferase
<b>Gy</b>	Gray
<b>H<sub>2</sub>O<sub>2</sub></b>	Hydrogen Peroxide
<b>HCT116</b>	Human Colon Cancer cell line
<b>HEK</b>	Human Embryonic Kidney 293 cells
<b>HeLa</b>	Human cervical adenocarcinoma epithelial cells
<b>His</b>	Histidine (H)
<b>Ile</b>	Isoleucine (I)
<b>IPTG</b>	isopropyl β-D-1- thiogalactopyranoside
<b>JBS</b>	Johanson–Blizzard Syndrome
<b>Jurkat</b>	human T lymphocyte cells
<b>K562</b>	Chronic myelogenous leukemia cells
<b>LB</b>	Luria Broth
<b>Leu</b>	Leucine (L)

<b>Lys</b>	Lysine (K)
<b>Met</b>	Methionine (M)
<b>MTAP</b>	Metalloprotease
<b>MCL</b>	Mantle Cell Lymphom
<b>MM</b>	Multiple Myeloma
<b>MOE</b>	Molecular Operating Environment
<b>MTT</b>	Thiazolyl tetrazolium bromide
<b>NTAN1</b>	N-Terminal Asparagine Amidase
<b>NTAQ1</b>	N-Terminal Glutamine Amidase
<b>PAC1</b>	Procaspase Activator Factor-1
<b>PBS</b>	Phosphate Buffered Saline
<b>PCA</b>	Para-chloramphetamine
<b>Phe</b>	Phenylalanine (F)
<b>PI</b>	Propidium iodine
<b>PDK-1</b>	Phosphoinositide-dependent kinase
<b>PKC</b>	Protein Kinase C
<b>PMSF</b>	phenylmethanesulphonyl fluoride
<b>PPCP</b>	3-phenyl-2-[[9(2-phenylethyl) carbamoyl] amino} propanoic acid
<b>Pro</b>	Proline (P)
<b>PTM</b>	Post-translation modification
<b>Ptr1</b>	Peptide transporter 1
<b>Ser</b>	Serine (S)
<b>STS</b>	Stausporine
<b>Thr</b>	Threonine (T)
<b>Trp</b>	Tryptophan (W)
<b>Tyr</b>	Tyrosine (Y)
<b>Tyr</b>	Tyrosine (Y)

<b>Ub</b>	Ubiquitin
<b>UBR 1</b>	Ubiquitin protein ligase E3 component n-recognin 1
<b>UBR 2</b>	Ubiquitin protein ligase E3 component n-recognin 2
<b>UPS</b>	Ubiquitin-Proteasome System
<b>Val</b>	Valine (V)
<b>Zn<sup>2+</sup></b>	Zinc ion
<b>Z-VAD-fmk</b>	Carbobenzoxy-valyl-alanyl-aspartyl-[O-methyl]-fluoromethylketone

Note:

<sup>1</sup> Amino acid residues of a protein will be written in the three-letter code followed by the residue number (ex. Ser331)

<sup>2</sup> N-terminal amino acid specificity will be written in the three-letter code (ex. Met)

# CHAPTER 1 . INTRODUCTION

Part of this chapter is published as:

Eldeeb MA, Leitao LCA, and Fahlman RP (2017) Emerging branches of the N-end rule pathways are revealing the sequence complexities of N-termini

dependent protein. *Biochem. Cell Biol.* 00: 1–6 (0000)

[dx.doi.org/10.1139/bcb-2017-0274](https://doi.org/10.1139/bcb-2017-0274)

## **1. Protein degradation pathways**

Protein degradation (proteolysis) is a prominent regulatory process to maintain the organism's homeostasis. The selective degradation of intracellular proteins controls cell responses and empirical products in a variety of physiological and biochemical processes from yeast to mammals. Not only the targeted protein degradation is involved in controlling the levels of regulatory proteins but also in eliminating misfolded and abnormal proteins. In mammalian cells, the intracellular selective protein degradation is mainly carried out by the Ubiquitin-Proteasome System (UPS) in association with autophagy, molecular chaperones, and lysosomal proteolysis (Varshavsky, 2011).

The UPS and its chaperones determine the time-dependent probability of each protein being either in its functional state, targeted for degradation or perturbed in a manner that may or may not result in degradation. The intracellular proteolysis also can be mediated by cytosolic and nuclear proteases such as calpains and caspases. The fragmented proteins produced by these proteases are often target and degraded by the Ubiquitin mediated pathways (Eldeeb, Mohamed & Fahlman, 2016; Varshavsky, 2011).

### **1.1 Implications of the N-Termini Dependent Degradation**

The first selective degradation signal identified for proteins was the presence of destabilizing N-terminal residues, a pathway that has pivotal roles in physiological and pathological processes such as malignancies, cardiovascular disorders, and neurodegenerative diseases (Bachmair, Finley, & Varshavsky, 1986; Ciechanover & Kwon, 2015; Varshavsky, 2011). This N-termini dependent protein

degradation has been termed the N-end rule pathway and encompasses the set of different N-terminal destabilizing amino acid residues that dictates the *in vivo* half-life of a given protein (Varshavsky, 2017). The history and key milestones of our understanding of the N-end rule have been recently summarized, and investigations over the past years have revealed that the N-end rule pathway degrades a number of proteins that are central to a wide spectrum of cellular and biological processes in eukaryotes such as genome stability and repair (Hwang, Shemorry, & Varshavsky, 2009; Piatkov, Colnaghi, Békés, Varshavsky, & Huang, 2012; Rao, Uhlmann, Nasmyth, & Varshavsky, 2001), apoptosis (Ditzel et al., 2003; Eldeeb, Mohamed, Fahlman, Esmaili, & Ragheb, 2018; Xu, Payoe, & Fahlman, 2012), autophagy (Cha-Molstad et al., 2015; Jiang et al., 2016; Yamano & Youle, 2013), neurodegeneration (Brower, Christopher S., Piatkov, & Varshavsky, 2013), development (Weaver, Weaver, Mitani, & Han, 2017), and nitric oxide sensing of G-protein regulators (Hu et al., 2005; Lee, M. J. et al., 2012).

While the biological roles of the N-end rule pathways have been mostly implicated because of the identification and characterization of particular protein substrates, the overall function of the N-end rule in these processes is likely very complex as a result of the large number of various proteins that can be targeted by the pathway, **Table 1-1**. For example, many pro-apoptotic protein fragments generated by proteolytic cleavage have been demonstrated to be targeted for degradation via the N-end rule pathway (Ditzel et al., 2003; Eldeeb, Mohamed A. & Fahlman, 2016; Piatkov et al., 2012; Xu et al., 2012).

**Table 1-1. Physiological cleaved fragments and implications of the mammalian Arg/N-end Rule Pathway.**

<b>N-termini</b>	<b>Cleaved C-terminal fragment</b>	<b>Physiological Function</b>
Type I	Cys2-RGS4 Cys2-RGS5 Cys2-RGS16	GPCR signaling pathway Cardiac development
	Arg208-TDP43 Asp219-TDP43 Asp247-TDP43	Amyotrophic lateral sclerosis (ALS) Frontotemporal lobar degeneration (FTLD)
	Gln79-synuclein	Parkinson's disease (PD)
	Asp-Ab42	Alzheimer's disease (AD)
	Glu3-Tau	
	Glu19-Bip1	Protein quality control through autophagy
	PINK1	Mitochondrial quality control through mitophagy
Type II	Leu2-RGS2	Hypertension Cardiovascular homeostasis
Type I and Type II	Proapoptotic protein fragments	Apoptosis regulation
	Myofibrils	Muscle wasting
	Ate1 -/-	Heart development Angiogenesis Hyperphagia Hyperkinesia Infertility Metabolic defects
	UBR1 -/-	Johanson-Blizzard syndrome (JBS)
	UBR1 -/- UBR2 -/-	Neurogenesis Cardiogenesis
	UBR4 -/-	Regulation of autophagic flux

\* Adapted from Lee, J. H. et al., 2015.

In addition, there are examples demonstrating that the inhibition of the N-end rule or knockouts of components of the N-end rule pathway, such as UBR1 and UBR2, sensitize cells to cell stress and cell death (Agarwalla & Banerjee, 2016; Deka, Singh, Chakraborty, Mukhopadhyay, & Saha, 2016; Piatkov et al., 2012). With these examples, it appears that the N-end rule plays an active role in inhibiting cell death, although additional reports demonstrated that the N-end rule also degrades anti-apoptotic protein fragments (Eldeeb, Mohamed A. & Fahlman,



2014) and components of the N-end rule pathway promote cell death and cell cycle arrest (Kumar et al., 2016). These findings demonstrate that the biological function of the N-end rule pathway may not be simply defined as pro- or anti-apoptotic but appears to participate in the crucial balance of both pro- and anti-apoptotic proteins.

The complexity in the role of the N-end rule pathway is exemplified by the Johanson–Blizzard Syndrome (JBS), a genetic disease resulting from inactivating mutations to one of the redundant ubiquitin E3 ligases involved in the N-end rule pathway (Hwang et al., 2011; Zenker et al., 2005). The complexities of the Johanson–Blizzard syndrome being a multisystem congenital disorder affecting many tissues in the body when only a single redundant component of the N-end rule is mutated suggests key roles for this pathway in diverse tissues in the body. The JBS is caused by mutations that abolish UBR1 activity, whereas it has been reported that single-residue changes, involve positions in the RING-H2 and UBR domains of UBR1 that are conserved among eukaryotes (Hwang et al., 2011).

The N-end Rule physiological functions have been elucidated in mouse knockouts, human disease-gene mapping and in vivo characterizations (Balogh, McDowell, & Denenberg, 2002; Kwon, Xia, Davydov, Lecker, & Varshavsky, 2001). Previous studies demonstrated that this pathway participates in a wide range of physiological and developmental processes including spermatogenesis, hypertension, neural tube formation, autophagy, oxygen sensing, and chromosomal stability (Varshavsky, 2011). The double knockout of UBR1 and UBR2, ubiquitin enzymes, in mice, was reported to cause early embryonic lethality in females and abnormal spermatocytes formation in male mice (Kwon et al., 2001; Ouyang et al., 2006).

## 1.2 Characteristics of the N-End-Rule Pathway

As outlined in **Figure 1-1.A**, in eukaryotes there are a series of primary N-terminal destabilizing residues that include the type I positively charged Arg, Lys, and His amino acids in addition to the type II large hydrophobic, Leu, Phe, Tyr, Trp, and Ile amino acids. Proteins with these 2 types of N-terminal destabilizing residues are recognized by different protein domains on a series of E3 ubiquitin ligases in eukaryotes that include UBR1 in *Saccharomyces cerevisiae* (Bartel, Wüning, & Varshavsky, 1990), UBR11 in *Schizosaccharomyces pombe* (Fujiwara, Tanaka, Yamashita, & Kitamura, 2013), and UBR1, UBR2, UBR4, and UBR5 in mammals (Tasaki et al., 2005). The redundant UBR1 and UBR2 proteins possess an N-terminal UBR domain for the recognition of Type I N-termini and an N-domain for the recognition of Type II N-termini, **Figure 1-1.B**. In addition, UBR4(p600) and UBR5(EDD) proteins only possess a Type I UBR domain (Tasaki et al., 2005).

Similar, yet distinct versions of N-end rule pathways are present in diverse organisms that have been investigated, including the bacterium *Escherichia coli* (Tobias, Shrader, Rocap, & Varshavsky, 1991), yeast (Bachmair et al., 1986), plants (Potuschak et al., 1998), and mammals (Gonda et al., 1989).

In mammals, this pathway is divided into three branches regarding the destabilizing residues: the Arg/N-end rule, the Ac/N-end rule and the newly identified Pro-N-end rule pathway (Chen, Wu, Wadas, Oh, & Varshavsky, 2017). The Ac/N-end rule targets the N-terminal acetylated residue. Whereas, the Arg/N-end rule branch has as its destabilizing residue unacetylated N-terminal Cys, Asn, Gln, Asp, Glu, Arg, Lys, and His (type I destabilizing residues) along with Trp, Tyr, Ile, Phe, and Leu (type II amino acids), **Figure 1-1.C**. The process which leads to this destabilizing N-terminals is either by cotranslation removal of Met by Met-

aminopeptidases (MetAPs) or through the posttranslational and conditional cleavage by proteases such as calpains, caspases, and separases (Varshavsky, 2011). This study is mainly focused on studies pertaining to the classical Arg-N-end rule pathway.

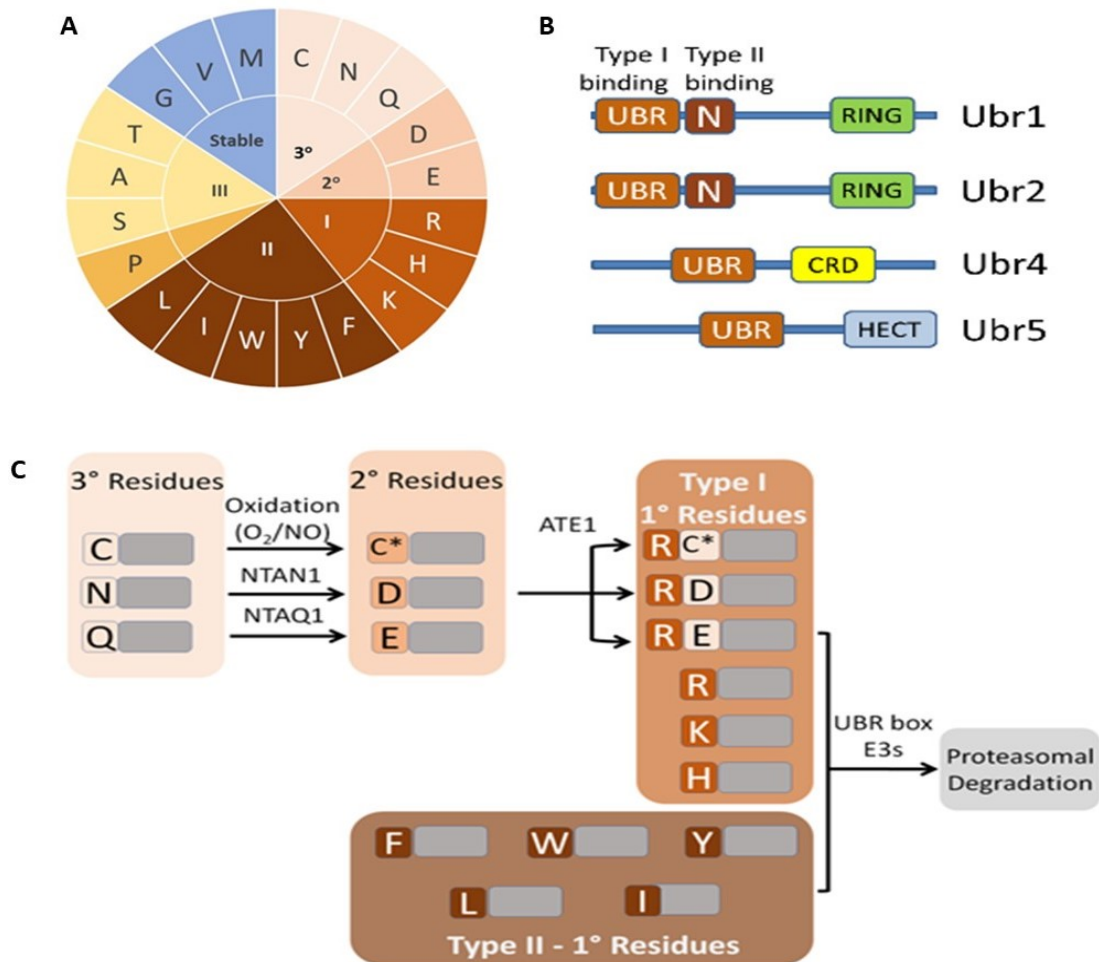


**Figure 1-1. Destabilizing N-Terminal Amino Acids.**

**A.** A summary of the destabilizing amino acids in eukaryotes with the exclusion of the complexities of the Ac-N-end rule pathway (Park et al., 2015). Blue highlights the stable N-terminal residues. The different shades of orange highlight the distinct destabilizing residues recognized by the canonical Arg-N-end Rule pathway; the tertiary, secondary and Type I and Type II primary destabilizing residues. Gold

highlights the recent identification of Pro as an N-terminal destabilizing residue and yellow emphasizes the poorly defined type III N-termini. **B.** Schematic of the domain structure of four UBR proteins implicated in the N-End rule, the UBR1, UBR2, UBR4 and UBR5. **C.** Schematic of the hierarchical structure of the canonical mammalian N-End Rule pathway and the key steps leading to proteasomal dependent degradation. The type I residues divided into three groups, the tertiary residues (Cys, Asn, Gln), the secondary residues (oxidized Cys, Asp, Glu) and the primary residues (Arg, Lys, His). The type II primary residues being Phe, Trp, Tyr, Leu, Ile.

The canonical N-end rule type I destabilizing Nt-residues are divided into three groups: tertiary (Cys, Asn, and Gln), secondary (oxidized Cys, Asp, and Glu), and primary (Arg, Lys, and His) residues. The tertiary Nt-residue Cys is oxidized by O<sub>2</sub> or Nitric Oxide to secondary destabilizing residue Cys-sulfinate or Cys-sulfonate. Whereas, the Asn and Gln tertiary Nt-residues are deaminated to Asp and Glu, by N-terminal amidases (NTAN1 and NTAQ1, respectively). These secondary residues are then, argynilated by R-transferase (ATE1), **Figure 1-1.c.** The positively charged amino acids (Arg, His, and Lys) and the hydrophobic residues (Trp, Tyr, Ile, Phe, and Leu) are recognized and poly-ubiquitinated by ubiquitin enzymes (Varshavsky, 2011).

### **1.1.1 Poly-ubiquitination targets the destabilizing N-terminals for degradation**

The Ubiquitination process is mediated by three enzymes – E1, E2, and E3, **Figure 1-2.** First, the ubiquitin-activating enzyme (E1) that activates the ubiquitin in an ATP-dependent manner, it forms a thioester bond among ubiquitin C-terminus and E1 catalytic cysteine. Further, the Ubiquitin is transferred to the catalytic Cys of the ubiquitin-conjugating enzyme (E2). Consequently, the ubiquitin

is carried to the substrate by the complex formation between ubiquitin ligase (E3) and E2 (Morreale & Walden, 2016).

There are over 40 E2s and more than 600 E3s in humans which confers these enzymes a high substrate specificity (Morreale & Walden, 2016). Forthwith, the ubiquitin ligases are classified in three categories (RINGs E3, HECTs E3, RBRs E3) according to the domain structure and organization and regarding the ubiquitin transfer to the target protein. My studies focus on, the UBR1 and UBR2, redundant bona fide E3 ligases that are classified as RING E3s, the most abundant E3 ubiquitin ligase in mammalian cells (present in cytosol), **Figure 1-1** (Metzger, Hristova, & Weissman, 2012). This type of ubiquitin ligase has a zinc-binding domain called RING (Really Interesting New Gene) that is involved in the binding of the ubiquitin-charged E2 and ubiquitin transfer (Morreale & Walden, 2016).

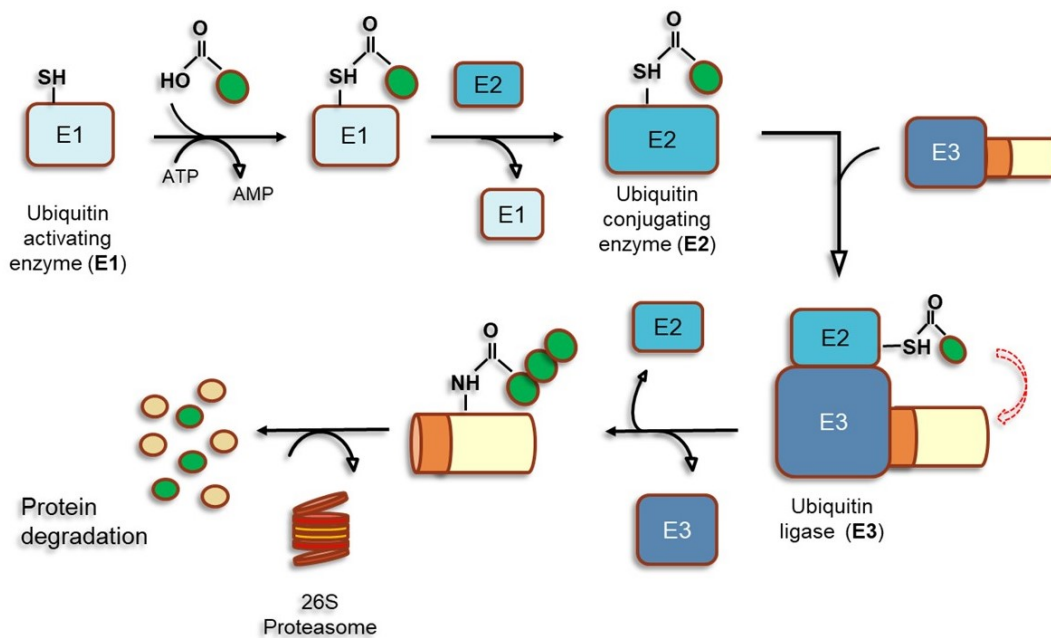


**Figure 1-2. Diagram illustrating the poly-ubiquitination in mammalian cells.**

The ubiquitin enzymes are represented by "E1", "E2", and "E3" (ubiquitin activating enzyme, ubiquitin conjugating enzyme, and ubiquitin ligase, respectively). The E1

activate the ubiquitin (green oval) in an ATP dependent manner and transfer active ubiquitin to E2. The E2 form a complex with E3 and the substrate, targeting the destabilizing N-terminal substrate with ubiquitin. The process is repeated several times until the protein is poly-ubiquitinated. The target substrate is recognized by the 26S proteasome, which cleaves the complex (the poly-ubiquitinated substrate) into short peptides. Adapted from Morreale and Walden(2016).

Other than the Ring domain, both UBR1/UBR2 have two key recognition domains. One is known as the UBR box domain, which independently functions as binding sites for type I (basic amino acids as Arg, His and Lys), and the other is the N-domain type II (Trp, Leu, Phe, Ile and Tyr N-terminal destabilizing amino acids) (Eldeeb, Mohamed A. & Fahlman, 2014; Matta-Camacho, Kozlov, Li, & Gehring, 2010). Studies have shown that mutation of V122L, present in JBS, disrupts the UBR-box binding sites and inhibits the recruitment of the substrate(Muñoz-Escobar, Matta-Camacho, Cho, Kozlov, & Gehring, 2017).

Recently, it was demonstrated that the UBR-box domain recognizes the N-terminal through two interacting pockets, one is a negative charge cavity and the other is a hydrophobic groove named the secondary pocket (Matta-Camacho et al., 2010; Muñoz-Escobar et al., 2017; Sriram et al., 2013). Interestingly, it has been shown that besides the N-terminal residue the identity of the amino acid in the second position has a significant role in the specificity of binding. Furthermore, the UBR-box structure suggests that a free  $\alpha$ -amino group, a basic side chain and part of the second last N-terminal amino acid are essential for its recognition (Choi et al., 2010; Lee, J. H., Jiang, Kwon, & Lee, 2015; Matta-Camacho et al., 2010).

### 1.2.1 UBR box structure

Previous studies determined the structure of the UBR box from human UBR1 and UBR2 that consist of two antiparallel  $\beta$ -strands; two  $\alpha$ -helices; and two long ordered loops. For the UBR2, an extra  $\beta$ -sheet is present between the loops. The UBR box is stabilized by three zinc ions forming two contiguous zinc fingers. Two zinc ions are each tetrahedrally coordinated with a shared cysteine ligand (Cys127). The other zinc finger coordinating residues are located in between strand  $\beta$ 1 and helix  $\alpha$ 1 (Cys112 and Cys115), the helix  $\alpha$ 2 (His133) and one in the linker between  $\alpha$ 2 and  $\beta$ 2 (His136)(Morreale & Walden, 2016), **Figure 1-3**.

Most of the zinc-coordinating residues are conserved throughout the UBR family, where the UBR1 and UBR2 UBR boxes share 76% identity and over 69 common residues. A DaliLite structural similarity search showed that the UBR box represents a novel structural fold, distinct from known zinc fingers and RING domains (Holm, Kivriinen, Rosenström, & Schenkel, 2008; Matta-Camacho et al., 2010).

Previous studies, utilizing the crystal structure of the UBR1 and UBR2 in complex with the tetrapeptide (RIAA and RLWS) showed that the interaction of the N-terminal amino group and the UBR box domain is crucial for binding as in the case of the arginine unstable N-terminal, **Figure 1-3.B** (Matta-Camacho et al., 2010). For all arginine and methylated arginine structures, the backbone and side chains of the domain remain in the same conformation as in the unbound structure.

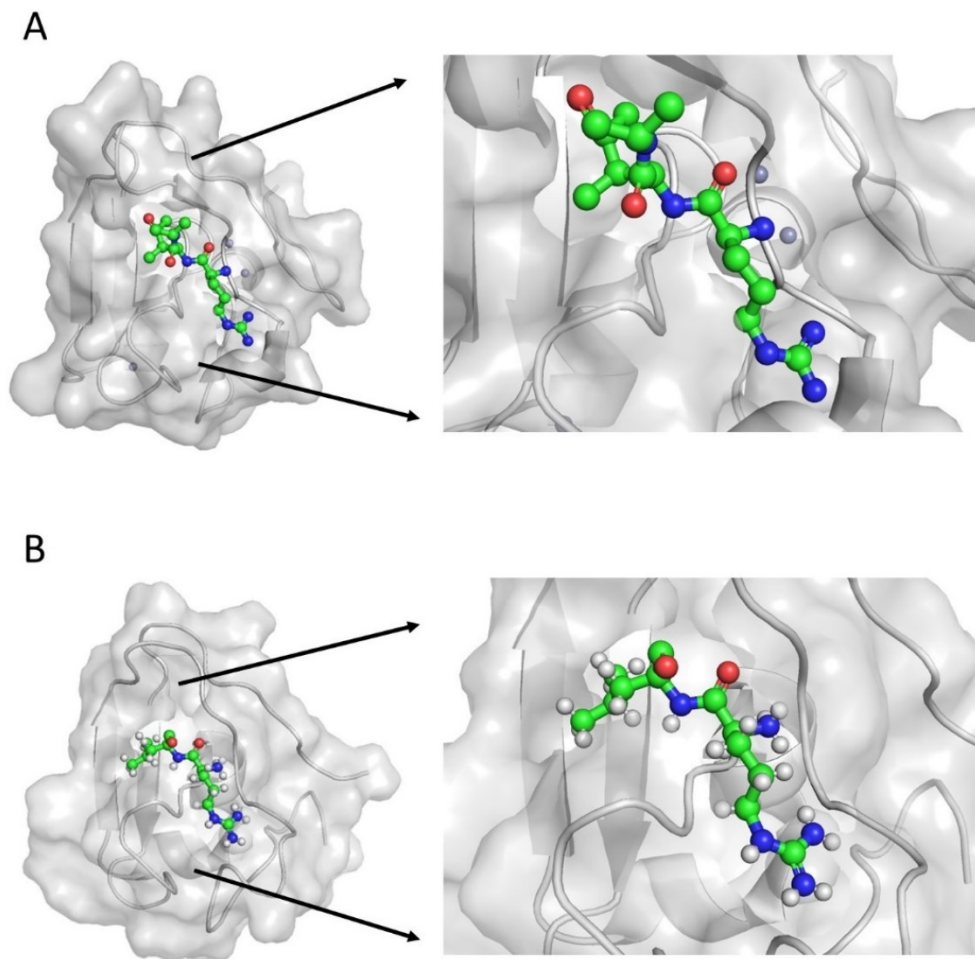


**Figure 1-3. Crystal structure of the UBR-box domain in complex with type I residue**

**A.** Molecular surface showing the UBR box domain of the UBR1 ligase. The crystal structure is shown in gray and the ligand RIA is shown in color. This image was prepared from a protein data bank file, PDB ID: 3NIH, using PyMOL Molecular Graphics System, Version 1.3. **B.** Molecular surface showing the UBR box domain of the UBR2 ligase. The molecule is shown in gray and the ligand RL is shown in color. The image was prepared from a protein data bank file, PDB ID: 5TDA, using PyMOL Molecular Graphics System, Version 1.3.



## 2. Sequence specificity in N-terminal dependent protein degradation

It was previously reported that Arg/N-end rule requires additional sequence elements in the N-terminal peptide sequence. In the case of cysteine oxidation by nitric oxide in mammals, there is a requirement for the penultimate amino acid to be a basic residue to enable the chemical S-nitrosylation of the N-terminal Cys by nitric oxide (Hu et al., 2005). Systematic analysis of substrate selectivity of the aminoacyl tRNA transferases, which catalyze the addition of destabilizing amino acids to the N-termini of secondary destabilizing N-termini, **Figure 1-4.A**, have also revealed some selectivity for the second amino acid for both the bacterial (Kawaguchi, Maejima, Kuroiwa, & Taki, 2013) and eukaryotic (Wadas, Piatkov, Brower, & Varshavsky, 2016) enzymes. With the eukaryotic aminoacyl tRNA transferase, ATE1, investigations revealed a general low preference for proline and tryptophan at the penultimate position for the four different spliced isoform of ATE1 tested. Besides, there were differences between the isoforms; for example, the ATE11B7B spliced isoform exhibits an additional low specificity for aspartate and glutamate penultimate amino acids (Wadas et al., 2016), **Figure 1-4.B**.

Structural and biochemical investigations of the UBR domain from the E3 ligases that bind type I destabilizing N-termini, have also revealed a role for the penultimate amino acid in the binding of peptides to this protein (Choi et al., 2010; Matta-Camacho et al., 2010; Muñoz-Escobar et al., 2017). Intriguingly, while the UBR proteins are highly conserved within eukaryotes, there appears to be some divergence in the binding specificity as a result of the identity of the penultimate amino acid for the yeast (Choi et al., 2010) and human (Muñoz-Escobar et al., 2017) UBR domains.

With the interconnection of ATE1 products being substrates for the UBR proteins, a systematic comparison of the reported penultimate amino acid specificity is presented, **Figure 1-4.B**. With ATE1 recognizing acidic N-terminal residues, the products it generates have a penultimate acidic residue as dictated by its substrate specificity. When one then compares this with the reported specificity of the UBR proteins, it appears that the yeast UBR1 protein exhibits a low specificity for acidic penultimate residues (Choi et al., 2010), such that ATE1 products in yeast are suboptimal substrates for UBR1. Further investigations may reveal this apparent dichotomy may be to tune the half-life of protein substrates or may correlate with emerging alternative roles for protein arginylation (Chamolstad et al., 2015; Cornachione et al., 2014; Jiang et al., 2016; Saha, Sougata et al., 2010; Zhang et al., 2015).

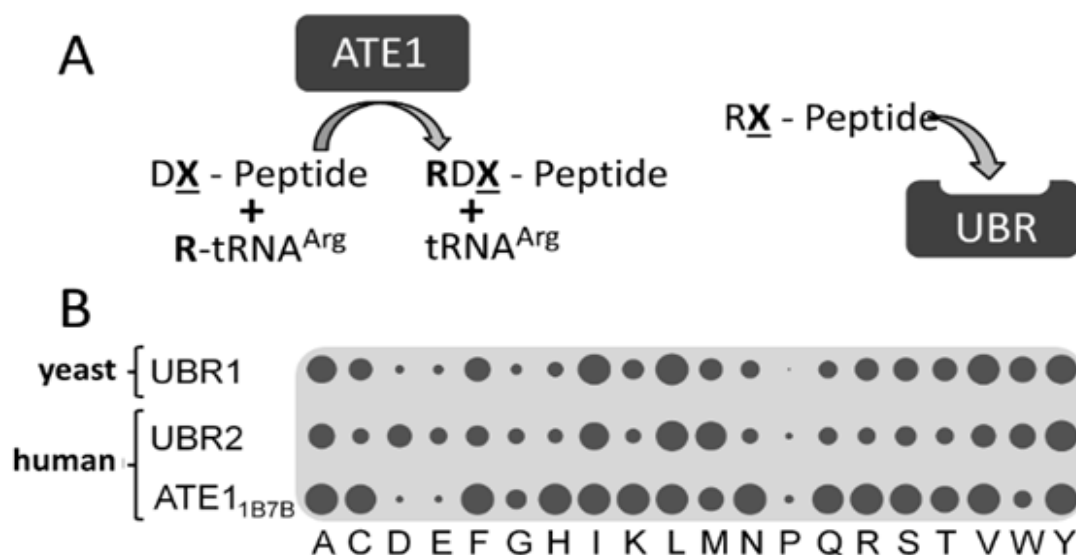


**Figure 1-4. Summary of the penultimate amino acid effects.**

**A.** Schematics of biochemical investigations used for investigating the effects of penultimate residues (X) on arginylation by ATE1 or binding to UBR protein domains. **B.** Summary of the quantified data reported for penultimate amino acid (X) effects for the enzymatic activity of human ATE1(Wadas et al., 2016), the

binding affinity for the UBR domain from human UBR2 (Munoz-Escobar et al., 2017), or the UBR domain from yeast UBR1 (Choi et al., 2010). The areas of the circles presented in the dot blot is proportional to the relative activity for ATE1 or binding for the UBR proteins.

The implications of these additional sequence requirements may have evolved to regulate the specific half-life of individual proteins with destabilizing N-termini. Furthermore, it shall provide the molecular basis for a potential cellular mechanism that can coordinate the degradation of a protein via post-translational modifications that may be analogously identified in the future, as it was previously demonstrated for an internal phosphorylation site modulating the degradation of the BMX kinase by the N-end rule pathway (Eldeeb, Mohamed A. & Fahlman, 2016).

### **3. Pharmacological inhibition of N-end Rule Pathway**

Given their importance in regulating the N-end Rule Pathway, the UBR binding domains (UBR-box and the N-domain) became potential targets for the modulation by small molecules with similar characteristics of the cognate destabilizing N-terminal residues (Agarwalla & Banerjee, 2016; Jiang et al., 2013; Kwon, Levy, & Varshavsky, 1999). Although several N-end rule inhibitors have been investigated (Jiang et al., 2014; Lee, J. H. et al., 2015) the lack of binding specificity still represents a challenge towards functional studies and pharmacological applications.

### 3.1 Dipeptide Ligands

So far, few chemicals have been used for modulation of the N-end Rule Pathway. The most used inhibitors are the dipeptides, which are often employed to investigate the degradation pathway. These small peptides successfully promote the competitive inhibition of type I and type II destabilizing N-terminal, with high stereospecificity which supports the rationale that *in vivo* modulation of the N-end Rule Pathway can be done using small-molecule inhibitors or activators of the ubiquitin enzymes (Baker & Varshavsky, 1991; Sriram et al., 2013).

The inhibition of the N-end rule pathway by dipeptides was first tested in yeast cells expressing model substrate (Lee, J. H. et al., 2015). Through ubiquitin fusion technic the Ub-X- $\beta$ -gal was co-translationally cleaved by the deubiquitinating enzymes (DUBs) into X- $\beta$ -gal fragment bearing a desired N-terminal residues (Baker & Varshavsky, 1991; Lee, J. H. et al., 2015). The results showed that the dipeptide Arg-Ala selectively increased the steady-state of X- $\beta$ -gal type I N-terminal, with similar results being observed for type II dipeptides. Interestingly, the mutation of the N-terminal residue for the Arg- $\beta$ -gal fragment to D-form stereoisomer resulted in a severe loss in the inhibitory effect, with no virtually inhibition of the N-end rule proteasome degradation even in high concentrations of the dipeptides (up to 6 mM) (Sriram et al., 2013). These results were confirmed by *in vitro* ubiquitination and degradation assays employing rabbit reticulocyte lysates (Gonda et al., 1989; Lee, J. H. et al., 2015).

In the human body, several dipeptides are originated from polypeptides and proteins by different peptidases (Silk, Grimble, & Rees, 1985), as well as, extracellular dipeptides are imported into cells by specific transport systems (Craft, Geddes, Hyde, Wise, & Matthews, 1968; NEWAY & SMYTH, 1960). In essence,

these intracellular dipeptides could modulate the N-end rule pathway in human cells, which was exemplified by previous studies with UBR1/Ptr1–Cup9–Ptr2 circuit (Alagramam, Naider, & Becker, 1995; Byrd, Turner, & Varshavsky, 1998; Turner, Du, & Varshavsky, 2000). The peptide transporter 1 (Ptr1), an enzyme with high similarity to the yeast UBR1, has a crucial role for peptide transport in *S. cerevisiae* (Alagramam et al., 1995). Studies revealed that imported dipeptides could bind to UBR1 and expedite the ubiquitination and proteolysis of the Cup9 homeodomain. The Cup9 is allosterically triggered by dipeptides with destabilizing N-terminal residues. As a positive feedback circuit, there is a suppress of the Ptr2 expression and the increase on the cell's capacity to import peptides (Byrd et al., 1998; Turner et al., 2000).

### **3.2. Heterovalent Ligands**

The synthetic heterovalent compounds have also demonstrated positive results inhibiting the N-end Rule Pathway. An example of these ligands is the RF-C11, which showed high inhibitory efficacy for *in vitro* proteasome degradation (Jiang et al., 2013; Lee, M. J. et al., 2008). The RF-C11 is formed by an N-terminal Arg (type I) and an N-terminal Phe (type II) chemically linked by two C11 hydrocarbon chains. *In vitro* analysis showed an inhibitory efficacy of 16 mM, whereas the homovalent controls RR-C11 and Arg–Ala required higher concentration for inhibitory activity, 67 mM and 283 mM, respectively (Brower, Christopher S. et al., 2013). The synthetic heterovalent compound also inhibited the degradation of a physiological N-end rule substrate, RGS4, in living cells without no apparent cytotoxicity (Jiang et al., 2013).

The multivalent interactions are employed by nature to increase protein–protein or protein–ligand interactions, not only thermodynamically, with enhanced binding affinity, but also kinetically, with reduced dissociation rate (Lee, M. J. et al., 2008). As such, most multivalent synthetic molecules have been created to employ cooperative interactions of multivalent ligands to target molecules. To date, most synthetic compounds are inter-homovalent, where two homovalent ligands interact with the same binding site of two identical proteins on the membrane of viruses, bacteria, or cells (Huskens, 2006; Lee, M. J. et al., 2008). The multivalent interaction to a single protein remains predominantly unexplored probably because of the scarcity of appropriate model systems (Lee, M. J. et al., 2008).

The optimal linker length of the RF-C11 was determined by *in vitro* degradation assays and *in silico* docking computational studies for binding energy (Jiang et al., 2013; Lee, M. J. et al., 2008). The distance between the two ligands was designed to be approximately 45 Å at the equilibrium conformation so the heterovalent compound would reach both binding sites (Lee, M. J. et al., 2008). With that, the length of the flexible linker being close to the size of the space between the binding sites prevents the compound of creating a steric obstruction or decreasing conformational entropy (Jiang et al., 2013). Heterovalent inhibitors with an *in vivo* applicability, optimal linker sizes and more potent N-terminal ligands could be useful not only for probing substrate–UBR protein interactions but also for identifying novel physiological functions of the Arg/N-end rule pathway (Lee, J. H. et al., 2015).

### 3.3 Monomeric inhibitors

Previous studies demonstrated that Phe-derived monomeric molecules have a significant *in vitro* inhibitory efficiency for ubiquitination and protein degradation by the N-end rule pathway (Jiang et al., 2014; Kwon et al., 1999; Lee, J. H. et al., 2015). It was shown that an L-conformation, protonated  $\alpha$ -amine group, and hydrophobic side chain are essential pharmacophores for effective N-end rule inhibitor. Using a systemic approach, it was identified that several Phe-derived monomeric molecules, including simple sympathomimetic amines, such as amphetamine and *para*-chloroamphetamine (PCA), significantly delay the degradation of both type I and II N-end rule substrates simultaneously (Sriram et al., 2013).

Important to mention that *in silico* analysis of PCA computational docking revealed that this compound has robust and specific interactions with both UBR1 domains, the UBR box and N-domain (Lee, J. H. et al., 2015). The PCA is known to pass through the blood-brain barrier (Jiang et al., 2014), stabilize endogenous RGS4 in the hippocampus and frontal cortex (Erdely et al., 2004), and impairment of the GPCR downstream effectors (Lee, J. H. et al., 2015). Furthermore, a study using PCA unveiled that the N-end Rule dependent degradation of the pathologic C-terminal fragments of TDP43 (Arg- TDP25) (Sriram et al., 2013).

Previous studies reveal a similar phenotype of the amphetamine effects in animals with those from knockout mouse analysis of UBR1 and UBR2, such as cardiac abnormality and neural tube defects (Brower, C. S. & Varshavsky, 2009; Dougan, Micevski, & Truscott, 2012). With that, the PCA highly-efficient systemic delivery to the brain (Jiang et al., 2014) could be useful for studying the neuroprotective roles of the degradation pathway. Nevertheless, PCA is not likely

to be used as drug treatment because of its neurological side effects (Lee, J. H. et al., 2015). Moreover, these chemicals are likely to be useful as tools for understanding the N-end Rule Pathway aside from being employed as drug treatment.

### **3.4. Upstream inhibitors**

The deletion of upstream N-end Rule regulators has been reported in several pathogenesises. To mention, the absence of ATE1 causes embryonic lethality due to defective cardiac development and angiogenic remodelling (Brower, C. S. & Varshavsky, 2009). A single element of the pathway may be involved in multiple regulatory circuits, which makes the upstream components a potential target for inhibition of the N-end rule pathway and a promising strategy to treat diseases generated by abnormal N-end rule activity (Lee, J. H. et al., 2015). Although the development of small-molecule ligands to regulate upstream components of the N-end rule pathway remain rather unexplored, screening of chemical libraries revealed two inhibitors of ATE1, tannic acid and merbromin, that delayed *in vivo* proteasomal degradation of RGS4 (Saha, S. et al., 2012). It is still to be determined how the mechanism of ATE1 R-transferase inhibition works.

Another upstream inhibitor of the N-end Rule pathway is the fumagillin, an antibiotic obtained from a fungus called *Aspergillus fumigatus fresenius*, that binds to metalloprotease 2 (METAP-2) and irreversibly inactivates this enzyme through covalent modification (Yin, Wang, Zhang, & Liu, 2012). The METAPs co-translationally produces N-terminal alanine, valine, serine, threonine, or cysteine, which, could be ubiquitinated and degraded by the UPS. The fumagillin also promotes the inhibition of endothelial cells without causing apoptosis (Ingber et



al., 1990). Its synthetic analogs, CKD-732, TNP-470, and PPI-2458, have been tested through clinical trials with a more potent effect than fumagillin (Yin et al., 2012).

#### **4. N-end Rule implication on apoptosis regulation**

The apoptosis, a programmed cell death, is mediated by proteases activated in response to intracellular stress or extracellular signals. These proteases, called caspases, are responsible for making sequence-specific cuts in several proteins. Cleavages of cytosolic and nuclear proteins by proteases such as separases, caspases, and specific deubiquitylases can generate fragments that bear destabilizing N-terminal residues. Several of these C-terminal fragments are short-lived N-end rule substrates, with demonstrated or predicted functional ramifications (Piatkov, Colnaghi, B♦k♦s, Varshavsky, & Huang, 2012; Piatkov, Oh, Liu, & Varshavsky, 2014)

Caspases or calpains execute sequence specific cleavages in several cellular proteins, which abrogate or change the functions of these proteins (Cao, Deng, & May, 2003; Chen et al., 2017; Dizin, Ray, Suau, Voeltzel, & Dalla Venezia, 2008; Eldeeb, Mohamed et al., 2018; Li, Zhang, Bottaro, Li, & Pierce, 1997; Utz & Anderson, 2000). Part of the cleaved fragments, such as Bax (Cao et al., 2003), BID (Li et al., 1997), BIMel (Dizin et al., 2008), and BRCA (Dizin et al., 2008) have a detrimental pro-apoptotic activity, while other cleaved fragments have anti-apoptotic functions, such as Lyn Kinase (Gamas et al., 2009), synphilin-1 (Giaime et al., 2006), and P27kip1 (Eymin et al., 1999). Additionally, our lab demonstrated that the stabilization of the pro-apoptotic fragment BMX, the bone marrow kinase on chromosome X, increased the sensitivity of PC3 cells to docetaxel, a

chemotherapeutic that induces cell death by mitotic catastrophe and caspase-dependent apoptosis (Eldeeb, Mohamed A. & Fahlman, 2016; Gan, Wang, Xu, & Yang, 2011; Mediavilla-Varela et al., 2009).

The difference in the stability between different proteolytically activated fragments, either pro-apoptotic or anti-apoptotic, would be a possible regulatory avenue of such proteolytic cascade (Eldeeb, Mohamed et al., 2018). Then, the new generated N-terminal fragments represent a regulatory feature during the proteolytic cascade and may impact the apoptotic pathway by the selective protein degradation through the N-end Rule (Bachmair et al., 1986; Eldeeb, Mohamed et al., 2018; Piatkov, Brower, & Varshavsky, 2012).

Several C-terminal cleaved fragments still have unknown protein stability. In this study, I investigated the protein degradation of the PKC $\delta$ , a novel isoform from the protein kinase C family. This protein is cleaved by caspase 3 after cell stress, generating a C-terminal fragment bearing an unstable N-terminal Asn. Interestingly, the data showed that additionally to the N-terminal, the second position amino acid (Ser) has a crucial role in the protein degradation by the N-end Rule Pathway.

Additionally, to the endogenous regulation of the proteasomal degradation, the modulation of the N-end Rule Pathway via the inhibition of E3 ligase was developed as a prospective strategy to sensitize malignant cells to chemotherapy. In the upcoming data chapters, it is shown the investigation of a selective type I N-end Rule Pathway inhibitor that binds to the UBR box domain, of the UBR1 and UBR2, increasing the half-life of type I residues (Cys, Asn, Gln, Asp, Glu, Arg, Lys, and His).

## References

- Agarwalla, P., & Banerjee, R. (2016). N-end rule pathway inhibition assists colon tumor regression via necroptosis. *Molecular Therapy-Oncolytics*, 3
- Alagramam, K., Naider, F., & Becker, J. M. (1995). A recognition component of the ubiquitin system is required for peptide transport in *saccharomyces cerevisiae*. *Molecular Microbiology*, 15(2), 225-234.
- Bachmair, A., Finley, D., & Varshavsky, A. (1986). In vivo half-life of a protein is a function of its amino-terminal residue. *Science*, 234(4773), 179-186.
- Baker, R. T., & Varshavsky, A. (1991). Inhibition of the N-end rule pathway in living cells. *Proceedings of the National Academy of Sciences*, 88(4), 1090-1094.
- Balogh, S. A., McDowell, C. S., & Denenberg, V. H. (2002). Behavioral characterization of mice lacking the ubiquitin ligase UBR1 of the N-End rule pathway. *Genes, Brain and Behavior*, 1(4), 223-229.
- Bartel, B., Wüning, I., & Varshavsky, A. (1990). The recognition component of the n-end rule pathway. *The EMBO Journal*, 9(10), 3179-3189.
- Brower, C. S., & Varshavsky, A. (2009). Ablation of arginylation in the mouse N-end rule pathway: Loss of fat, higher metabolic rate, damaged spermatogenesis, and neurological perturbations. *PloS One*, 4(11), e7757. doi:10.1371/journal.pone.0007757 [doi]

- Brower, C. S., Piatkov, K. I., & Varshavsky, A. (2013). Neurodegeneration-associated protein fragments as short-lived substrates of the N-end rule pathway. *Molecular Cell*, 50(2), 161-171.
- Byrd, C., Turner, G. C., & Varshavsky, A. (1998). The N-end rule pathway controls the import of peptides through degradation of a transcriptional repressor. *The EMBO Journal*, 17(1), 269-277. doi:10.1093/emboj/17.1.269 [doi]
- Cao, X., Deng, X., & May, W. S. (2003). Cleavage of bax to p18 bax accelerates stress-induced apoptosis, and a cathepsin-like protease may rapidly degrade p18 bax. *Blood*, 102(7), 2605-2614.
- Cha-Molstad, H., Sung, K. S., Hwang, J., Kim, K. A., Yu, J. E., Yoo, Y. D., . . . Kim, J. G. (2015). Amino-terminal arginylation targets endoplasmic reticulum chaperone BiP for autophagy through p62 binding. *Nature Cell Biology*, 17(7), 917.
- Chen, S., Wu, X., Wadas, B., Oh, J., & Varshavsky, A. (2017). An N-end rule pathway that recognizes proline and destroys gluconeogenic enzymes. *Science*, 355(6323), eaal3655.
- Choi, W. S., Jeong, B., Joo, Y. J., Lee, M., Kim, J., Eck, M. J., & Song, H. K. (2010). Structural basis for the recognition of N-end rule substrates by the UBR box of ubiquitin ligases. *Nature Structural & Molecular Biology*, 17(10), 1175.

- Ciechanover, A., & Kwon, Y. T. (2015). Degradation of misfolded proteins in neurodegenerative diseases: Therapeutic targets and strategies. *Experimental & Molecular Medicine*, 47(3), e147.
- Cornachione, A. S., Leite, F. S., Wang, J., Leu, N. A., Kalganov, A., Volgin, D., . . . Yates III, J. R. (2014). Arginylation of myosin heavy chain regulates skeletal muscle strength. *Cell Reports*, 8(2), 470-476.
- Craft, I. L., Geddes, D., Hyde, C. W., Wise, I. J., & Matthews, D. M. (1968). Absorption and malabsorption of glycine and glycine peptides in man. *Gut*, 9(4), 425-437.
- Deka, K., Singh, A., Chakraborty, S., Mukhopadhyay, R., & Saha, S. (2016). Protein arginylation regulates cellular stress response by stabilizing HSP70 and HSP40 transcripts. *Cell Death Discovery*, 2, 16074.
- Ditzel, M., Wilson, R., Tenev, T., Zachariou, A., Paul, A., Deas, E., & Meier, P. (2003). Degradation of DIAP1 by the N-end rule pathway is essential for regulating apoptosis. *Nature Cell Biology*, 5(5), 467.
- Dizin, E., Ray, H., Suau, F., Voeltzel, T., & Dalla Venezia, N. (2008). Caspase-dependent BRCA1 cleavage facilitates chemotherapy-induced apoptosis. *Apoptosis*, 13(2), 237-246.
- Dougan, D. A., Micevski, D., & Truscott, K. N. (2012). The N-end rule pathway: From recognition by N-recognins, to destruction by AAA+proteases. *Biochimica Et Biophysica Acta*, 1823(1), 83-91.  
doi:10.1016/j.bbamcr.2011.07.002 [doi]

- Eldeeb, M. A., & Fahlman, R. P. (2014). The anti-apoptotic form of tyrosine kinase lyn that is generated by proteolysis is degraded by the N-end rule pathway. *Oncotarget*, 5(9), 2714.
- Eldeeb, M. A., & Fahlman, R. P. (2016). Phosphorylation impacts N-end rule degradation of the proteolytically activated form of BMX kinase. *Journal of Biological Chemistry*, 291(43), 22757-22768.
- Eldeeb, M., & Fahlman, R. (2016). The-N-end rule: The beginning determines the end. *Protein and Peptide Letters*, 23(4), 343-348.
- Eldeeb, M., Fahlman, R., Esmaili, M., & Ragheb, M. (2018). Regulating apoptosis by degradation: The N-end rule-mediated regulation of apoptotic proteolytic fragments in mammalian cells. *International Journal of Molecular Sciences*, 19(11), 3414.
- Erdely, H. A., Lahti, R. A., Lopez, M. B., Myers, C. S., Roberts, R. C., Tamminga, C. A., & Vogel, M. W. (2004). Regional expression of RGS4 mRNA in human brain. *The European Journal of Neuroscience*, 19(11), 3125-3128.  
doi:10.1111/j.0953-816X.2004.03364.x [doi]
- Eymin, B., Sordet, O., Droin, N., Munsch, B., Haugg, M., Van de Craen, M., . . . Solary, E. (1999). Caspase-induced proteolysis of the cyclin-dependent kinase inhibitor p27 Kip1 mediates its anti-apoptotic activity. *Oncogene*, 18(34), 4839.
- Fujiwara, H., Tanaka, N., Yamashita, I., & Kitamura, K. (2013). Essential role of UBR11, but not UBR1, as an n-end rule ubiquitin ligase in *Schizosaccharomyces pombe*. *Yeast*, 30(1), 1-11.

- Gamas, P., Marchetti, S., Puissant, A., Grosso, S., Jacquet, A., Colosetti, P., . . . Auburger, P. (2009). Inhibition of imatinib-mediated apoptosis by the caspase-cleaved form of the tyrosine kinase lyn in chronic myelogenous leukemia cells. *Leukemia*, 23(8), 1500.
- Gan, L., Wang, J., Xu, H., & Yang, X. (2011). Resistance to docetaxel-induced apoptosis in prostate cancer cells by p38/p53/p21 signaling. *The Prostate*, 71(11), 1158-1166.
- Giaime, E., Sunyach, C., Herrant, M., Grosso, S., Auburger, P., McLean, P. J., . . . Da Costa, C. A. (2006). Caspase-3-derived C-terminal product of synphilin-1 displays antiapoptotic function via modulation of the p53-dependent cell death pathway. *Journal of Biological Chemistry*, 281(17), 11515-11522.
- Gonda, D. K., Bachmair, A., Wüning, I., Tobias, J. W., Lane, W. S., & Varshavsky, A. (1989). Universality and structure of the N-end rule. *Journal of Biological Chemistry*, 264(28), 16700-16712.
- Holm, L., Kriinen, S., Rosenström, P., & Schenkel, A. (2008). Searching protein structure databases with DaliLite v. 3. *Bioinformatics*, 24(23), 2780-2781.
- Hu, R., Sheng, J., Qi, X., Xu, Z., Takahashi, T. T., & Varshavsky, A. (2005). The N-end rule pathway as a nitric oxide sensor controlling the levels of multiple regulators. *Nature*, 437(7061), 981.
- Huskens, J. (2006). Multivalent interactions at interfaces. *Current Opinion in Chemical Biology*, 10(6), 537-543. doi:S1367-5931(06)00147-5 [pii]

- Hwang, C., Shemorry, A., & Varshavsky, A. (2009). Two proteolytic pathways regulate DNA repair by cotargeting the Mgt1 alkylguanine transferase. *Proceedings of the National Academy of Sciences*, 106(7), 2142-2147.
- Hwang, C., Sukalo, M., Batygin, O., Addor, M., Brunner, H., Aytes, A. P., . . . Zenker, M. (2011). Ubiquitin ligases of the N-end rule pathway: Assessment of mutations in UBR1 that cause the johanson-blizzard syndrome. *PLoS One*, 6(9), e24925.
- Ingber, D., Fujita, T., Kishimoto, S., Sudo, K., Kanamaru, T., Brem, H., & Folkman, J. (1990). Synthetic analogues of fumagillin that inhibit angiogenesis and suppress tumour growth. *Nature*, 348(6301), 555-557. doi:10.1038/348555a0 [doi]
- Jiang, Y., Choi, W. H., Lee, J. H., Han, D. H., Kim, J. H., Chung, Y., . . . Lee, M. J. (2014). A neurostimulant para-chloroamphetamine inhibits the arginylation branch of the N-end rule pathway. *Scientific Reports*, 4, 6344.
- Jiang, Y., Lee, J., Lee, J. H., Lee, J. W., Kim, J. H., Choi, W. H., . . . Kwon, Y. T. (2016). The arginylation branch of the N-end rule pathway positively regulates cellular autophagic flux and clearance of proteotoxic proteins. *Autophagy*, 12(11), 2197-2212.
- Jiang, Y., Pore, S. K., Lee, J. H., Sriram, S., Mai, B. K., Han, D. H., . . . Banerjee, R. (2013). Characterization of mammalian N-degrons and development of heterovalent inhibitors of the N-end rule pathway. *Chemical Science*, 4(8), 3339-3346.



- Kawaguchi, J., Maejima, K., Kuroiwa, H., & Taki, M. (2013). Kinetic analysis of the leucyl/phenylalanyl-tRNA-protein transferase with acceptor peptides possessing different n-terminal penultimate residues. *FEBS Open Bio*, 3(1), 252-255.
- Kumar, A., Birnbaum, M. D., Patel, D. M., Morgan, W. M., Singh, J., Barrientos, A., & Zhang, F. (2016). Posttranslational arginylation enzyme Ate1 affects DNA mutagenesis by regulating stress response. *Cell Death & Disease*, 7(9), e2378.
- Kwon, Y. T., Levy, F., & Varshavsky, A. (1999). Bivalent inhibitor of the N-end rule pathway. *Journal of Biological Chemistry*, 274(25), 18135-18139.
- Kwon, Y. T., Xia, Z., Davydov, I. V., Lecker, S. H., & Varshavsky, A. (2001). Construction and analysis of mouse strains lacking the ubiquitin ligase UBR1 (E3a) of the N-end rule pathway. *Molecular and Cellular Biology*, 21(23), 8007-8021.
- Lee, J. H., Jiang, Y., Kwon, Y. T., & Lee, M. J. (2015). Pharmacological modulation of the N-end rule pathway and its therapeutic implications. *Trends in Pharmacological Sciences*, 36(11), 782-797.
- Lee, M. J., Kim, D. E., Zakrzewska, A., Yoo, Y. D., Kim, S., Kim, S. T., . . . Oh, U. (2012). Characterization of arginylation branch of N-end rule pathway in G-protein-mediated proliferation and signaling of cardiomyocytes. *Journal of Biological Chemistry*, 287(28), 24043-24052.
- Lee, M. J., Pal, K., Tasaki, T., Roy, S., Jiang, Y., An, J. Y., . . . Kwon, Y. T. (2008). Synthetic heterovalent inhibitors targeting recognition E3

components of the N-end rule pathway. *Proceedings of the National Academy of Sciences*, 105(1), 100-105.

Li, W., Zhang, J., Bottaro, D. P., Li, W., & Pierce, J. H. (1997). Identification of serine 643 of protein kinase C- $\delta$  as an important autophosphorylation site for its enzymatic activity. *Journal of Biological Chemistry*, 272(39), 24550-24555.

Matta-Camacho, E., Kozlov, G., Li, F. F., & Gehring, K. (2010). Structural basis of substrate recognition and specificity in the N-end rule pathway. *Nature Structural & Molecular Biology*, 17(10), 1182.

Mediavilla-Varela, M., Pacheco, F. J., Almaguel, F., Perez, J., Sahakian, E., Daniels, T. R., . . . Lilly, M. B. (2009). Docetaxel-induced prostate cancer cell death involves concomitant activation of caspase and lysosomal pathways and is attenuated by LEDGF/p75. *Molecular Cancer*, 8(1), 68.

Metzger, M. B., Hristova, V. A., & Weissman, A. M. (2012). HECT and RING finger families of E3 ubiquitin ligases at a glance. *J Cell Sci*, 125(3), 531-537.

Morreale, F. E., & Walden, H. (2016). Types of ubiquitin ligases. *Cell*, 165(1), 248. e1.

Muñoz-Escobar, J., Matta-Camacho, E., Cho, C., Kozlov, G., & Gehring, K. (2017). Bound waters mediate binding of diverse substrates to a ubiquitin ligase. *Structure*, 25(5), 729. e3.

NEWBY, H., & SMYTH, D. H. (1960). Intracellular hydrolysis of dipeptides during intestinal absorption. *The Journal of Physiology*, 152, 367-380.

- Ouyang, Y., Kwon, Y. T., An, J. Y., Eller, D., Tsai, S., Diaz-Perez, S., . . . Marahrens, Y. (2006). Loss of UBR2, an E3 ubiquitin ligase, leads to chromosome fragility and impaired homologous recombinational repair. *Mutation Research/Fundamental and Molecular Mechanisms of Mutagenesis*, 596(1-2), 64-75.
- Park, S., Kim, J., Seok, O., Cho, H., Wadas, B., Kim, S., . . . Hwang, C. (2015). Control of mammalian G protein signaling by N-terminal acetylation and the N-end rule pathway. *Science*, 347(6227), 1249-1252.
- Piatkov, K. I., Brower, C. S., & Varshavsky, A. (2012). The N-end rule pathway counteracts cell death by destroying proapoptotic protein fragments. *Proceedings of the National Academy of Sciences*, 109(27), E1847.
- Piatkov, K. I., Colnaghi, L., Boksis, M., Varshavsky, A., & Huang, T. T. (2012). The auto-generated fragment of the Usp1 deubiquitylase is a physiological substrate of the N-end rule pathway. *Molecular Cell*, 48(6), 926-933.
- Piatkov, K. I., Colnaghi, L., Békés, M., Varshavsky, A., & Huang, T. T. (2012). The auto-generated fragment of the Usp1 deubiquitylase is a physiological substrate of the N-end rule pathway. *Molecular Cell*, 48(6), 926-933.
- Piatkov, K. I., Oh, J., Liu, Y., & Varshavsky, A. (2014). Calpain-generated natural protein fragments as short-lived substrates of the N-end rule pathway. *Proceedings of the National Academy of Sciences*, , 201401639.
- Potuschak, T., Stary, S., Schlögelhofer, P., Becker, F., Nejinskaia, V., & Bachmair, A. (1998). PRT1 of *Arabidopsis thaliana* encodes a component of

the plant N-end rule pathway. *Proceedings of the National Academy of Sciences*, 95(14), 7904-7908.

Rao, H., Uhlmann, F., Nasmyth, K., & Varshavsky, A. (2001). Degradation of a cohesin subunit by the N-end rule pathway is essential for chromosome stability. *Nature*, 410(6831), 955.

Saha, S., Wang, J., Buckley, B., Wang, Q., Lilly, B., Chernov, M., & Kashina, A. (2012). Small molecule inhibitors of arginyltransferase regulate arginylation-dependent protein degradation, cell motility, and angiogenesis. *Biochemical Pharmacology*, 83(7), 866-873. doi:10.1016/j.bcp.2012.01.012 [doi]

Saha, S., Mundia, M. M., Zhang, F., Demers, R. W., Korobova, F., Svitkina, T., . . . Kashina, A. (2010). Arginylation regulates intracellular actin polymer level by modulating actin properties and binding of capping and severing proteins. *Molecular Biology of the Cell*, 21(8), 1350-1361.

Silk, D. B., Grimble, G. K., & Rees, R. G. (1985). Protein digestion and amino acid and peptide absorption. *The Proceedings of the Nutrition Society*, 44(1), 63-72. doi:S0029665185000167 [pii]

Sriram, S., Lee, J. H., Mai, B. K., Jiang, Y., Kim, Y., Yoo, Y. D., . . . Lee, M. J. (2013). Development and characterization of monomeric N-end rule inhibitors through in vitro model substrates. *Journal of Medicinal Chemistry*, 56(6), 2540-2546.

Tasaki, T., Mulder, L. C., Iwamatsu, A., Lee, M. J., Davydov, I. V., Varshavsky, A., . . . Kwon, Y. T. (2005). A family of mammalian E3 ubiquitin ligases that

contain the UBR box motif and recognize N-degrons. *Molecular and Cellular Biology*, 25(16), 7120-7136.

Tobias, J. W., Shrader, T. E., Rocap, G., & Varshavsky, A. (1991). The N-end rule in bacteria. *Science*, 254(5036), 1374-1377.

Turner, G. C., Du, F., & Varshavsky, A. (2000). Peptides accelerate their uptake by activating a ubiquitin-dependent proteolytic pathway. *Nature*, 405(6786), 579-583. doi:10.1038/35014629 [doi]

Utz, P. J., & Anderson, P. (2000). Life and death decisions: Regulation of apoptosis by proteolysis of signaling molecules. *Cell Death and Differentiation*, 7(7), 589.

Varshavsky, A. (2011). The n-end rule pathway and regulation by proteolysis. *Protein Science*, 20(8), 1298-1345.

Varshavsky, A. (2017). The ubiquitin system, autophagy, and regulated protein degradation. *Annual Review of Biochemistry*, 86, 123-128.

Wadas, B., Piatkov, K. I., Brower, C. S., & Varshavsky, A. (2016). Analyzing N-terminal arginylation through the use of peptide arrays and degradation assays. *Journal of Biological Chemistry*, 291(40), 20976-20992.

Weaver, B. P., Weaver, Y. M., Mitani, S., & Han, M. (2017). Coupled caspase and N-end rule ligase activities allow recognition and degradation of pluripotency factor LIN-28 during non-apoptotic development. *Developmental Cell*, 41(6), 673. e6.

- Xu, Z., Payoe, R., & Fahlman, R. P. (2012). The C-terminal proteolytic fragment of the breast cancer susceptibility type 1 protein (BRCA1) is degraded by the N-end rule pathway. *Journal of Biological Chemistry*, 287(10), 7495-7502.
- Yamano, K., & Youle, R. J. (2013). PINK1 is degraded through the N-end rule pathway. *Autophagy*, 9(11), 1758-1769.
- Yin, S. Q., Wang, J. J., Zhang, C. M., & Liu, Z. P. (2012). The development of MetAP-2 inhibitors in cancer treatment. *Current Medicinal Chemistry*, 19(7), 1021-1035. doi:BSP/CMC/E-Pub/2012/089 [pii]
- Zenker, M., Mayerle, J., Lerch, M. M., Tagariello, A., Zerres, K., Durie, P. R., . . . Rehder, H. (2005). Deficiency of UBR1, a ubiquitin ligase of the N-end rule pathway, causes pancreatic dysfunction, malformations and mental retardation (johanson-blizzard syndrome). *Nature Genetics*, 37(12), 1345.
- Zhang, F., Patel, D. M., Colavita, K., Rodionova, I., Buckley, B., Scott, D. A., . . . Chernov, M. (2015). Arginylation regulates purine nucleotide biosynthesis by enhancing the activity of phosphoribosyl pyrophosphate synthase. *Nature Communications*, 6, 7517.

## CHAPTER 2 . MATERIALS AND METHODS

## **1. Materials**

### **1.1 Cell Culture**

I have used four cell lines, HEK (Human Embryonic Kidney 293 cells), HeLa (human cervical adenocarcinoma epithelial cells), K562 (chronic myelogenous leukemia) and Jurkat (human T lymphocyte cells). HEK and HeLa cells were maintained in Dulbecco's Modified Eagle's medium (DMEM) supplemented with 10% FBS. K562 and Jurkat cells were maintained in RPMI-1640 Medium with L-glutamine supplemented with 10% FBS.

### **1.2 DNA plasmids and Stable Expression of Constructs**

To express the cleaved PKC $\delta$  and Lyn fragments, we cloned the cleaved fragments as a fusion between an N-terminal ubiquitin and the C-terminal end of the proteins published previous in our lab (Xu, Payoe, & Fahlman, 2012; Eldeeb, & Fahlman, 2016). The final Ub- PKC $\delta$  -FLAG pcDNA 3.1 vector and Ub- PKC $\delta$  -FLAG pcDNA 3.1 vector were verified by DNA sequencing, same for the Ub-X-Lyn $\Delta$ N -FLAG pcDNA 3.1 vectors. The full-length substrates were similarly cloned with a C-terminal 3xFLAG in a pcDNA 3.1 plasmid.

### **1.3 Antibodies**

Mouse anti-FLAG<sup>®</sup> antibody was purchased from Sigma. Mouse anti- $\beta$ -actin (I-19, catalog number sc-1616-R) and PKC $\delta$  (C-20, sc-937) were purchased from Santa Cruz Biotechnology. Secondary antibody for Western blot analysis (goat



anti-mouse 680RD, LIC-926-32220, and goat anti-rabbit 680RD, LIC-926-32221) coupled to IRDyes® were purchased from LI-COR.

## **1.4 Cell culture of Escherichia coli**

The bacterial cells were grown in liquid culture Luria Broth (LB) Base, Miller, Difco, (0.5g NaCl & Pancreatic Digest of Casein) at 1% (w/v). For solid culture medium it was used the LB Agar, Miller (Luria-Bertani), Difco. For plasmid selection antibiotics were added to the medium (final concentration: ampicillin 50 µg/mL, kanamycin 25 µg/mL).

## **2. Methods**

### **2.1 Cell Transfections**

HeLa cells were transfected with Lipofectamine™ 3000 Transfection Reagent (Invitrogen) according to the manufacturer's recommended procedures. HEK 293T cells were transfected using the calcium phosphate-based method (Jordan, Schallhorn, & Wurm, 1996).

### **2.2 Protein Half-life Determination**

One day after transfection,  $6 \times 10^5$  cells (80 to 90% of confluency) were treated with 100 µg/ml of cycloheximide for the indicated amounts of time. Cells were then lysed in 50 µl of lysis buffer (50 mM Tris, pH 6.8, 8% glycerol (v/v), 0.016% SDS (w/v), 0.125% β-mercaptoethanol (v/v), 0.125% bromphenol blue

(w/v), 1 mM PMSF, and 1  $\mu$ g/ml of leupeptin) (Xu, Payoe, & Fahlman, 2012). The samples were then resolved by SDS-PAGE on 10% gels using Precision Plus All Blue protein prestained standards (Bio-Rad) as molecular weight markers. Protein amounts were visualized by Western blot analysis. **Figure 2-1** illustrated the process involved in the protein half-life determination.

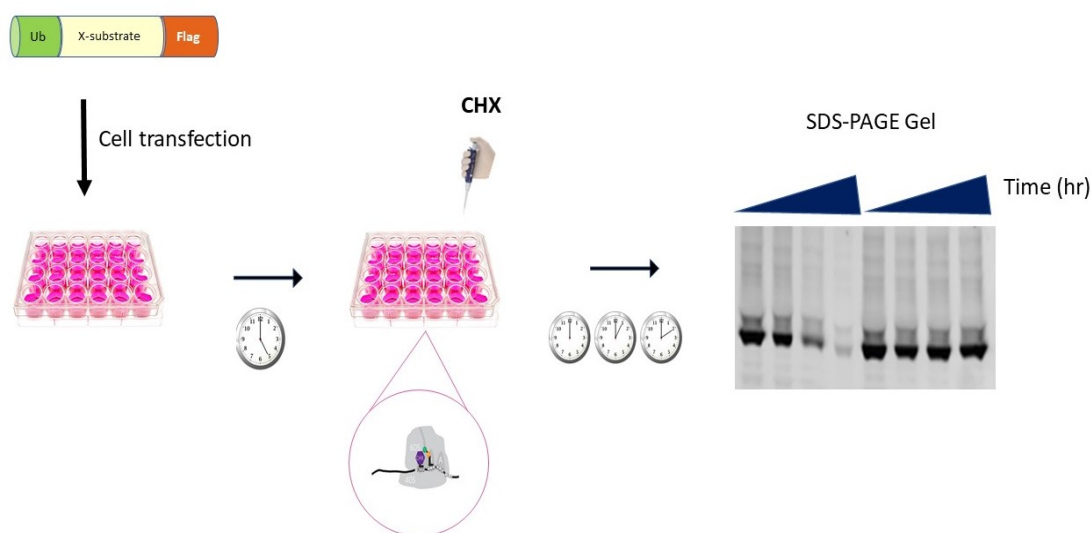


**Figure 2-1. Schematic of Protein Stability**

The figure illustrates the protein degradation analysis, including the cell transfection followed by Cycloheximide treatment to inhibit protein synthesis and the analysis of protein abundance in different timepoints.

### 2.3 Western Blot Analysis

Cell lysates were run in SDS-PAGE gel (30% acrylamide, 4x running buffer, 10% SDS, MiliQ H<sub>2</sub>O, 10% ASP, TEMED) 12% and 10% depending on the protein molecular weight. After SDS-PAGE, proteins were transferred onto nitrocellulose membranes (LI-COR Biosciences). The membranes were blocked with blocking

buffer (1xPBS, 2.5% Fish Gelatin), probed with primary and secondary antibodies, and imaged with an Odyssey® Fc Imaging System using the manufacturer's recommended procedures (LI-COR).

For endogenous proteins, after running the SDS-PAGE the protein was transfer to nitrocellulose membrane following the wet transfer protocol. The gel, membrane, two sheets of filter paper, and transfer cassette pads were soaked in transfer buffer (25mM Tris, 192mM glycine, pH 8.3, 20% methanol) for 10 minutes, then assembled into the transfer apparatus. Transfer was completed in 75 min at 100V or 400mA at 4°C.

## **2.4 Protein expression and purification**

Human UBR1 UBR-box and UBR2 UBR-box domain were kindly provided by Dr. Kalle Gehring from McGill University (Muñoz-Escobar, Matta-Camacho, Cho, Kozlov, & Gehring, 2017). The plasmids listed above together with the GST-protein, were transformed in BL21 cells and expressed in Luria-Bertani media containing ampicillin. Transformed cells were grown to mid-log phase, approximately 0.5 O.D. 600nm, and then induced with 1mM isopropyl  $\beta$ -D-1-thiogalactopyranoside (IPTG) and 100 $\mu$ M ZnCl<sub>2</sub> (only for UBR1 and 2) overnight at 37°C. Cells were harvested by centrifugation and, then, lysed by sonication in buffer A (50mM HEPES pH 7.5, 200mM NaCl, 10  $\mu$ M ZnCl<sub>2</sub>, 5% glycerol, and 5 mM  $\beta$ -mercaptoethanol buffer) containing 0.1 mM of the protease inhibitor phenylmethylsulphonyl fluoride (PMSF). The lysates were passed through a 1 mL GSTrap FF Column (GE Healthcare). After substantial wash with buffer A, the proteins attached to the column were eluted in constant gradient with buffer A containing 20mg glutathione. Purification was performed using affinity

chromatography with Glutathione S-transferase (GST) immobilized in agarose beads followed by elution with reduced glutathione and removal of the GST tag. The final step consisted of size exclusion chromatography using UBR-wash buffer (25mM Hepes, 25mM NaCl, 0.5mM DDT, 0.01% triton), followed by UBR lysis buffer (wash buffer, 1mM PMSF) and finally eluted with fresh GST elution buffer (20 mM HEPES pH 7.5, 100 mM NaCl, 2 mM  $\beta$ -mercaptoethanol and 10  $\mu$ M ZnCl<sub>2</sub> buffer, glutathione 3mg/mL).

The eluted fractions were analyzed by 12% SDS-PAGE gel. The fractions containing the purified proteins were pooled together and dialyzed into storage buffer (25mM mM Tris-Cl (pH 7.4), 25 mM NaCl). Standard Bradford protein assay (Bio-Rad) and Bovine Serum Albumin (BSA) standards were used to determine the concentration of purified proteins. The purified proteins were aliquoted into 100  $\mu$ L per tube and stored at -80 °C.

## **2.5 Site-directed Mutagenesis**

Mutagenesis of the codon for the Asp corresponding to the N-termini and Ser corresponding to the second position of the cleaved PKC $\delta$  protein was performed by site-directed mutagenesis. The change of the codon contemplates the following sequences: Asp (GAC), Asn (AAC), Thr (ACG), Ala (GCC), Pro (CCG), Glu (GAG) and Val (GTG). Similarly, the kinase-dead form of cleaved PKC $\delta$  was obtained through mutating Lys378 into Arginine (CGG) by site-directed mutagenesis.

## **2.6 Cell Cycle Analysis**

HeLa cells were grown in 6-well plates and treated with the indicated compounds (PPCP, Phe-Nh<sup>2</sup>, and DMSO as control). Post-treatment, cells were trypsinized, centrifuged (230xg) for 10 minutes and washed with 1XPBS. Cell pellets were gently resuspended in ice-cold 70% ethanol. A single cell suspension was made by gentle vortexing followed two to 24 hours storage at -20°C(Kim & Sederstrom, 2015). Ethanol-fixed cells were centrifuged (500xg) and washed twice with 1XPBS at 4°C. Propidium iodide staining of the cells was performed by incubating cell pellets in DNA staining solution (0.1% TritonX-100, 100µg/ml DNase free RNase A, 20µg/ml propidium iodide in 1XPBS) at 37°C for 40min followed by filtration through a nylon mesh (50µM exclusion limit) to remove cell clumps. Flow cytometric analysis of was performed on a BD Accuri cell analyzer.

## **2.7 Acridine Orange/ Ethidium Bromide (AO/EB) staining**

HeLa cells were analyzed using Acridine Orange and ethidium bromide (AO/EB) staining to identify the cell apoptosis after indicated treatment. The double staining is an accurate method that has been used to distinguish cell viability by differentiating the red and green stain, dead and live cells, respectively(Kasibhatla et al., 2006; Liu, Liu, Liu, & Wu, 2015). The cells at a final concentration of approximately  $4 \times 10^5$ /ml were left untreated or treated with 200uM of PPCP in the presence or absence of 16uM, 32uM, or 64uM of PAC1 (Procaspase Activating Factor-1) in a 24 well plate. After 24 and 48 hours, the media was removed and a dual fluorescent staining solution (500 µl) containing 100 µg/ml AO and 100 µg/ml EB in 1xPBS was added to each well. The morphology of apoptotic cells was

examined, and  $1 \times 10^3$  cells were counted using a fluorescent microscope (ZOE™ Fluorescent Cell Imager). Dual AO/EB staining method was done in triplicate.

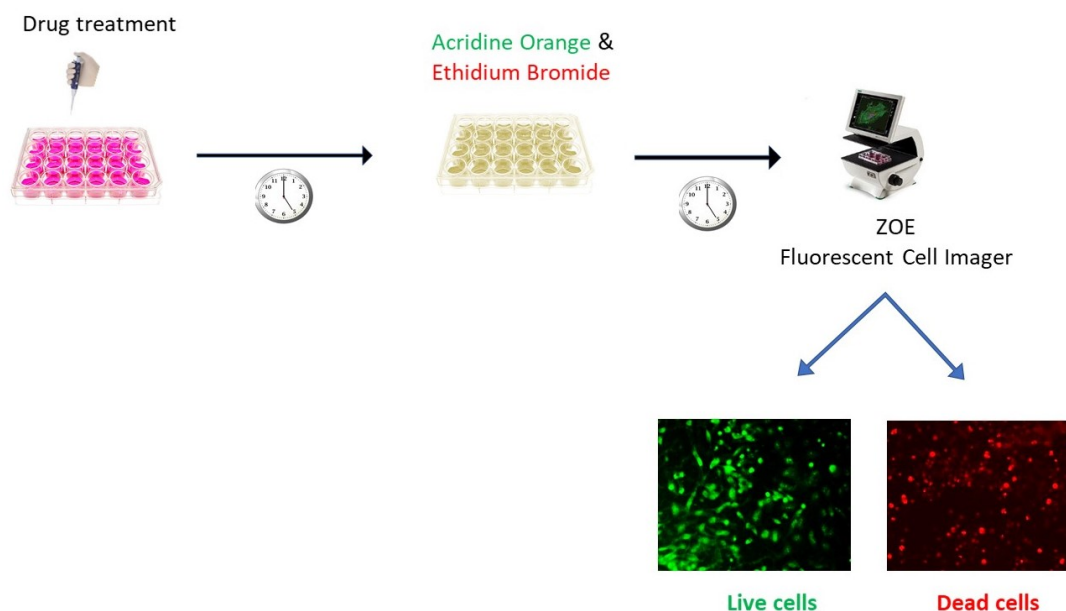


### Figure 2-2. Cell viability assay through double staining

Schematic of the Acridine Orange and Ethidium Bromide staining with the Fluorescent cell imager ZOE™, 175x to 700x zoom.

## 2.8 Metabolic activity

MTT (Thiazolyl tetrazolium bromide) was dissolved in PBS at 5 mg/ml and filtered to sterilize and remove a small amount of insoluble residue present in some batches of MTT. 24 hours after drug treatment, stock MTT solution (10  $\mu$ l per 100  $\mu$ l medium) was added to all wells of an assay, and plates were incubated at 37°C for 3.5 h. Acid-isopropanol (100  $\mu$ l of 0.04 N HCl in isopropanol) was added to all wells and mixed thoroughly to dissolve the dark blue crystals. After fifteen minutes at room temperature to ensure that all crystals were dissolved, the plates

were read on a  $\mu$ Quant reader, using a test wavelength of 590 nm, a reference wavelength of 630 nm, and a calibration setting of 1.99. Plates were normally read within 1 h of adding the isopropanol (Menyhárt et al., 2016; Mosmann, 1983).

## **2.9 Thermal Shift Assays**

The thermal shift assay was done by using the protocol previous described by Gehring's lab at McGill University (Muñoz-Escobar et al., 2017). Each of the reaction contained 20  $\mu$ l of solution with 1.5  $\mu$ M of Ubr1, 5  $\mu$ l of Protein Thermal Shift™ buffer, 1 $\times$  Protein Thermal Shift™ dye (Protein Thermal Shift Dye kit™, Life Technologies), buffer A and 9.5 mM peptide (REGK), with or without the Analogue II (10  $\mu$ M) and DMSO control. Peptide concentration was estimated based on amount of powder weighted and molecular weight. Samples were heated from 25 °C to 99 °C at a rate of 1 °C per minute and fluorescence signals were monitored by the quantitative real-time PCR system. The peptide was also tested alone (no protein control) and flat lines were observed at all temperatures during each experiment. The maximum change of fluorescence with respect to temperature was used to determine the T<sub>m</sub>.

## **3. Statistical Analysis**

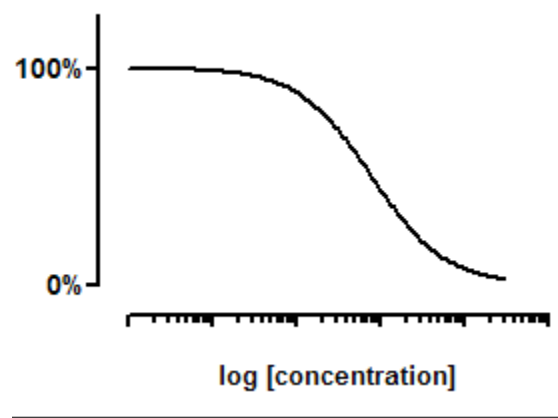
### **3.1 Effective Half Life Concentration**

To analyse the log (inhibitor) vs. response curves the data was plotted using the GraphPad Prim version 8.0. The data was normalized to run between 0% and 100%, with the goal of determining the EC<sub>50</sub> of the inhibitor - the concentration that provokes a response equal to 50%. The data was created as an XY data table,

with the concentration of the inhibitor being in X and response into Y. The experiments were performed in triplicates.

The data was analysed with the following settings: nonlinear regression; Dose-response curves – Inhibition; log(inhibitor) vs. normalized response equation; variable slope. The model of the equation is as follow:

$$Y=100/(1+10^{((\text{LogIC50}-X)*\text{HillSlope}))})$$



Two concepts are important to clarify. First, the EC50 that is the concentration of agonist that represents a halfway response. Prism reports both the EC50 and its log. Second, the Hill slope which describes the steepness of the family of curves. The Hill slope standard is -1.0 whereas the Hill slope more negative than -1 (e.g. -2) is steeper (Motulsky, 2007).

### **3.2 Data representation**

The graphs were created using GraphPad prism (GraphPad Software, La Jolla, CA, USA) and Microsoft Excel editor. The error bars on the bar graphs are presented as mean ± standard deviation. The statistical analysis of bar graphs was



done using two-tailed unpaired t-test at  $p$ . As per the statistical approach, if significant, the actual  $p$ -value is given up to three decimal places and if not significant written as ns.

## References

- Eldeeb, M. A., & Fahlman, R. P. (2016). Phosphorylation impacts N-end rule degradation of the proteolytically activated form of BMX kinase. *Journal of Biological Chemistry*, *291*(43), 22757-22768.
- Jordan, M., Schallhorn, A., & Wurm, F. M. (1996). Transfecting mammalian cells: Optimization of critical parameters affecting calcium-phosphate precipitate formation. *Nucleic Acids Research*, *24*(4), 596-601.
- Kasibhatla, S., Amarante-Mendes, G. P., Finucane, D., Brunner, T., Bossy-Wetzel, E., & Green, D. R. (2006). Acridine orange/ethidium bromide (AO/EB) staining to detect apoptosis. *Cold Spring Harbor Protocols*, *2006*(3), pdb.prot4493.
- Kim, K. H., & Sederstrom, J. M. (2015). Assaying cell cycle status using flow cytometry. *Current Protocols in Molecular Biology*, , 28.6. 11.
- Liu, K., Liu, P., Liu, R., & Wu, X. (2015). Dual AO/EB staining to detect apoptosis in osteosarcoma cells compared with flow cytometry. *Medical Science Monitor Basic Research*, *21*, 15.
- Menyhárt, O., Harami-Papp, H., Sukumar, S., Schäfer, R., Magnani, L., de Barrios, O., & Györfy, B. (2016). Guidelines for the selection of functional

assays to evaluate the hallmarks of cancer. *Biochimica Et Biophysica Acta (BBA)-Reviews on Cancer*, 1866(2), 300-319.

Mosmann, T. (1983). Rapid colorimetric assay for cellular growth and survival: Application to proliferation and cytotoxicity assays. *Journal of Immunological Methods*, 65(1-2), 55-63.

Motulsky, H. J. (2007). Prism 5 statistics guide, 2007. *GraphPad Software*, 31(1), 39-42.

Muñoz-Escobar, J., Matta-Camacho, E., Cho, C., Kozlov, G., & Gehring, K. (2017). Bound waters mediate binding of diverse substrates to a ubiquitin ligase. *Structure*, 25(5), 729. e3.

Xu, Z., Payoe, R., & Fahlman, R. P. (2012). The C-terminal proteolytic fragment of the breast cancer susceptibility type 1 protein (BRCA1) is degraded by the N-end rule pathway. *Journal of Biological Chemistry*, 287(10), 7495-7502.

CHAPTER 3 . PHOSPHORYLATION OF  
SER331 AND ITS ROLE IN THE N-END  
RULE PATHWAY REGULATION

## 1. Introduction to the PKC family

The protein kinase C (PKC) gene family is conserved throughout ten different isoforms: the conventional or classical isoforms ( $\alpha$ ,  $\beta$ I,  $\beta$ II, and  $\gamma$ ), which may be activated by calcium and diacylglycerol (DAG) or phorbol esters; the novel isoforms ( $\delta$ ,  $\epsilon$ ,  $\theta$ , and  $\eta$ ), which can be stimulated by DAG, but independent of calcium or phorbol ester; and the atypical isoforms ( $\zeta$ , and  $\iota$ ), which are activated in response to calcium, DAG and phorbol esters (Singh et al., 2017; Sun, Wu, Song, & Sun, 2018).

Conserved through the family, the structure comprises a C-terminal serine/threonine protein kinase domain that is linked through a variable 'V3' domain to a regulatory N-terminal domain, with three functional elements (1) the inhibitory region (pseudo-substrate site), (2) a C1 domain, and (3) the C2 or PB1 domain (Roffey et al., 2009). The conserved region 1 (C1) domains are individually folded Zn<sup>2+</sup> fingers of 50 amino acids, with the function of targeting native PKCs to DAG-containing endo-membranes (Igumenova, 2015). One of the importance of the PKCs to DAG affinity is its implication for the isoenzymes cellular localization and their response selectivity (Gallegos & Newton, 2008).

The C2 domains, on the other hand, are singly folded structural and functional modules composed by approximately 140 residues (Cho & Stahelin, 2006; Shao, Davletov, Sutton, Südhof, & Rizo, 1996). It has been reported that the electrostatic potential of C2 is modified by Ca<sup>2+</sup> which enables the domain to interact with anionic lipids (Murray & Honig, 2002). The C2 domain of novel PKC lacks the key residues for these interactions and does not bind either Ca<sup>2+</sup> or phospholipids (Verdaguer, Corbalan-Garcia, Ochoa, Fita, & Gómez-Fernández, 1999), instead, it binds phosphotyrosine residues (Benes et al., 2005; Yang, Y.,

Shu, Li, & Igumenova, 2018). Moreover, it was previously demonstrated that the chemical identity of a metal ion has consequences for protein-membrane interactions (Morales et al., 2011).

### **1.1 Overall view of the PKC enzymatic activation**

The PKC members are activated by allosteric inputs, such as lipids, proteins or a combination of both, while the inactivity is determined through the interaction between the regulatory domain and the catalytic domain (Keranen, Dutil, & Newton, 1995; Roffey et al., 2009). The optimal kinase domain functionality is when the kinase domain is appropriately phosphorylated on two ( $\zeta$ , and  $\iota$ ) or three ( $\alpha$ ,  $\beta$ ,  $\tau$ ,  $\delta$ ,  $\epsilon$ ,  $\theta$ , and  $\eta$ ) conserved sites (Parekh, Ziegler, & Parker, 2000; Roffey et al., 2009). Phosphorylation sites, such as threonine or serine residues, are well conserved through the PKC family members (Newton, 2001; Parekh et al., 2000). The phosphorylation of serine/threonine or tyrosine residues in PKC isoforms are implicated in the allosteric activation, activity control, cellular localization and function (Roffey et al., 2009).

First, the PKCs are phosphorylated by an upstream kinase, phosphoinositide-dependent kinase (PDK-1), in the activation loop (Kikkawa, Matsuzaki, & Yamamoto, 2002). After the “priming” phosphorylation the protein adopts a mature and stable conformation, translocate to the cytosol (Yang, Q., Langston, Tang, Kiani, & Kilpatrick, 2019) and is ready to interact with second messengers, the diacylglycerol or phorbol ester (Yang, Q. et al., 2019). Right after the first phosphorylation step is completed, the activation loop may be dephosphorylated (Keranen et al., 1995; Yang, Q. et al., 2019). Nevertheless, this is a somewhat oversimplified description of PKC activation and is essential to

acknowledge there are multiple points of intervention and particularities of each PKC family member.

## 1.2 The PKC $\delta$ isoform specificities

The PKC $\delta$  is a novel isoform, the overall structure consists of an N-terminal regulatory domain connected by a flexible linker region to a C-terminal kinase domain (Gong, Park, & Steinberg, 2017), **Figure 3-1.A**. Its activation, is regulated by the binding of the diacylglycerol and phorbol ester (Hurley, Newton, Parker, Blumberg, & Nishizuka, 1997; Kikkawa et al., 2002) as well as by molecular mechanisms such as phosphorylation and proteolytic reactions (Kikkawa et al., 2002). As previously mentioned, despite other isoforms, the C2 domain of the PKC $\delta$  do not bind Ca<sup>2+</sup> or membranes but rather serve as protein-protein interaction modules (Benes et al., 2005; Stahelin et al., 2012). Moreover, recent investigations revealed that PKC $\delta$  also moves to several subcellular compartments, such as mitochondria, endoplasmic reticulum (ER), Golgi apparatus, nuclei, and caveolae (Page et al., 2003; Qi & Mochly-Rosen, 2008; Rybin, Xu, & Steinberg, 1999).

The phosphorylation of the kinase Thr505 residue in the activation loop is important for PKC autophosphorylation (Dutil, Toker, & Newton, 2031; Le Good et al., 1998; Parekh et al., 2000). However, studies expressing *Escherichia coli*, with PKC $\delta$  WT and mutant (Thr505), suggested that the phosphorylation of the activation loop may not be necessary for its catalytic activity (Liu, Belkina, Graham, & Shaw, 2006; Stempka et al., 1997). These findings differ on the role of PKC $\delta$  activation loop phosphorylation biological functions (Cheng, He, Tian, Dinauer, & Ye, 2007). Additionally, reports shows a distinct lipid-independent mechanism that

leads to PKC $\delta$  activation (Konishi et al., 1997; Rybin et al., 2004) including Src activation by oxidative stress stimulus leading to the Src-dependent phosphorylation of PKC $\delta$  at Tyr313 and Tyr334 (Rybin et al., 2004).

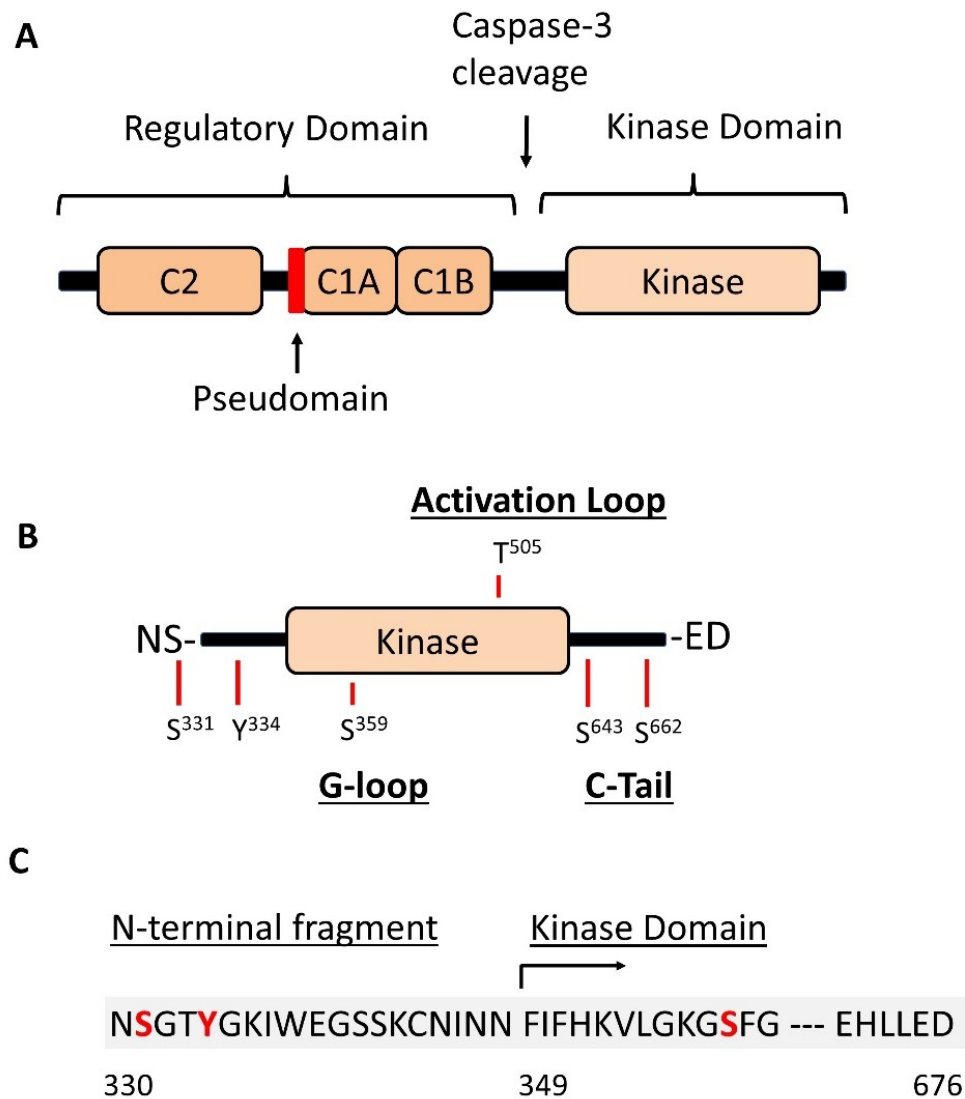


**Figure 3-1. Schematic of PKC $\delta$  structure.**

**A.** It shows the domain structure of PKC $\delta$ , divided in C2, Pseudodomain, C1A, C1B and Kinase domain. Noticed that between C1B and the kinase domain is the V3 region where also occurs the caspase cleavage. **B.** C-terminal fragment after caspase cleavage. In red it is highlighted the main phosphorylation sites. The G-

loop, activation loop and C-tail are also identified. **C.** Sequence of the C-terminal fragment, with the phosphorylation sites in red.

The main conserved threonine and serine phosphorylation sites for PKC $\delta$  are the Thr505 (activation loop), Ser643 (turn motif)(Kikkawa et al., 2002; Li, Zhang, Bottaro, Li, & Pierce, 1997), and Ser662 (hydrophobic motif)(Malavez, Gonzalez-Mejia, & Doseff, 2009), these two on the C-tail, **Figure 3-1.B**. However, with little phosphorylation in the activation loop in many cell types (Yang, Q. et al., 2019). Different than the other PKC family members, the mutations of Thr505 to Ala505 in PKC $\delta$  does not affect its catalytic activity, although it may be necessary for enzyme stability (Malavez et al., 2009; Stempka et al., 1997).

The Thr505 and Ser662 motifs are both recognized by an upstream kinase (Le Good et al., 1998; Ziegler et al., 1999) whereas the Ser643 is an autophosphorylation site (Parekh et al., 2000; Roffey et al., 2009). Overall, the phosphorylation of Ser643 and Ser662 is necessary for the catalytic activation of PKC $\delta$  and the Thr505 phosphorylation can enhance its catalytic activity (Le Good et al., 1998; Malavez et al., 2009; Stempka et al., 1999; Yang, Q. et al., 2019). Other than the already mentioned phosphorylation site, the Ser359, a site at the tip of the Gly-rich ATP-positioning loop (G-loop) in the kinase domain, contributes to redox-activated PKC $\delta$  responses in cardiomyocytes (Gong et al., 2017).

### **1.2.1 PKC $\delta$ Physiological Roles**

Unlike the other isoforms, PKC $\delta$  is expressed ubiquitously in mammalian tissues, such as brain, hematopoietic system, placenta, uterus, epidermis, lung, and kidney (Leibersperger, Gschwendt, Gernold, & Marks, 1991; Zhao, Xia, & Chen, 2012). Not surprisingly, mouse models study demonstrated that kinase



knockout is associated with defects in smooth muscle cells survival (Leitges et al., 2001), elimination of self-reactive B cells (Mecklenbräuker, Saijo, Zheng, Leitges, & Tarakhovsky, 2002), and excessive damage associated with ischemic preconditioning (Mayr et al., 2004; Roffey et al., 2009). Likewise, the PKC $\delta$  was also reported as an import regulator of the inflammatory response in sepsis (Yang, Q. et al., 2019), regulator of reperfusion injury (Chen, L. et al., 2001; Hahn et al., 2002; Inagaki et al., 2003), reduction in apoptosis (Reyland, M. E., 2007), and to be upregulated in several cancers (Safran et al., 2003; Sun et al., 2018), such as bladder and breast cancers.

In addition to the identified roles for the full length protein, PKC $\delta$  can undergo caspase cleavage in response to several stress factors such as tumor necrosis factor related to apoptosis in glioma cells (Okhrimenko et al., 2005), UV radiation in keratinocytes (Denning et al., 2002), cisplatin in glioma and small cell lung cancer (Billecke et al., 2006; Persaud, Hoang, Huang, & Basu, 2005), hydrogen peroxide (H<sub>2</sub>O<sub>2</sub>) in neuronal cells (Kaul et al., 2005), etoposide in glioma and acinar cells (Blass, Kronfeld, Kazimirsky, Blumberg, & Brodie, 2002; Reyland, Mary E., Anderson, Matassa, Barzen, & Quissell, 1999), and mitomycin C in gastric adenocarcinoma (Park et al., 2000). Caspase-3 is responsible for the substrate cleavage at the V3 region and generation of a  $\Delta$ N-PKC $\delta$  (330-676) fragment (Cross et al., 2000; Gong et al., 2017), **Figure 3-1.B and C**. The cleaved catalytic fragment is associated to apoptosis activity (Cross et al., 2000; Durrant, Liu, Yang, & Lee, 2004; Ren et al., 2002), and is predominantly localized in the nucleus (Blass et al., 2002; DeVries, Neville, & Reyland, 2002, DeVries-Seimon, Ohm, Humphries, & Reyland, 2007). Important to mention that the tyrosine phosphorylation of PKC $\delta$  preceded caspase-3 cleavage and influenced the PKC $\delta$  nuclear accumulation (Blass et al., 2002; Humphries, Ohm, Schaack, Adwan, &

Reyland, 2008), which was reinforced by a recent study that shows the phosphorylation at the activation loop, C-tail priming sites, Tyr334, and Ser359 at the G-loop as crucial factors for the  $\Delta$ N-PKC $\delta$  activity regulation (Gong et al., 2017).

Interestingly, ambiguous roles of PKC $\delta$  have been reported, where the full-length kinase and the cleaved catalytic fragment seems to have different signalling outcomes. While studies demonstrate the PKC $\delta$  activity as a tumour suppressor with anti-proliferative activity in different cell types (Jackson & FOSTER, 2004), other reports show PKC $\delta$  as having a pro-proliferative activity and a cancer-promoting gene (Kiley, Clark, Duddy, Welch, & Jaken, 1999). It was revealed that the nucleus import sequence identified in the PKC $\delta$  catalytic fragment is necessary for its pro-apoptosis role, and the nuclear expression of PKC $\delta$  dominant-negative mutant inhibits etoposide-induced apoptosis (DeVries et al., 2002). These findings indicate that the PKC $\delta$  cleaved fragment is partially active in the nucleus during apoptosis (Zhao et al., 2012). Furthermore, PKC $\delta$  fragment also functions as a feedforward for the complementary PKC $\delta$  and caspase-3 proteolytic activation (Chen, J. et al., 2009).

Nevertheless, the regulation of the PKC $\delta$  cleaved fragment by the N-end Rule Pathway would have a direct impact in its pro-apoptotic activity. As the cleaved fragment bears an unstable N-terminal Asn I sought to investigate its protein degradation rate. This analysis expands the understanding of the PKC $\delta$  pro-apoptotic fragment stability.

### 1.3 The PKC $\delta$ fragment as an N-end rule substrate

After caspase cleavage, the newly formed PKC $\delta$  fragment ( $\Delta$ N-PKC $\delta$ ) has a known tertiary unstable N-terminal, asparagine (N). The Neo-termini is a predicted N-end rule substrate and is expected to undergo through protein degradation by the Ubiquitin Proteasome System. This process includes the enzymatic deamination of the asparagine by N-terminal amidases (NTA1), followed by arginilation through ATE1 activity, polyubiquitination and proteasomal degradation.

The investigation of the  $\Delta$ N-PKC $\delta$  fragment degradation was possible by the ubiquitin fusion technique. Although virtually all proteins are translated with the first amino acid being a methionine, the ubiquitin fusion allows the expression of any desired residue as the N-termini. This is obtained by the activity of the endogenous ubiquitin hydrolases which cleaves the ubiquitin moiety and exposes the protein fragment with the desired amino acid at the N-terminal (Xu, Payoe, & Fahlman, 2012), **Figure 3-2.A and B.**

The stability of the proteins was investigated by using cycloheximide (CHX) treatment and Western blot analysis. CHX inhibits protein synthesis through blocking translocation of the ribosome on an mRNA transcripts (Kao et al., 2015). Once protein synthesis is inhibited by CHX treatment, any reduction in the abundance of proteins can be correlated to the degradation of the targeted protein.

First, the PKC $\delta$  cleavage was induced by the addition of a Procaspase Activator Factor-1 (PAC1). In **Figure 3-3.A**, it is shown the protein expression after PAC1, and the addition of Z-VAD-fmk (carbobenzoxy-valyl-alanyl-aspartyl-[O-methyl]- fluoromethylketone). The Z-VAD-fmk is a cell-permeable pan-caspase inhibitor that binds irreversibly to the catalytic site of caspase proteases. It was

observed the  $\Delta$ N-PKC $\delta$  fragment formed after caspase activation, PAC1 treatment. Interestingly, the cleaved fragment was also present after four hours of the caspase inhibitor suggesting that the cleaved PKC WT is stable. Additionally, it was demonstrated that the mutation of Asp329, with the substitution of the aspartate (D) to glutamate (E), inhibited the formation of the  $\Delta$ N-PKC $\delta$  fragment, validating that the Asp329 site is crucial for caspase recognition.

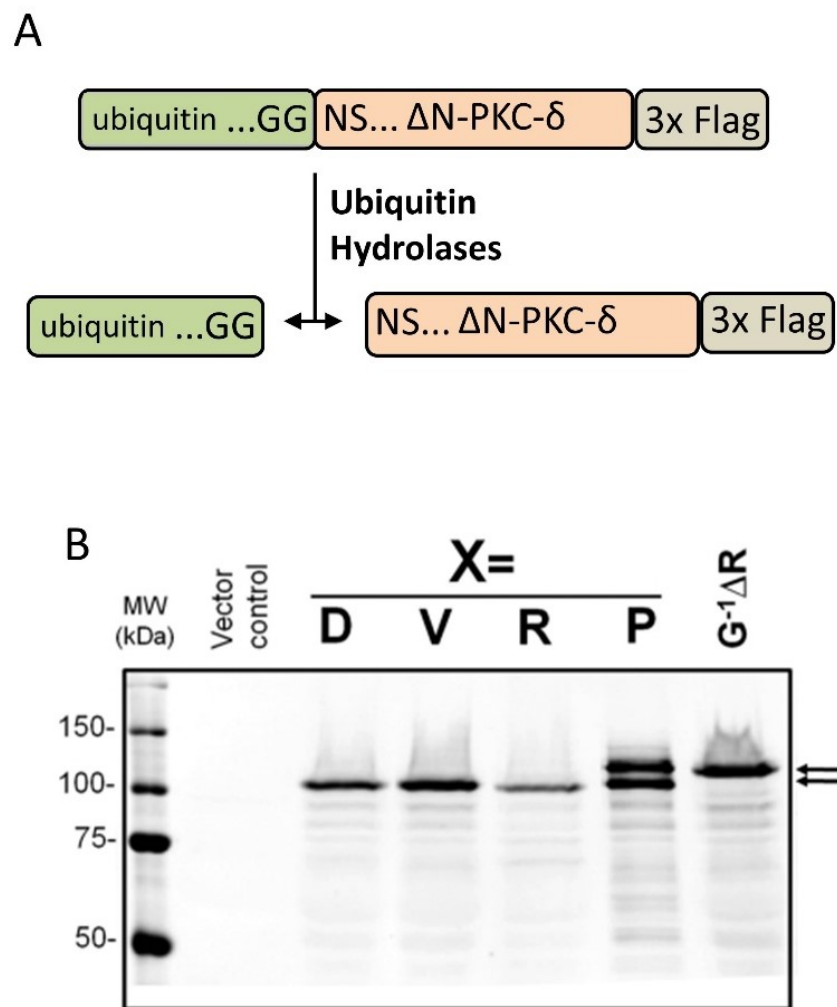


**Figure 3-2. Diagram of Ubiquitin Fusion Technique.**

**A.** Illustration of  $\Delta$ N-PKC $\delta$ -FLAG with the N-terminal fusion of ubiquitin. Followed by an endogenous ubiquitin hydrolase, allowing the exposure of the desired protein

fragment. **B.** Western Blot of different N-terminal BRCA1 protein fragment expressed by ubiquitin fusion technique. Proline (P) on the second last lane has doubled bands due to an inefficient cleavage by endogenous ubiquitin hydrolase. In the last lane, a mutation in C-terminal glycine of ubiquitin results in loss of hydrolase activity (shift in the size of protein band).

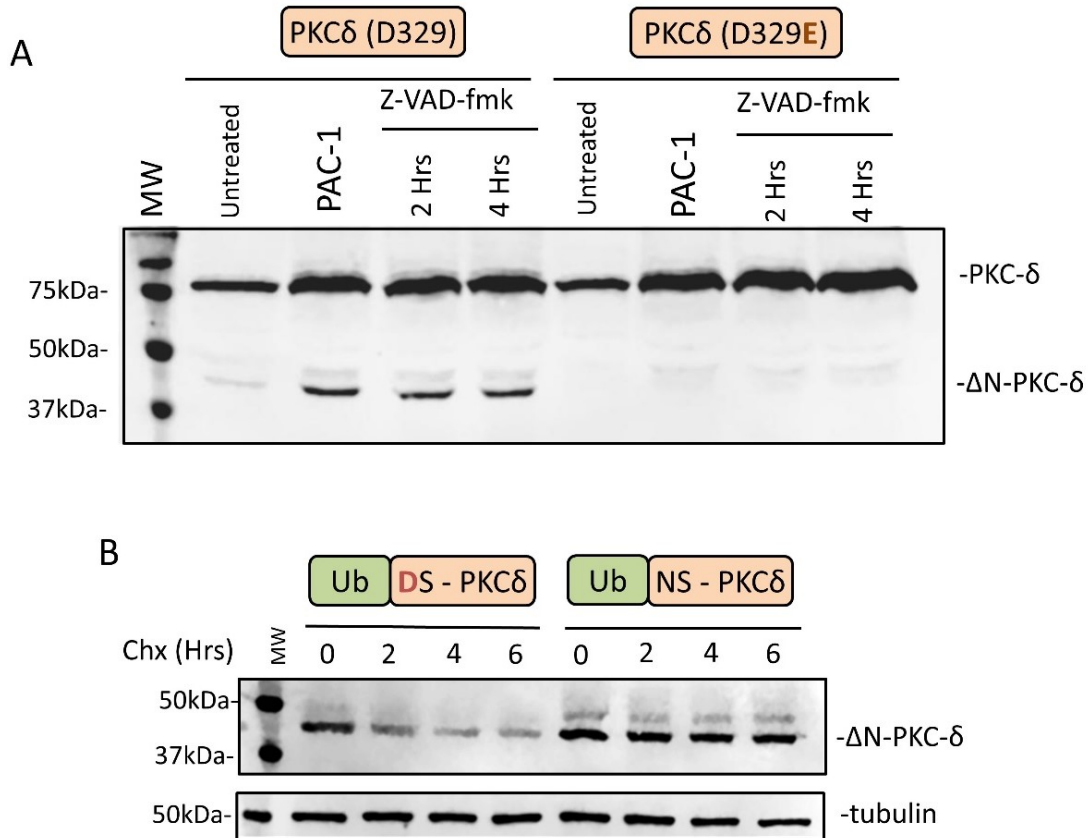


**Figure 3-3. PKCδ expression and C-terminal fragment stability.**

**A.** Protein expression of PKCδ and ΔN-PKCδ (fragment). First four lanes after the molecular weight shows wild type PKCδ, untreated, after PAC1 addition, and after 2 and 4 hours of Z-VAD-fmx treatment, respectively. The last four lanes show the mutated PKCδ (D329E), with the same treatment as the WT. **B.** Western blot of ΔN-PKCδ stability. First four lanes after MW shows the mutated Ub-DS-PKCδ degradation after CHX treatment, on the specific time points. On the right, it shows the WT Ub-NS-PKCδ after the same treatment and time course. Anti-body tubulin was used as a control.

Another unexpected outcome was observed after the wild-type NS-PKC $\delta$  cycloheximide treatment. The data shows that the cleaved fragment was stable even after six hours of CHX addition, despite the Asn residue being a well-known unstable N-terminal, **Figure 3-3.B**. Nevertheless, the DS-PKC $\delta$  mutant was degraded after CHX treatment as expected for a tertiary unstable N-termini. Since the Asp has the same recognition pathway as the Asn residue, the only difference being the activity of the NTAN1, it appears that the interaction between the Asn330 and the Nt-amidase has been disrupted.

This unforeseen outcome triggered further investigation, with a series of mutation in the  $\Delta$ N-PKC $\delta$  first and second position, **Figure 3-4.A to C**, to investigate the substrate stability. Applying the ubiquitin fusion method, it was shown that mutation of the N-terminal asparagine to aspartate resulted in protein degradation, as well as the mutation of the second amino acid to asparagine (N), threonine (T), alanine (A) and proline(P) derive in the  $\Delta$ N-PKC $\delta$  short half-life. Interestingly, the mutation of the serine (S) in the second position to glutamine (E) did not affect protein stability.

Although there is no clear relationship between these two residues (Ser and Glu), it is important to mention that the phosphorylated serine has a similar chemical configuration to the aspartic acid, both being negatively charged. The phosphorylation of Ser331, was already reported in previous phospho-proteomics study (Daub et al., 2008), and together with our findings suggests that the phosphorylation of the second position serine is implicated in the regulation of the PKC $\delta$  degradation after caspase cleavage resulting in the extended C-terminal fragment half-life.

This is not the first time our laboratory reports the phosphorylation as an essential player in the N-end Rule Pathway. It was previously demonstrated that the phosphorylation of the Try566 of BMX $\Delta$ N fragment inhibits its degradation through the N-end Rule Pathway (Eldeeb & Fahlman, 2016). It revealed an increased complexity of signalling networks and showed that phosphorylation could also regulate the outcome of some caspase products (Eldeeb & Fahlman, 2016; Lu, Lee, Xiang, Finniss, & Brodie, 2007).

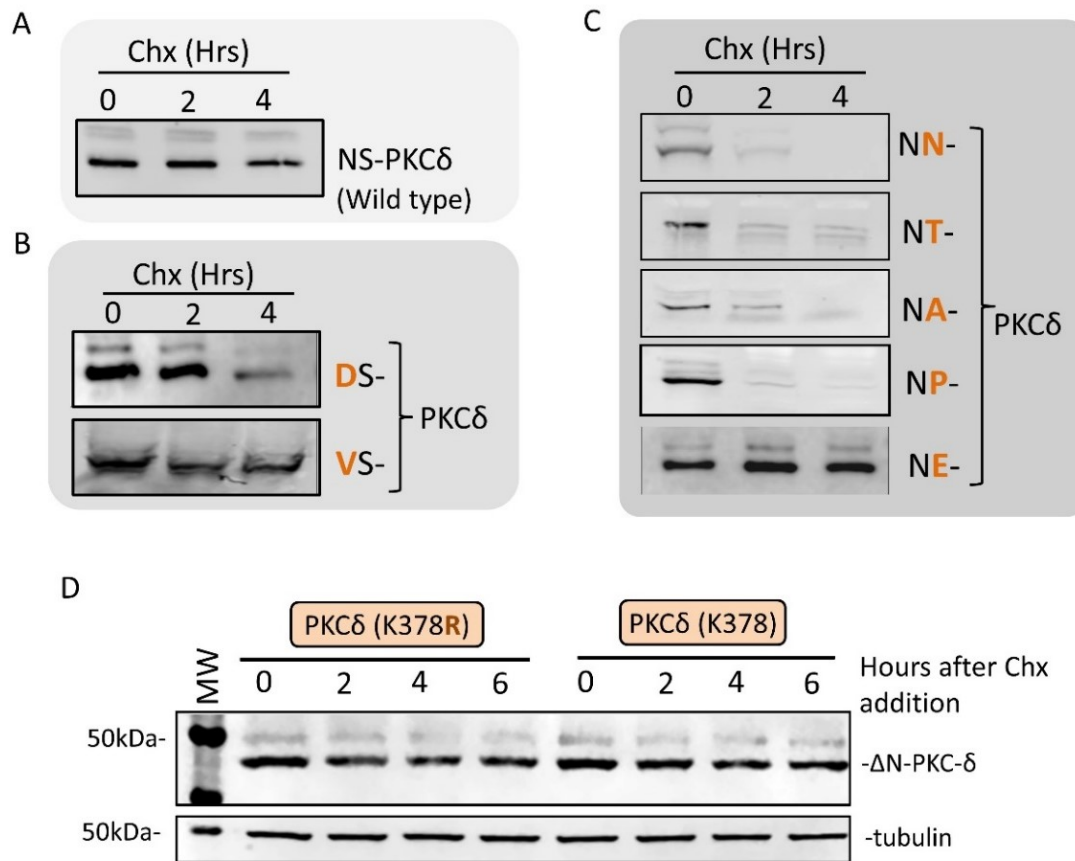


**Figure 3-4. Stability of  $\Delta$ N-PKC $\delta$  fragment after serial mutation.**

**A.** WT PKC $\delta$  fragment protein expression after CHX treatment, lysate was collected after 0, 2, and 4 hours. **B.** Shows the protein stability of two  $\Delta$ N-PKC $\delta$  mutant (DS-PKC $\delta$ , and VS-PKC $\delta$ ). Mutation were performed on the first N-terminal amino acid, N330D (unstable residue) and N330V (stable residue). Same procedure as in A. **C.**

Protein stability after second position mutation on the  $\Delta$ N-PKC $\delta$  fragment, S331N, S331T, S331A, S331P, and S331E. Same procedure as in A. **D.** Western blot of transfected cells with WT PKC $\delta$  (on the right) and mutant PKC $\delta$  (K378R) after 0,2,4, and six hours of CHX treatment. This mutation interferes on the kinase domain activity.

The Lys378 is part of the conserved PKC $\delta$  AxK motif, and has been previously reported in the regulation of the enzyme activity (Gong, Park, & Steinberg, 2017) Although there is no clear relationship between these two residues, it is important to mention that the phosphorylated serine has a similar chemical configuration to the E, both being negatively charged. The phosphorylation of Ser331, was already reported in previous phospho-proteomics study (Daub et al., 2008), and together with our findings suggests that the phosphorylation of the second position serine is implicated in the regulation of the PKC $\delta$  degradation after caspase cleavage resulting in the extended C-terminal fragment half-life.

### **1.3.1 PKC $\delta$ phosphorylation and its implication on protein degradation**

The PKC $\delta$  tyrosine phosphorylation has a critical role in the substrate activity, localization and its binding affinity (Kronfeld et al., 2000; Steinberg, 2004). The tyrosine phosphorylation of the catalytic domain improves the PKC $\delta$  activity, where the tyrosine phosphorylation in the regulatory domain impacts the cellular actions instead of the catalytic competence (Steinberg, 2008; Yang, Q. et al., 2019). An example is the Tyr313 site, that is implicated in redox-dependent changes in the substrate activity and Tyr334, a regulator of PKC $\delta$  fragment



catalytic activity (Gong et al., 2017). Other PKC $\delta$  tyrosine residues undergo into phosphorylation on different sites such as Tyr187 (Blass et al., 2002), Try155 (Okhrimenko et al., 2005), Try311 (Kajimoto et al., 2004), Tyr332 (Lu et al., 2007), Tyr512 (Kaul et al., 2005; Konishi et al., 1997), as a response of diverse apoptotic stimuli.

The scope of phosphorylation sites has been amplified by a phospho-proteomics study (Daub et al., 2008) that revealed other PKC $\delta$  phosphorylation sites at Ser331, Ser506, Ser647, Ser658, and Ser664. The phosphorylation of Ser331 is particularly meaningful to this study, as this finding supports the post-translation modification (PTM) on the second position residue of the C-terminal fragment and leading to proteasome degradation. So far, little is known about the Ser331 phosphorylation, or even if it is auto-phosphorylated by the kinase domain.

In order to identify if the PTM of Ser331 occurs through autophosphorylation, the PKC $\delta$  kinase domain was inactivated through mutation of the Lys378 (K) to an Arginine (R). HEK cells were transfected with the WT and mutated plasmid, then treated with CHX at specific time points, **Figure 3-4.D**. The results show that independent of the kinase activity, no change was observed on the stability of the  $\Delta$ N-PKC $\delta$  fragment, where the mutant was stable likewise the WT. These findings demonstrate that the autophosphorylation is not involved in the PTM of Ser331. Nevertheless, further investigation is required to identify what is the mechanism involved on the Ser331 phosphorylation and in which point of the caspase activation it might occur.

## 2. The second residue and the implication on N-termini recognition

Previous studies have shown the importance of the second residue to the N-end rule pathway substrate recognition by an E3 ligase (Choi et al., 2010; Matta-Camacho, Kozlov, Li, & Gehring, 2010; Muñoz-Escobar, Matta-Camacho, Cho, Kozlov, & Gehring, 2017a; Sriram et al., 2013). It has been observed that the UBR1, an E3 ubiquitin enzyme, recognizes the N-terminal through two different pockets (Muñoz-Escobar, Matta-Camacho, Cho, Kozlov, & Gehring, 2017b). The first residue is identified by the negative pocket, whereas the second residue accommodates in a hydrophobic groove, also known as the UBR1 secondary pocket. The disruption of the hydrogen bond with the second residue is enough to abolish binding, revealing the highest affinities for hydrophobic residues in the second position (Muñoz-Escobar et al., 2017a).

Surprisingly, the data shows for the first time, that the second position residue also plays an important role in the Nt-amidase substrate recognition. As previously mentioned, the electrically charged amino acids may disrupt the binding affinity to the N-end Rule enzymes, resulting in the endogenous regulation of the proteasome degradation. That would explain why the PKC $\delta$  fragment is stable even with an unstable N-terminal, asparagine. The hydrophilic phosphorylated Ser331 seems to disrupt the substrate binding to the Nt-amidase which inhibits the ubiquitination of the PKC $\delta$  fragment and subsequent protein degradation. The data presented in this study reveals that the mutation of the second position residue into an amino acid with no hydrophilic characteristics, enable the binding affinity to be reestablished.

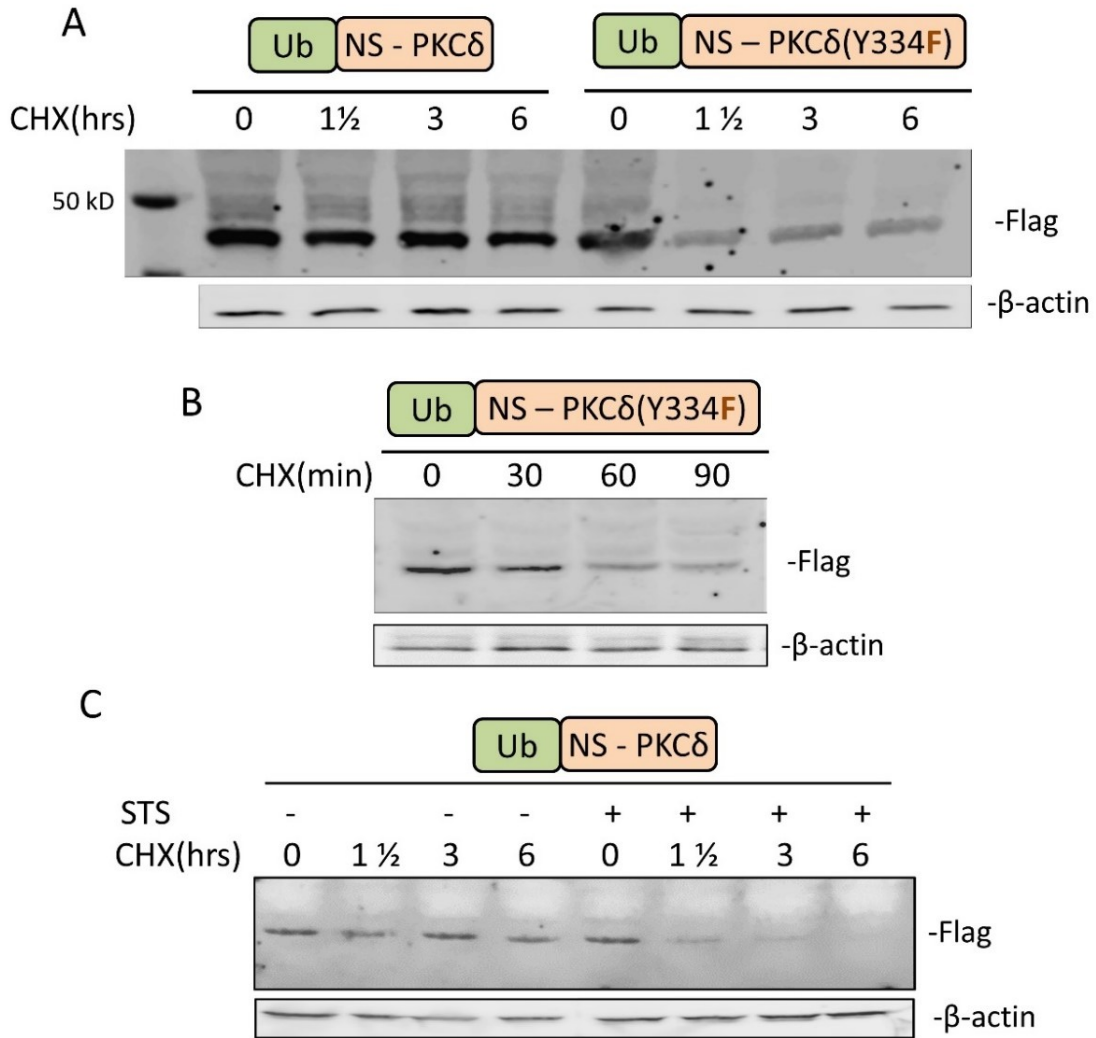


**Figure 3-5.  $\Delta$ N-PKC $\delta$  Stability after Tyr334 mutation.**

**A.** Western blot of Ub-NS-PKC $\delta$  WT and mutant (Y334F), after CHX treatment. Anti-flag antibody shows the protein abundance overtime.  $\beta$ -actin antibody is used as a control. **B.** Western blot of Ub-NS-PKC $\delta$  mutant (Y334F) after 0, 30, 60, and 90 minutes of CHX treatment. Same as in A. **C.** The Ub-NS-PKC $\delta$  WT treated with 1  $\mu$ M of Staurosporine (STS).  $\beta$ -actin antibody is used as a control.

## 2.1 The phosphorylation of internal tyrosine

The investigation of  $\Delta$ N-PKC $\delta$  stability after Staurosporine (STS) treatment, **Figure 3-5.C**, demonstrated that the inhibition of PKC $\delta$  phosphorylation resulted

in early protein degradation. The STS is a potent PKC inhibitor, although, with low selectivity (Roffey et al., 2009), it prevents phosphorylation and the appearance of the more slowly migrating phosphorylated PKC isoforms (Kiley, Parker, Fabbro, & Jaken, 1992). The data showed that after ninety (90) minutes after CHX treatment, the STS treated cells had a significant decrease of PKC $\delta$  fragment abundance, **Figure 3-5.C**.

While no kinase has been attributed to the Ser331 phosphorylation of PKC $\delta$  the nearby Tyr334 SRC target was investigated as there is a possibility that these phosphorylation sites are correlated. As such the data showed a correlation between the Tyr334 phosphorylation and protein degradation, potentially due to this phosphorylation being required prior to the Ser331 phosphorylation. PKC $\delta$  WT (Ub-NS-PKC $\delta$ ) and mutant (Ub-NS-PKC $\delta$  (Y334F)) were transfected in HEK cells and treated with CHX for the specified time points, **Figure 3-5.A and B**.

The results revealed a change in the abundance of  $\Delta$ N-PKC $\delta$  fragment over time only in the Ub-NS-PKC $\delta$  (Y334F) mutant at thirty (30) minutes whereas no significant difference was observed on the WT substrate in six (6) hours. It appears that without the Tyr334 phosphorylation the Ser331 phosphorylation is affected, and the unphosphorylated Ser331 is now recognized by the E3 ligase, resulting in the decrease of the  $\Delta$ N-PKC $\delta$  fragment abundance, and consequently its half-life. This brings a new model where Tyr334 needs to be phosphorylated before Ser331 is phosphorylated.

Although these finds present some limitations, we can assume that there is a strong relationship between the phosphorylation of Serine on the N-termini second position and the N-end Rule Pathway. Moreover, additional investigation is needed to better identify the mechanism of interaction and how do these findings apply to different substrates.

## References

- Benes, C. H., Wu, N., Elia, A. E., Dharia, T., Cantley, L. C., & Soltoff, S. P. (2005). The C2 domain of PKCdelta is a phosphotyrosine binding domain. *Cell*, *121*(2), 271-280. doi:S0092-8674(05)00164-9 [pii]
- Billecke, C., Finniss, S., Tahash, L., Miller, C., Mikkelsen, T., Farrell, N. P., & Bogler, O. (2006). Polynuclear platinum anticancer drugs are more potent than cisplatin and induce cell cycle arrest in glioma. *Neuro-Oncology*, *8*(3), 215-226. doi:15228517-2006-004 [pii]
- Blass, M., Kronfeld, I., Kazimirsky, G., Blumberg, P. M., & Brodie, C. (2002). Tyrosine phosphorylation of protein kinase cδ is essential for its apoptotic effect in response to etoposide. *Molecular and Cellular Biology*, *22*(1), 182-195.
- Chen, J., Lin, H. H., Kim, K., Lin, A., Ou, J. J., & Ann, D. K. (2009). PKCδ signaling: A dual role in regulating hypoxic stress-induced autophagy and apoptosis. *Autophagy*, *5*(2), 244-246.
- Chen, L., Hahn, H., Wu, G., Chen, C., Liron, T., Schechtman, D., . . . Bolli, R. (2001). Opposing cardioprotective actions and parallel hypertrophic effects of δPKC and εPKC. *Proceedings of the National Academy of Sciences*, *98*(20), 11114-11119.
- Cheng, N., He, R., Tian, J., Dinauer, M. C., & Ye, R. D. (2007). A critical role of protein kinase C delta activation loop phosphorylation in formyl-methionyl-leucyl-phenylalanine-induced phosphorylation of p47(phox) and rapid activation of nicotinamide adenine dinucleotide phosphate oxidase. *Journal of*

*Immunology (Baltimore, Md.: 1950)*, 179(11), 7720-7728. doi:179/11/7720  
[pii]

Cho, W., & Stahelin, R. V. (2006). Membrane binding and subcellular targeting of C2 domains. *Biochimica Et Biophysica Acta (BBA)-Molecular and Cell Biology of Lipids*, 1761(8), 838-849.

Choi, W. S., Jeong, B., Joo, Y. J., Lee, M., Kim, J., Eck, M. J., & Song, H. K. (2010). Structural basis for the recognition of N-end rule substrates by the UBR box of ubiquitin ligases. *Nature Structural & Molecular Biology*, 17(10), 1175.

Cross, T., Griffiths, G., Deacon, E., Sallis, R., Gough, M., Watters, D., & Lord, J. M. (2000). PKC- $\delta$  is an apoptotic lamin kinase. *Oncogene*, 19(19), 2331.

Daub, H., Olsen, J. V., Bairlein, M., Gnad, F., Oppermann, F. S., Körner, R., . . . Mann, M. (2008). Kinase-selective enrichment enables quantitative phosphoproteomics of the kinome across the cell cycle. *Molecular Cell*, 31(3), 438-448.

Denning, M. F., Wang, Y., Tibudan, S., Alkan, S., Nickoloff, B. J., & Qin, J. Z. (2002). Caspase activation and disruption of mitochondrial membrane potential during UV radiation-induced apoptosis of human keratinocytes requires activation of protein kinase C. *Cell Death and Differentiation*, 9(1), 40-52. doi:10.1038/sj.cdd.4400929 [doi]

DeVries, T. A., Neville, M. C., & Reyland, M. E. (2002). Nuclear import of PKC $\delta$  is required for apoptosis: Identification of a novel nuclear import sequence. *The EMBO Journal*, 21(22), 6050-6060.

- DeVries-Seimon, T. A., Ohm, A. M., Humphries, M. J., & Reyland, M. E. (2007). Induction of apoptosis is driven by nuclear retention of protein kinase c $\delta$ . *Journal of Biological Chemistry*, 282(31), 22307-22314.
- Durrant, D., Liu, J., Yang, H., & Lee, R. M. (2004). The bortezomib-induced mitochondrial damage is mediated by accumulation of active protein kinase C- $\delta$ . *Biochemical and Biophysical Research Communications*, 321(4), 905-908.
- Dutil, E. M., Toker, A., & Newton, A. C. (2031). Regulation of conventional protein kinase C isozymes by phosphoinositide-dependent kinase 1 (PDK-1). *Current Biology : CB*, 8(25), 1366-1375. doi:S0960-9822(98)00017-7 [pii]
- Eldeeb, M. A., & Fahlman, R. P. (2016). Phosphorylation impacts N-end rule degradation of the proteolytically activated form of BMX kinase. *Journal of Biological Chemistry*, 291(43), 22757-22768.
- Gallegos, L. L., & Newton, A. C. (2008). Spatiotemporal dynamics of lipid signaling: Protein kinase C as a paradigm. *IUBMB Life*, 60(12), 782-789.
- Gong, J., Park, M., & Steinberg, S. F. (2017). Cleavage alters the molecular determinants of protein kinase C- $\delta$  catalytic activity. *Molecular and Cellular Biology*, 37(20), 324.
- Hahn, H. S., Yussman, M. G., Toyokawa, T., Marreez, Y., Barrett, T. J., Hilty, K. C., . . . Dorn, G. W. (2002). Ischemic protection and myofibrillar cardiomyopathy: Dose-dependent effects of in vivo  $\delta$ PKC inhibition. *Circulation Research*, 91(8), 741-748.

- Humphries, M. J., Ohm, A. M., Schaack, J., Adwan, T. S., & Reyland, M. E. (2008). Tyrosine phosphorylation regulates nuclear translocation of PKC $\delta$ . *Oncogene*, 27(21), 3045.
- Hurley, J. H., Newton, A. C., Parker, P. J., Blumberg, P. M., & Nishizuka, Y. (1997). Taxonomy and function of C1 protein kinase C homology domains. *Protein Science*, 6(2), 477-480.
- Igumenova, T. I. (2015). Dynamics and membrane interactions of protein kinase C. *Biochemistry*, 54(32), 4953-4968.
- Inagaki, K., Chen, L., Ikeno, F., Lee, F. H., Imahashi, K., Bouley, D. M., . . . Mochly-Rosen, D. (2003). Inhibition of  $\delta$ -protein kinase C protects against reperfusion injury of the ischemic heart in vivo. *Circulation*, 108(19), 2304-2307.
- Jackson, D. N., & FOSTER, D. A. (2004). The enigmatic protein kinase c $\delta$ : Complex roles in cell proliferation and survival. *The FASEB Journal*, 18(6), 627-636.
- Kajimoto, T., Shirai, Y., Sakai, N., Yamamoto, T., Matsuzaki, H., Kikkawa, U., & Saito, N. (2004). Ceramide-induced apoptosis by translocation, phosphorylation, and activation of protein kinase c $\delta$  in the golgi complex. *Journal of Biological Chemistry*, 279(13), 12668-12676.
- Kao, S., Wang, W., Chen, C., Chang, Y., Wu, Y., Wang, Y., . . . Hong, T. (2015). Analysis of protein stability by the cycloheximide chase assay. *Bio-Protocol*, 5(1)



- Kaul, S., Anantharam, V., Yang, Y., Choi, C. J., Kanthasamy, A., & Kanthasamy, A. G. (2005). Tyrosine phosphorylation regulates the proteolytic activation of protein kinase c $\delta$  in dopaminergic neuronal cells. *Journal of Biological Chemistry*, 280(31), 28721-28730.
- Keranen, L. M., Dutil, E. M., & Newton, A. C. (1995). Protein kinase C is regulated in vivo by three functionally distinct phosphorylations. *Current Biology : CB*, 5(12), 1394-1403. doi:S0960-9822(95)00277-6 [pii]
- Kikkawa, U., Matsuzaki, H., & Yamamoto, T. (2002). Protein kinase c $\delta$  (PKC $\delta$ ): Activation mechanisms and functions. *The Journal of Biochemistry*, 132(6), 831-839.
- Kiley, S. C., Clark, K. J., Duddy, S. K., Welch, D. R., & Jaken, S. (1999). Increased protein kinase c $\delta$  in mammary tumor cells: Relationship to transformation and metastatic progression. *Oncogene*, 18(48), 6748.
- Kiley, S. C., Parker, P. J., Fabbro, D., & Jaken, S. (1992). Selective redistribution of protein kinase C isozymes by thapsigargin and staurosporine. *Carcinogenesis*, 13(11), 1997-2001.
- Konishi, H., Tanaka, M., Takemura, Y., Matsuzaki, H., Ono, Y., Kikkawa, U., & Nishizuka, Y. (1997). Activation of protein kinase C by tyrosine phosphorylation in response to H<sub>2</sub>O<sub>2</sub>. *Proceedings of the National Academy of Sciences*, 94(21), 11233-11237.
- Kronfeld, I., Kazimirsky, G., Lorenzo, P. S., Garfield, S. H., Blumberg, P. M., & Brodie, C. (2000). Phosphorylation of protein kinase c $\delta$  on distinct tyrosine

residues regulates specific cellular functions. *Journal of Biological Chemistry*, 275(45), 35491-35498.

Le Good, J. A., Ziegler, W. H., Parekh, D. B., Alessi, D. R., Cohen, P., & Parker, P. J. (1998). Protein kinase C isotypes controlled by phosphoinositide 3-kinase through the protein kinase PDK1. *Science*, 281(5385), 2042-2045.

Leibersperger, H., Gschwendt, M., Gernold, M., & Marks, F. (1991). Immunological demonstration of a calcium-unresponsive protein kinase C of the delta-type in different species and murine tissues. predominance in epidermis. *Journal of Biological Chemistry*, 266(22), 14778-14784.

Leitges, M., Mayr, M., Braun, U., Mayr, U., Li, C., Pfister, G., . . . Xu, Q. (2001). Exacerbated vein graft arteriosclerosis in protein kinase c $\delta$ -null mice. *The Journal of Clinical Investigation*, 108(10), 1505-1512.

Li, W., Zhang, J., Bottaro, D. P., Li, W., & Pierce, J. H. (1997). Identification of serine 643 of protein kinase C- $\delta$  as an important autophosphorylation site for its enzymatic activity. *Journal of Biological Chemistry*, 272(39), 24550-24555.

Liu, Y., Belkina, N. V., Graham, C., & Shaw, S. (2006). Independence of protein kinase C- $\delta$  activity from activation loop phosphorylation structural basis and altered functions in cells. *Journal of Biological Chemistry*, 281(17), 12102-12111.

Lu, W., Lee, H., Xiang, C., Finniss, S., & Brodie, C. (2007). The phosphorylation of tyrosine 332 is necessary for the caspase 3-dependent cleavage of PKC $\delta$  and the regulation of cell apoptosis. *Cellular Signalling*, 19(10), 2165-2173.

- Malavez, Y., Gonzalez-Mejia, M. E., & Doseff, A. I. (2009). PRKCD (protein kinase C, delta). *Atlas of Genetics and Cytogenetics in Oncology and Haematology*,
- Matta-Camacho, E., Kozlov, G., Li, F. F., & Gehring, K. (2010). Structural basis of substrate recognition and specificity in the N-end rule pathway. *Nature Structural and Molecular Biology*, *17*(10), 1182.
- Mayr, M., Metzler, B., Chung, Y., McGregor, E., Mayr, U., Troy, H., . . . Griffiths, J. R. (2004). Ischemic preconditioning exaggerates cardiac damage in PKC- $\delta$  null mice. *American Journal of Physiology-Heart and Circulatory Physiology*, *287*(2), H956.
- Mecklenbräuker, I., Saijo, K., Zheng, N., Leitges, M., & Tarakhovsky, A. (2002). Protein kinase  $\delta$  controls self-antigen-induced B-cell tolerance. *Nature*, *416*(6883), 860.
- Morales, K. A., Lasagna, M., Gribenko, A. V., Yoon, Y., Reinhart, G. D., Lee, J. C., . . . Igumenova, T. I. (2011). Pb<sup>2+</sup> as modulator of protein-membrane interactions. *Journal of the American Chemical Society*, *133*(27), 10599-10611. doi:10.1021/ja2032772 [doi]
- Muñoz-Escobar, J., Matta-Camacho, E., Cho, C., Kozlov, G., & Gehring, K. (2017a). Bound waters mediate binding of diverse substrates to a ubiquitin ligase. *Structure*, *25*(5), 729. e3.
- Muñoz-Escobar, J., Matta-Camacho, E., Cho, C., Kozlov, G., & Gehring, K. (2017b). Bound waters mediate binding of diverse substrates to a ubiquitin ligase. *Structure*, *25*(5), 729. e3.

- Murray, D., & Honig, B. (2002). Electrostatic control of the membrane targeting of C2 domains. *Molecular Cell*, 9(1), 145-154. doi:S1097-2765(01)00426-9 [pii]
- Newton, A. C. (2001). Protein kinase C: Structural and spatial regulation by phosphorylation, cofactors, and macromolecular interactions. *Chemical Reviews*, 101(8), 2353-2364.
- Okhrimenko, H., Lu, W., Xiang, C., Ju, D., Blumberg, P. M., Gomel, R., . . . Brodie, C. (2005). Roles of tyrosine phosphorylation and cleavage of protein kinase cδ in its protective effect against tumor necrosis factor-related apoptosis inducing ligand-induced apoptosis. *Journal of Biological Chemistry*, 280(25), 23643-23652.
- Page, K., Li, J., Zhou, L., Iasvoyskaia, S., Corbit, K. C., Soh, J., . . . Hershenson, M. B. (2003). Regulation of airway epithelial cell NF-κB-dependent gene expression by protein kinase cδ. *The Journal of Immunology*, 170(11), 5681-5689.
- Parekh, D. B., Ziegler, W., & Parker, P. J. (2000). Multiple pathways control protein kinase C phosphorylation. *The EMBO Journal*, 19(4), 496-503.
- Park, I. C., Park, M. J., Hwang, C. S., Rhee, C. H., Whang, D. Y., Jang, J. J., . . . Lee, S. H. (2000). Mitomycin C induces apoptosis in a caspases-dependent and fas/CD95-independent manner in human gastric adenocarcinoma cells. *Cancer Letters*, 158(2), 125-132. doi:S0304383500004894 [pii]
- Persaud, S. D., Hoang, V., Huang, J., & Basu, A. (2005). Involvement of proteolytic activation of PKCdelta in cisplatin-induced apoptosis in human

small cell lung cancer H69 cells. *International Journal of Oncology*, 27(1), 149-154.

Qi, X., & Mochly-Rosen, D. (2008). The PKC $\delta$ -abl complex communicates ER stress to the mitochondria—an essential step in subsequent apoptosis. *J Cell Sci*, 121(6), 804-813.

Ren, J., Datta, R., Shioya, H., Li, Y., Oki, E., Biedermann, V., . . . Kufe, D. (2002). p73 $\beta$  is regulated by protein kinase c $\delta$  catalytic fragment generated in the apoptotic response to DNA damage. *Journal of Biological Chemistry*, 277(37), 33758-33765.

Reyland, M. E. (2007). No title. *Protein Kinase C $\delta$  and Apoptosis*,

Reyland, M. E., Anderson, S. M., Matassa, A. A., Barzen, K. A., & Quissell, D. O. (1999). Protein kinase C  $\delta$  is essential for etoposide-induced apoptosis in salivary gland acinar cells. *Journal of Biological Chemistry*, 274(27), 19115-19123.

Roffey, J., Rosse, C., Linch, M., Hibbert, A., McDonald, N. Q., & Parker, P. J. (2009). Protein kinase C intervention—the state of play. *Current Opinion in Cell Biology*, 21(2), 268-279.

Rybin, V. O., Guo, J., Sabri, A., Elouardighi, H., Schaefer, E., & Steinberg, S. F. (2004). Stimulus-specific differences in protein kinase c $\delta$  localization and activation mechanisms in cardiomyocytes. *Journal of Biological Chemistry*, 279(18), 19350-19361.

- Rybin, V. O., Xu, X., & Steinberg, S. F. (1999). Activated protein kinase C isoforms target to cardiomyocyte caveolae: Stimulation of local protein phosphorylation. *Circulation Research*, *84*(9), 980-988.
- Safran, M., Chalifa-Caspi, V., Shmueli, O., Olender, T., Lapidot, M., Rosen, N., . . . Feldmesser, E. (2003). Human gene-centric databases at the weizmann institute of science: GeneCards, UDB, CroW 21 and HORDE. *Nucleic Acids Research*, *31*(1), 142-146.
- Shao, X., Davletov, B. A., Sutton, R. B., Südhof, T. C., & Rizo, J. (1996). Bipartite Ca<sup>2+</sup>-binding motif in C2 domains of synaptotagmin and protein kinase C. *Science*, *273*(5272), 248-251.
- Singh, R. K., Kumar, S., Gautam, P. K., Tomar, M. S., Verma, P. K., Singh, S. P., & Acharya, A. (2017). Protein kinase C- $\alpha$  and the regulation of diverse cell responses. *Biomolecular Concepts*, *8*(3-4), 143-153.
- Sriram, S., Lee, J. H., Mai, B. K., Jiang, Y., Kim, Y., Yoo, Y. D., . . . Lee, M. J. (2013). Development and characterization of monomeric N-end rule inhibitors through in vitro model substrates. *Journal of Medicinal Chemistry*, *56*(6), 2540-2546.
- Stahelin, R. V., Kong, K. F., Raha, S., Tian, W., Melowic, H. R., Ward, K. E., . . . Cho, W. (2012). Protein kinase ctheta C2 domain is a phosphotyrosine binding module that plays a key role in its activation. *The Journal of Biological Chemistry*, *287*(36), 30518-30528. doi:10.1074/jbc.M112.391557 [doi]

- Steinberg, S. F. (2004). Distinctive activation mechanisms and functions for protein kinase c $\delta$ . *Biochemical Journal*, 384(3), 449-459.
- Steinberg, S. F. (2008). Structural basis of protein kinase C isoform function. *Physiological Reviews*, 88(4), 1341-1378.
- Stempka, L., Girod, A., Müller, H., Rincke, G., Marks, F., Gschwendt, M., & Bossemeyer, D. (1997). Phosphorylation of protein kinase c $\delta$  (PKC $\delta$ ) at threonine 505 is not a prerequisite for enzymatic activity EXPRESSION OF RAT PKC $\delta$  AND AN ALANINE 505 MUTANT IN BACTERIA IN A FUNCTIONAL FORM. *Journal of Biological Chemistry*, 272(10), 6805-6811.
- Stempka, L., Schnölzer, M., Radke, S., Rincke, G., Marks, F., & Gschwendt, M. (1999). Requirements of protein kinase c $\delta$  for catalytic function ROLE OF GLUTAMIC ACID 500 AND AUTOPHOSPHORYLATION ON SERINE 643. *Journal of Biological Chemistry*, 274(13), 8886-8892.
- Sun, S., Wu, Q., Song, J., & Sun, S. (2018). Protein kinase C  $\delta$ -dependent regulation of ubiquitin-proteasome system function in breast cancer. *Cancer Biomarkers*, 21(1), 1-9.
- Verdaguer, N., Corbalan-Garcia, S., Ochoa, W. F., Fita, I., & Gómez-Fernández, J. C. (1999). Ca<sup>2+</sup> bridges the C2 membrane-binding domain of protein kinase c $\alpha$  directly to phosphatidylserine. *The EMBO Journal*, 18(22), 6329-6338.
- Xu, Z., Payoe, R., & Fahlman, R. P. (2012). The C-terminal proteolytic fragment of the breast cancer susceptibility type 1 protein (BRCA1) is degraded by the N-end rule pathway. *Journal of Biological Chemistry*, 287(10), 7495-7502.

- Yang, Q., Langston, J. C., Tang, Y., Kiani, M. F., & Kilpatrick, L. E. (2019). The role of tyrosine phosphorylation of protein kinase C delta in infection and inflammation. *International Journal of Molecular Sciences*, *20*(6), 1498.
- Yang, Y., Shu, C., Li, P., & Igumenova, T. I. (2018). Structural basis of protein kinase  $\alpha$  regulation by the C-terminal tail. *Biophysical Journal*, *114*(7), 1590-1603.
- Zhao, M., Xia, L., & Chen, G. (2012). Protein kinase  $\delta$  in apoptosis: A brief overview. *Archivum Immunologiae Et Therapiae Experimentalis*, *60*(5), 361-372.
- Ziegler, W. H., Parekh, D. B., Le Good, J. A., WHeLan, R., Kelly, J. J., Frech, M., . . . Parker, P. J. (1999). Rapamycin-sensitive phosphorylation of PKC on a carboxy-terminal site by an atypical PKC complex. *Current Biology*, *9*(10), 522-529.



CHAPTER 4 . SELECTIVE INHIBITION OF  
UBR1/UBR2 E3 LIGASE BY A SMALL  
MOLECULE

## 1. The identification of a selective N-end rule inhibitor

The investigation of E3 ligases as a potential therapeutic target has exponentially gained more interesting of academic and pharmaceutical research as these ubiquitin enzymes selectively stabilize cellular proteins. In theory, the inhibition of these enzymes would achieve a high level of specificity with less associated toxicity (Sun, 2003). As such, the E3 ubiquitin ligase UBR1 and UBR2 have been reported as having an essential role in neurogenesis (Ciechanover & Kwon, 2015; David et al., 2002), cardiogenesis (Lee, M. J. et al., 2012; Tasaki et al., 2005) and carcinogenesis (Lee, J. H., Jiang, Kwon, & Lee, 2015a; Varshavsky, 2011). In the present days, only a few chemicals have been used to target the N-end Rule Pathway. The inhibitors available are the dipeptides (e.g. arg-ala, phe-ala, lys-ala)(Baker & Varshavsky, 1991; Sriram et al., 2013), the synthetic heterovalent compounds (RF-C11) (Kwon, Lavy, & Varshavsky, 1999), and Phe-derived monomeric molecules (e.g. para-chloramphetamine – PCA) (Jiang et al., 2014; Lee, J. H. et al., 2015a). Some of the challenges that limits the use of this inhibitors are the high effective concentration required, its neurological side effects (Lee, J. H. et al., 2015a), the need of endopeptidase inhibitor for the dipeptide-base small molecules (Sriram et al., 2013), and the non-selectivity to type I or type II protein degradation.

To overcome the disadvantages of the currently available inhibitors, I have investigated small molecules with affinity to type I binding domain of the UBR1/2 E3 ubiquitin enzymes (Matta-Camacho, Kozlov, Li, & Gehring, 2010). The UBR-box domain, which is known for targeting type I protein degradation, has a vast number of substrates, including regulators of G proteins Rgs4, Rgs5, and Rgs16 (Hu et al., 2005; Lee, M. J. et al., 2005), caspase fragments products such as Arg-MYC

oncoprotein (Conacci-Sorrell, Ngouenet, & Eisenman, 2010), Cys-MDM2 (Chen, Marechal, Moreau, Levine, & Chen, 1997), Asn-PKC $\delta$  (Leverrier, Vallentin, & Joubert, 2002), Lys-PKC $\theta$  (Datta, Kojima, Yoshida, & Kufe, 1997), and pro-apoptotic substrates as Asp-BCL(XL), Arg-BID, and Arg-BIM(EL) (Lee, J. H., Jiang, Kwon, & Lee, 2015b; Piatkov, Brower, & Varshavsky, 2012). Thus, the inhibition of the UBR-box domain could be used as a potential drug treatment in several infirmities.

As an example of therapeutical application of the N-end Rule inhibitor is the increase of the pro-apoptotic signalling cascade and reduction of the cellular resistance to apoptosis-inducing drugs, as in cancer chemotherapeutical treatment. The combination of a proteasome inhibitor with chemotherapy have been successfully reported in different types of cancers, such as lung cancer (Sooman et al., 2017), esophageal squamous cell carcinoma (Dang et al., 2014), and pediatric Hodgkin lymphoma (Horton et al., 2015). The studies shows that the drug combination treatment have synergistic effects *in vitro* (Sooman et al., 2017), and that the combined treatment is safe for cancer patients (Horton et al., 2015).

Another possible use for the N-end Rule inhibitor is to become a cancer therapy by itself as an upstream proteasome inhibitor. Nowadays, this class of inhibitors, such as Bortezomib (BTZ) and Carfilzomib (CFZ), are already being used in the clinical treatment of Multiple Myeloma (MM) and Mantle Cell Lymphoma (MCL) (Manasanch & Orlowski, 2017; Papanagnou et al., 2018). Although, the MM is still incurable and treated patients usually become refractory to therapeutic proteasome inhibitors, which also exert several adverse effects (Cavaletti et al., 2010; Richardson et al., 2006), the investigation and development of a target-specific treatment upstream the proteasome degradation could lead to lower cytotoxicity to normal cells versus cancer cells.

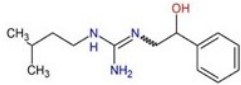
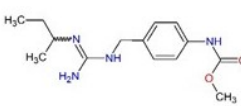
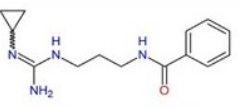
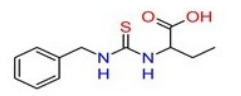
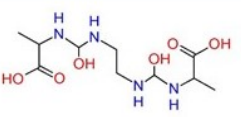
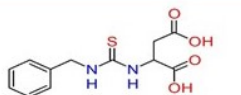
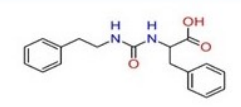
## 1.1 Chemical compounds with binding affinity with UBR-box domain

With the complexity of the organization of functional UBR domain being present on four proteins with divergent alternative functions, we have focused our efforts on the identification of a novel inhibitor targeting the UBR domain. We have focused on the UBR domain instead of the N-domain as a result of available structures for the UBR domains of human UBR1 and UBR2 proteins (Matta-Camacho et al., 2010; Muñoz-Escobar, Matta-Camacho, Cho, Kozlov, & Gehring, 2017) and due the protein with Type I N-termini exhibit significantly faster rates of degradation than those with Type II termini (Bachmair, Finley, & Varshavsky, 1986), suggesting these proteins are required to be more rapidly degraded in the cell.

In collaboration with Dr. Tuszynski laboratory, we were able to identify small molecule inhibitors by molecular docking using *in silico* screening of over 35 million compounds in the ZINC database (Sterling & Irwin, 2015). This technique allowed us to identify potential small molecules commercially available that could bind to the UBR domain. The structure of the UBR domain of UBR1 was initially minimized using forcefield Amber 10: EHT of the Molecular Operating Environment software (Molecular Operating Environment (MOE), 2013) and partial charges were added prior to minimization of the structure. This was a blind docking simulation where entire structure was explored for the determination of possible binding sites. Top ten compounds with the highest binding affinity to the UBR-box domain were selected, from those, only seven chemicals were commercially available for further investigation, **Table 4-1**.

**Table 4-1. Chemical compounds selected through in silico docking.**

The seven chemical compounds tested and the respective structure, empirical formula, chemical name and molecular weight available through the Vitas lab.

	Structure	Empirical Formula	Chemical Name	Molecular Weight
A		C14H24IN3O	2-(2-hydroxy-2-phenylethyl)-1-(3-methylbutyl)guanidine hydroiodide	377.26
B		C14H23IN4O2	methyl N-{4-[2-(butan-2-yl)carbamimidamidomethyl]phenyl}carbamate hydroiodide	406.26
C		C14H21BrN4O	N-[3-(2-cyclopropylcarbamimidamido)propyl]benzamide hydrobromide	341.24
D		C12H16N2O2S	2-[(benzylcarbamothioyl)amino]butanoic acid	252.34
E		C10H18N4O6	2,11-dimethyl-4,9-dioxo-3,5,8,10-tetraazadodecane-1,12-dioic acid (non-preferred name)	290.28
F		C12H14N2O4S	N-(benzylcarbamothioyl)aspartic acid	282.32
PPCP		C16H20N2O3	3-phenyl-2-[[9(2-phenylethyl)carbamoyl]amino]propanoic acid	288.34

We therefore performed in vivo analysis in HeLa cells to identify the inhibitory activity of the selected compounds, **Figure 4-1.A**. Although two of them demonstrated some inhibitory activity, the 3-phenyl-2-[[9(2-phenylethyl)carbamoyl]amino]propanoic acid, PPCP, showed a consistent result in prolonging

the protein metabolic stability of type I destabilizing amino acid, **Figure 4-1. B to D.**

This molecule consists of two benzene rings connected by an amino parent chain, with a carboxylate group attached at the second carbon and a carbonyl atom on the third carbon of the parent chain. To screen against non-specific effects of compounds that may inhibit down-stream steps of protein degradation, the compounds were also investigated in assays for the degradation of the same reporter protein, but with a Type II N-termini. As observed in **Figure 4-2.A**, inhibition was specific for Type I substrate degradation.

## 1.2 Small molecule affects type I N-terminal protein stability

Following the identification of the PPCP inhibitory activity, I analyzed the half-life of type I and type II destabilizing N-terminal amino acids with and without the addition of PPCP. The expression of the fragments was achieved by the ubiquitin fusion technique where the N-terminal of X-Lyn $\Delta$ N and X-PKC $\delta$  $\Delta$ N were fused to the ubiquitin moiety, and their C-terminal were combined with a 3 X FLAG tag for detection purpose (Ub-X-Lyn $\Delta$ N-FLAG and Ub-X-PKC $\delta$  $\Delta$ N-FLAG).

In **Figure 4-2.A and B**, both a type I and a type II substrates were tested to evaluate the inhibitor specificity. If the compound inhibited the proteasome or another downstream target of N-End rule degradation both substrates would have the degradation inhibited. As predicted by the *in silico* analysis, the results show type I substrate N-end Rule inhibition but no significant change in type II protein degradation suggesting that PPCP targets an upstream enzyme specific to type I N-Terminal.

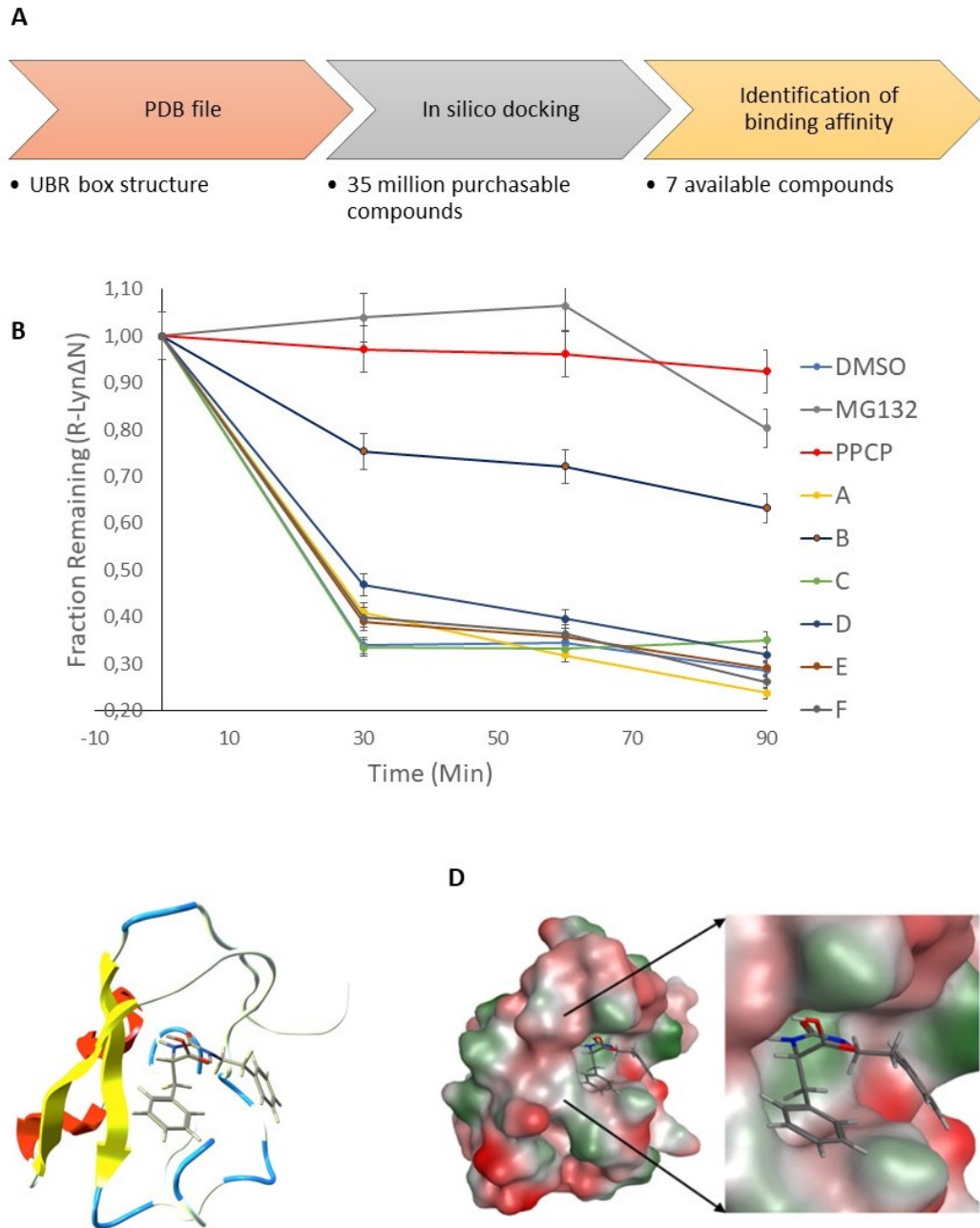


**Figure 4-1. Molecular docking workflow and the quantification of degradation rate after drug treatment.**

**A.** Flowchart of binding affinity analysis from *in silico* docking assay. **B.** Quantification of the reporter protein (R-Lyn $\Delta$ N) fraction remaining after treatment with DMSO (negative control), MG132 (positive control), and the selected compounds (A, B, C, D, E, F, and PPCP). **C.** Docking model of PPCP, as determined by *in silico* screening, bound to the UBR domain of UBR1. **D.** Molecular surface

showing the electrostatic potential of the UBR box. Negatively and positively charged surfaces are shaded red and green, respectively. The bound peptide is shown in grey.

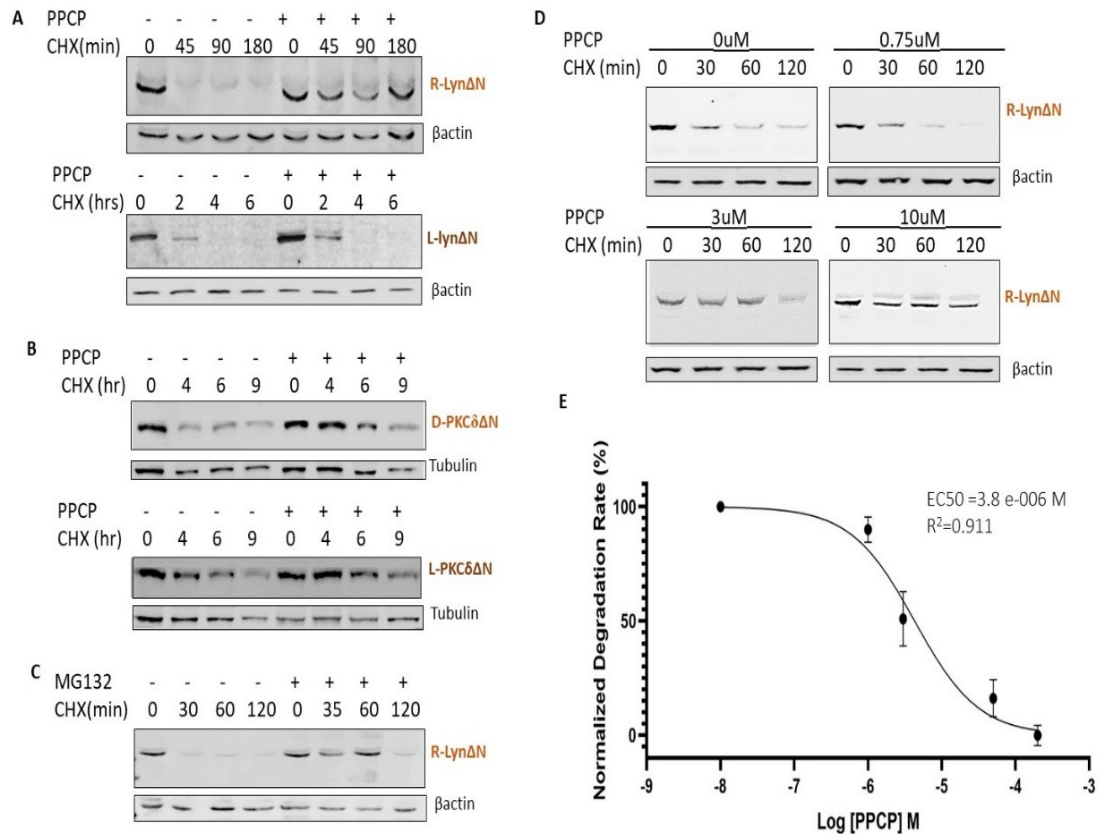


**Figure 4-2. Selective inhibition of the N-end Rule Pathway.**

**A.** The stability of L- LynΔN (type II) and R-LynΔN (type I) were determined in transfected HeLa cells, in the presence or absence of 200μM of PPCP, treated with 100μg/mL cycloheximide (CHX) at the indicated times to inhibit protein synthesis. The cells were lysed and analysed via Western Blotting. An anti-FLAG antibody was used to detect LynΔN and an anti-Tubulin antibody was employed as a loading control. **B.** Stability of D-PKCγΔN (type I) and L-PKCγΔN (type II), analysed as in (A). **C.** R-LynΔN treated with MG132 (20μM), a proteasome inhibitor, analysed as in (A). **D.** Analyses of R-LynΔN stability in different PPCP concentration, analysed as in (A). **E.** Quantification of the degradation of R-LynΔN after treatment with different concentrations of PPCP. The data was plotted to fit an apparent first order reaction.



As reporter protein, I utilized the cleaved Lyn kinase protein fragment (X-Lyn $\Delta$ N, where X represents different amino acid residues), and cleaved protein kinase C delta (X-PKC $\delta$  $\Delta$ N). Both protein fragments are catalytically inactivated by caspase cleavage which has been previously reported by our lab (Eldeeb & Fahlman, 2014) . The importance to use two different reporter proteins was to ensure that the data collected was not specific to an artifact for any particular protein.

Additionally, it was shown that the inhibition of type I degradation is directly proportional to the drug concentration with a half maximal effective concentration (EC<sub>50</sub>) of 3.8  $\mu$ M, **Figure 4-2.C and D**. It was observed that even at a low concentration (3  $\mu$ M) of PPCP treatment the type I protein (R-Lyn $\Delta$ N) presented an extended half-life equivalent to eight times (231 minutes) longer than the protein with no treatment (28 minutes). No significant change was observed on the protein stability of type II substrates, supporting the molecular modelling prediction.

### **1.3 The link between cellular stress response and protein degradation**

To investigate if the protein stability obtained after PPCP treatment could be an indirect result of the cellular stress response, I analyzed the protein degradation of different N-terminal substrates in the presence of two distinct cell stressors, **Figure 4-3.A and B**. I treated the cells with Staurosporine (STS) a non-selective inhibitor of protein kinases and apoptosis inducer (Belmokhtar, Hillion, & Sogal-Bendirdjian, 2001), and Hydrogen Peroxide (H<sub>2</sub>O<sub>2</sub>) a potent oxidizing agent.

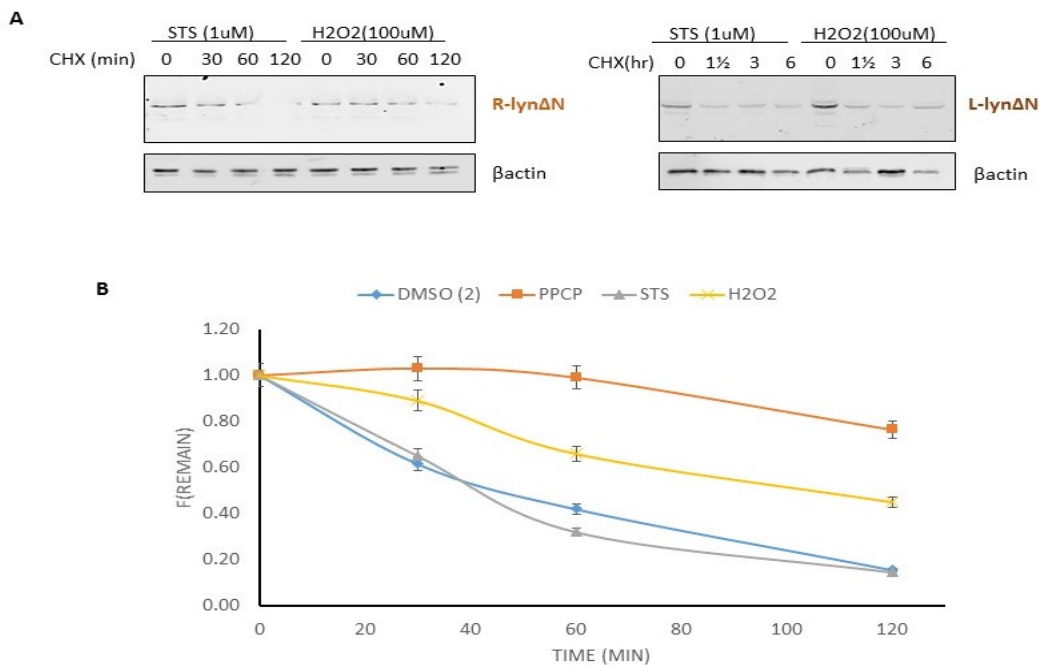


**Figure 4-3. Protein stability after cell stress after PPCP treatment.**

**A.** Stability of type I and type II reporter proteins after treatment of 1  $\mu\text{M}$  STS and 100  $\mu\text{M}$  of  $\text{H}_2\text{O}_2$ . The protein stability was investigated by treating HeLa cells with 100  $\mu\text{g}/\text{ml}$  CHX and collecting lysates at the indicated times. Then, the lysates were resolved by 10% SDS-PAGE, and the amount of protein remaining was determined by WB analysis with either an anti-FLAG or anti-actin antibody. **B.** Quantification of the remain fraction of type I reporter over the indicated time.

The results showed no relevant effect of STS treatment on protein stability compared with PPCP treatment, as well as, no difference in protein stability between type I and type II N-terminal. In regards to the  $\text{H}_2\text{O}_2$  data, there was a slight shift in protein stability compared to the control. This finding could be explained by the effect of oxidative stress in protein degradation. As an example, oxidized forms of some proteins are resistant to proteolysis, and, also, they can inhibit the ability of proteases to degrade the oxidized forms of other

proteins(Berlett & Stadtman, 1997; Friguet, Stadtman, & Szweda, 1994; RIVETT, 1986).

Despite the limitation of these findings, it shows that the impact of PPCP on protein degradation is likely to be intrinsic to the N-end rule pathway. Nevertheless, it is still relevant to investigate more deeply the binding of PPCP and the UBR box domain.

#### **1.4 Cell proliferation is affected by the selective inhibition of the N-end Rule pathway**

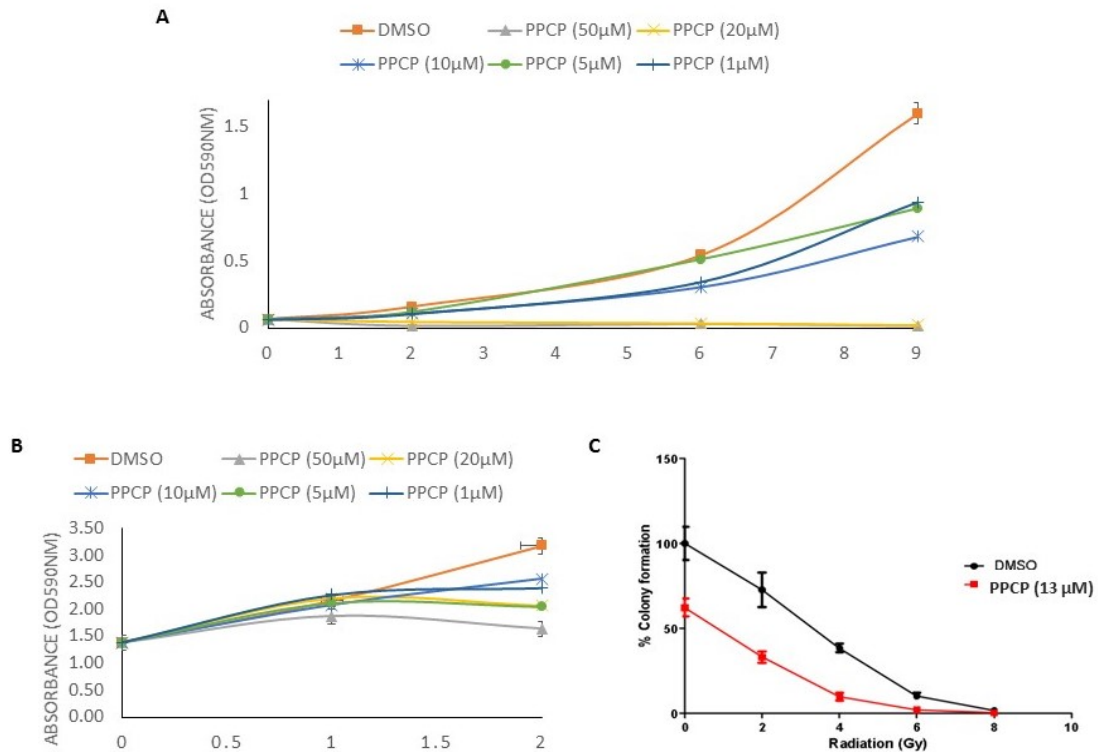
In eukaryotes, during the prophase phase of cell division, the bulk of cohesin-mediated confinement of sister chromatids is removed through openings of cohesin rings, which until the end of metaphase continue to be held the sister chromatids together to a large extent through the intact cohesin rings at the centromeres. At the end of metaphase, the activated separase cleaves cohesion subunits, in mammals the Rad21 subunit and Scc1 in yeast, resulting in their opening and allowing the separation of sister chromatids (Haarhuis, Elbatsh, & Rowland, 2014; Nasmyth & Haering, 2009; Panigrahi, Zhang, Mao, & Pati, 2011; Zhang et al., 2013). In *S. cerevisiae*, the Scc1 cohesin fragment subunit bears N-terminal Arg that is formed late in mitosis upon the activation of separase, being rapidly destroyed by the N-end rule pathway (Liu, Y. et al., 2016; Rao, Uhlmann, Nasmyth, & Varshavsky, 2001). Previous studies showed that a failure to eliminate this short-lived Scc1 fragment results in chromosome instability (Rao et al., 2001). In mammals, the separase-generated C-terminal fragments of the Rad21 subunit of mitotic cohesin and the Rec8 subunit of meiotic cohesin bear a tertiary type I N-terminal Glu being degraded by the same proteolytic path (Liu, Y. et al., 2016).

Through the MTT (Thiazolyl tetrazolium bromide) assay, **Figure 4-4. A and B**, I analyzed the cell proliferation of HeLa cells after treatment with DMSO and different concentrations of PPCP for the described time points. As a result, there was a decrease in the cellular growth rate even in the lower concentrations of PPCP treatment (1 $\mu$ M) compared with the control (DMSO). Nevertheless, the impact on cell proliferation was directed related to the increase of the PPCP concentration. Although this effect is more evident in cultures with initial low cell density (7,500 cell/ml), it still can be seen in high initial cell concentration (75,000 cell/ml). The growth pattern of the cells can explain the difference in the growth rate between the high and low cell density in the culture, where the cells proceed from the lag phase following seeding to the log phase. This exponential proliferation is significantly reduced or entirely ceased once the cells reach confluency.

In agreement with the MTT assay, the decrease in cell proliferation was also observed in a clonogenic assay. The analysis was performed in HCT116 cells, a human colon cancer cell line. The cells were treated with DMSO (control) and 13  $\mu$ M of PPCP, **Figure 4-4.C**, with 0 to 10 grey (Gy) of ionic radiation. Even though no difference was observed in the colony formation curve, the data shows a decrease in cell growth after PPCP treatment, a finding that could be related to the N-end rule essential role in chromosome stability (Rao et al., 2001).

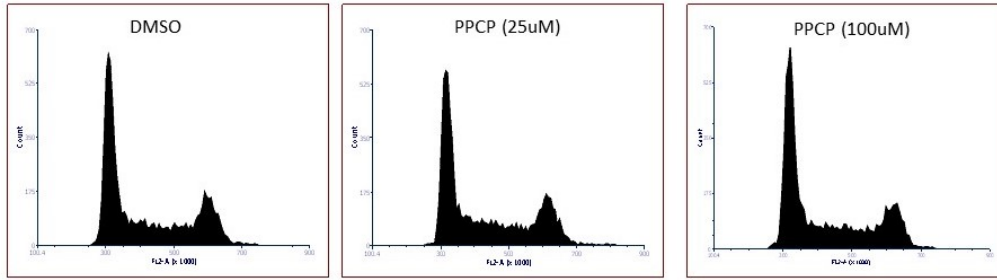
Next, I analyzed by flow cytometry if there is any change in the cell cycle of two different cell lines, HeLa and K562 (chronic myelogenous leukemia), after the inhibitor treatment, **Figure 4-5.A and B**. After the cells were treated with different concentrations of PPCP (25 $\mu$ M and 100 $\mu$ M) and DMSO for 24 hours the cells were stained with propidium iodide (PI) and posterior deconvolution of the DNA content frequency histograms. This method allows the analysis of cells distribution in three major phases of the cell cycle (G1 vs S vs G2/M) (Jayat & Ratinaud, 1993;

Pozarowski & Darzynkiewicz, 2004). Surprisingly, no significant change was observed in any of the major phases, G1 phase (cell growth), S phase (DNA synthesis), nor the G2 phase (cell growth).



**Figure 4-4. Proliferation assay after PPCP treatment.**

**A.** MTT assay beginning at a low cell confluency (7,500 cells/ml) after treatment with DMSO and PPCP (50 μM, 10 μM, 5 μM, and 1 μM), during two, six, and nine days. The data represent the average and S.D. (error bars) from three independent experiments. **B.** MTT assay absorbance quantification starting with high cell confluency (75,000 cells/ml) after 24 hours and 48 hours treatment with DMSO and PPCP (50 μM, 5 μM, and 1 μM). The data represent the average and S.D. (error bars) from three independent experiments. **C.** The data represents the cell survival after irradiation via clonogenic assay. In black is the control (DMSO), and in red is the 13 μM PPCP treatment. The data represent the average and S.D. (error bars) from three independent experiments.

**A****B**

	Cycle	G1 Mean	G1 CV	%G1	G2 Mean	G2 CV	%G2	%S	G2/G1	%Total	D.I.	B.A.D.
DMSO	Diploid	319253.51	4.65	47.97	688180.92	4.65	0.00	52.03	2.16	90.13	n/a	0.15
	Aneuploid A	609680.16	3.05	98.46	1226752.14	3.05	0.00	1.54	2.01	9.88	1.91	0.05
PPCP 25µM	Diploid	326118.80	4.51	45.29	661383.49	4.50	2.53	52.18	2.03	90.67	n/a	0.28
	Aneuploid A	625137.86	3.02	95.24	1260617.02	3.02	0.00	4.76	2.02	9.33	1.92	0.05
PPCP 100µM	Diploid	325134.29	4.77	46.90	711743.81	4.78	0.00	53.10	2.19	89.24	n/a	2.20
	Aneuploid A	624275.32	3.10	98.57	1250314.36	3.10	0.00	1.43	2.00	10.76	1.92	0.66

**Figure 4-5. Representative histograms for cells stained with PI after DMSO and PPCP treatment.**

**A.** HeLa cells were incubated with DMSO (control) or PPCP (25 µM or 100 µM) for 24 hours. Control and drug-treated cells were fixed then stained with PI. For each sample, 20 µl of cell sample (at  $\sim 4 \times 10^6$  cells / mL) was loaded in a BD Accuri cell analyzer. **B.** Fluorescence intensity measurement, same procedure as in A.

### 1.5 PPCP influences the programmed cell death

Additionally, I analyzed the cell viability of HeLa cells by double staining assay (Kasibhatla et al., 2006; Liu, K., Liu, Liu, & Wu, 2015) after treatment with different concentrations of the inhibitor. As a result, I found that PPCP has no impact on cell death when used alone, **Figure 4-6. A and B.** Conversely, the data shows that

cells under stress (addition of Procaspase Activator Factor-1, PAC1) treated with PPCP had an increase of cell death compared to the ones treated exclusively with PAC1. The experiments were repeated at least three times, and the results were confirmed with trypan blue staining. This evidence reinforces that the selective N-termini inhibitor could be used to enhance cell death in combination with the existent cancer treatment that induce the caspase activity in cell.

Moreover, when the cells were treated with different concentrations of PAC1, the concomitant treatment with PPCP showed higher cytotoxicity even in lower levels of the caspase activator, **Figure 4-6.C**. Thus, the use of the N-end rule inhibitor potentialize the programmed cell death triggered by apoptotic treatments. This diminishing the concentration of pro-apoptotic drug required for the same cellular effect.

In the literature, the combined effect of two or more drugs is described as additive, synergism or antagonism. By definition, synergism is more than an additive effect, were they demonstrate action that is higher than what is expected from their individual potencies and efficacies (Tallarida, 2011), and antagonism is less than an additive effect (Chou, Ting-Chao, 2010). The synergic activity has been of particular interest in cancer prevention and treatment (Gravitz, 2011; Tallarida, 2011). Interestingly, this seems to be the case for PAC1 combined with PPCP, as literature shows that in synergistic drug interaction there is a strong relation depending on the doses of each in the combination (Tallarida, 2000; Tallarida, 2011), as it was observed in **Figure 4-6.C**.

To quantify the combined effect of PPCP and PAC1, I followed the Chou-Talalay Method (Chou, Ting-Chao, 2010) using the third-generation "CompuSyn" software (Chou, T. C. & Martin, 2005), which uses the extended version of the general equation for the multiple drug effect. The isobologram equation provides

the theoretical basis for the combination index (CI) that allows quantitative determination of drug interactions, where  $CI < 1$ ,  $= 1$ , and  $> 1$  represents synergism, additive effect, and antagonism, respectively (Chou, Ting-Chao, 2006; Chou, Ting-Chao, 2010).

The results showed that the inhibitor administered concomitant with the caspase activator resulted in a synergic effect, with CI below one for all the concentrations tested, **Figure 4-7.A and B**. The graphic demonstrates the relation between the CI and the fraction affected ( $f_a$ ), the percentage of inhibition divided by hundred. See chapter 2 for a more detailed description of the equations.

## **2. Analysis of PPCP analogs enlighten the understanding of its inhibitory activity**

To clarify the functionality of the chemical structure of PPCP, seven analog compounds (commercially obtained – Vitascreen) were screened through western blotting analyses. As demonstrated in **Table 4-2**. The analogs differ from the main compound by the addition, substitution or removal of diverse chemical groups. The compounds I, II, III, VI, and VII show different composition on the amino parent chain by the presence of two methyl groups, the absence of the carboxyl group, the presence of a  $C_3O_2H_3$ , an  $N_2H_3$ , and benzene, respectively. On the other hand, the analog IV has a  $SNO_2H_2$  attached to one of the benzenes, whereas the compound V has the presence of fluorine at the benzene ring and a  $C_2H_3O_2$  instead of the carboxyl group existent on the PPCP.



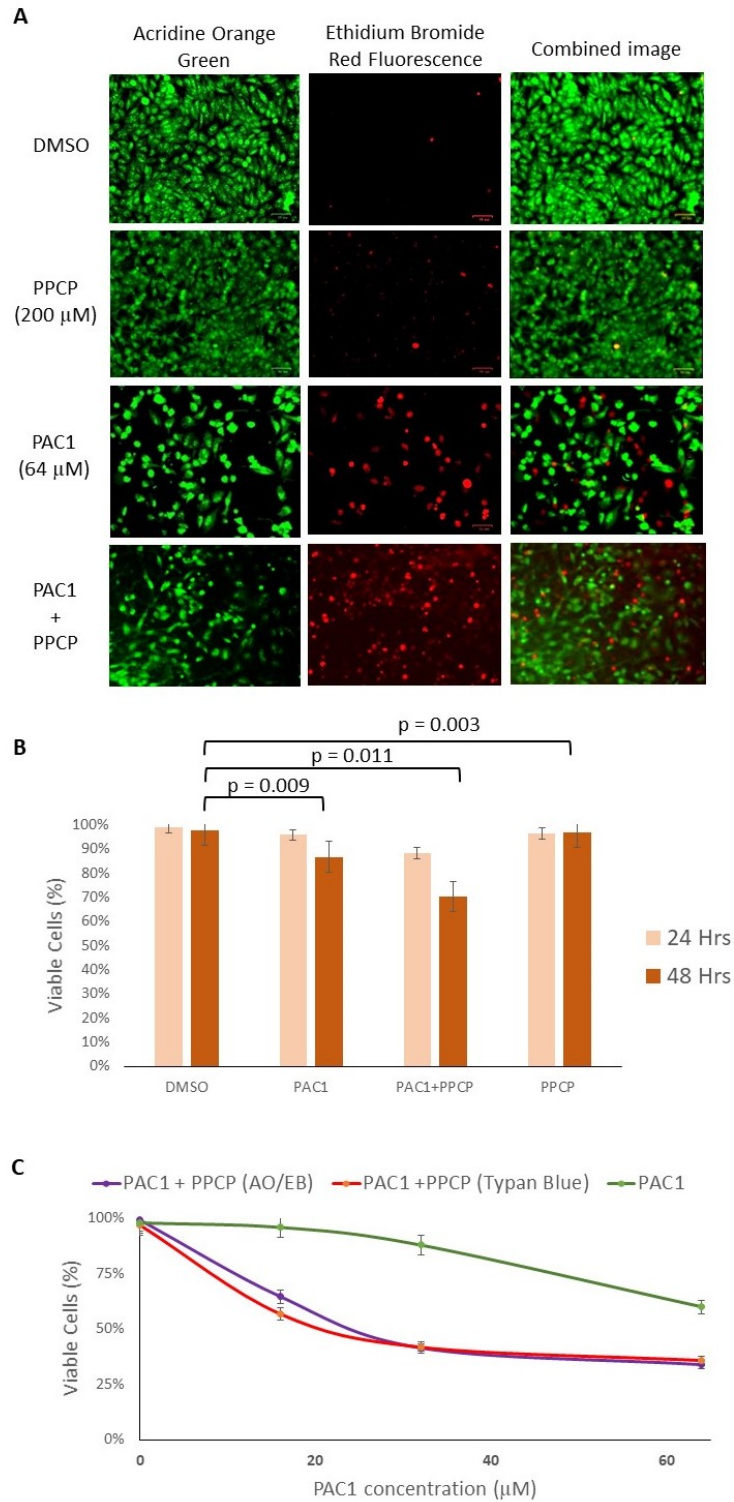


**Figure 4-6. Cell Viability after UBR-box inhibition.**

**A.** AO/EB double staining of HeLa cells after 48 hrs of the indicated treatment (DMSO; PPCP; PAC1; PPCP+PAC1). **B.** The data represent the average and S.D. (error bars) from three independent experiments. The cells were treated for 24 and 48 hours of DMSO, PPCP (200 $\mu$ M), PAC1 (64 $\mu$ M) or the combined treatment as indicated in the graphic. **C.** HeLa cells were treated with PAC1 in different concentrations, in the presence or absence of PPCP (200 $\mu$ M). Two methods were used for cell viability analyses, AO/EB and trypan blue staining. The data represents the average and standard deviation from three independent experiments, and *p* values were derived from paired two-tailed *t* tests.

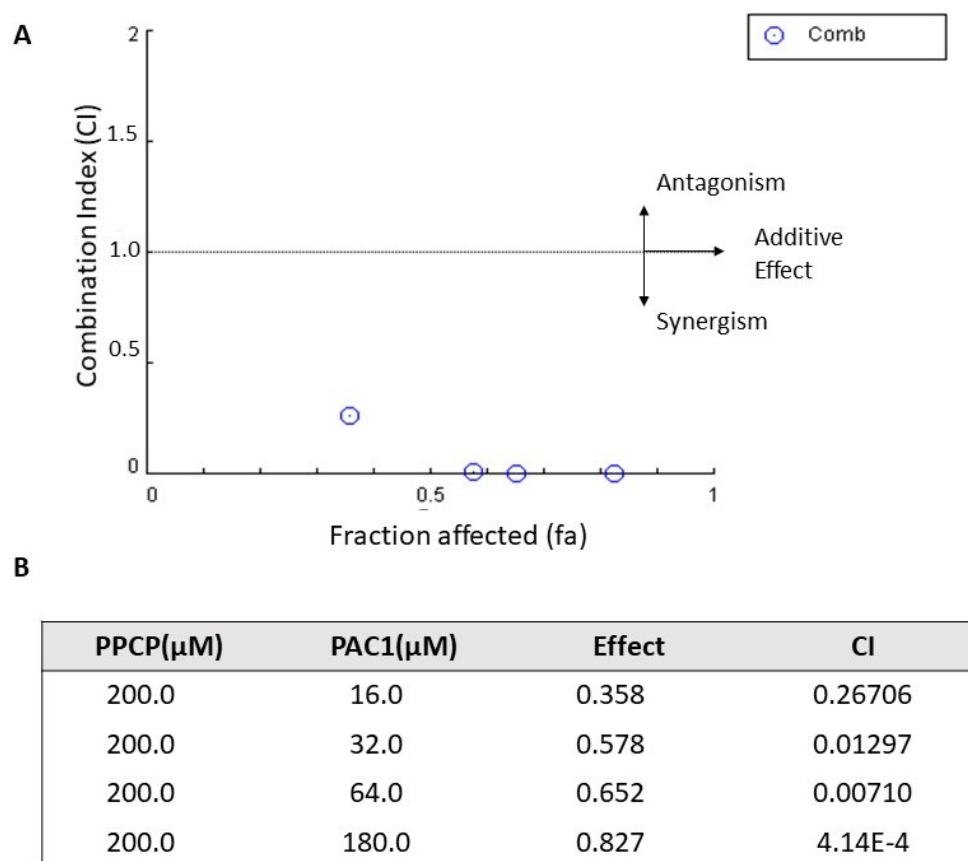


**Figure 4-7. Quantification of the combination index for PPCP and PAC1 drug interaction.**

**A.** Quantitative diagnostic graphic generated by the computer simulation, the Fa-CI plot, based on Chou-Talalay plot (Chou, Ting-Chao, 2010). Where *fa* is fraction affected and COMBO represents the combination of the two drugs. **B.**

Quantification of CI of different PPCP and PAC1 combinations. The effect was quantified by the percentage of cell viability after 24 hours of drug treatment, and represents the average from three independent experiments

## 2.1 Aromatic groups are essential to the inhibitory activity

The investigation of the analogs aimed to identify if similar chemicals would uphold the inhibitory activity, as demonstrated with PPCP treatment. First, I transfected type I and type II reporter substrates in HeLa cells and treated them with 50  $\mu\text{M}$  of each analog. After one hour of incubation, I added CHX and lysate the cells at the indicated time points. The quantification of the remaining protein was done by the analysis of western blotting, **Figure 4-8.A to C**. The results showed that four of the analogs (I, II, III, and VII), **Table 4-2**, had similar inhibitory activity as PPCP at the same concentration (50  $\mu\text{M}$ ). While analogs IV, V, and VI had little to no effect on the protein degradation rate. Important to mention that, except for the analog IV, no other compound affected the type II protein stability, data not shown.

In a second phase, the assay was repeated with a lower concentration (3  $\mu\text{M}$ , 1  $\mu\text{M}$  and 0.5  $\mu\text{M}$ ) only for the compounds that presented a positive result, **Figure 4-9.A to C**. Surprisingly, two of the analogs (I and II) showed a more efficient inhibition of type I protein degradation than PPCP at the same concentration. Both analogs (I and II) proved to have a lower EC50 (An I - 1.1  $\mu\text{M}$ , An II - 0.8  $\mu\text{M}$ ) then PPCP (3.8  $\mu\text{M}$ ), **Figure 4-9.D**.

### 2.1.1 Binding affinity to UBR box domain

To demonstrate direct binding *in vitro* to the UBR box domain, the construct to express the UBR domain from UBR1 was obtained from Dr Gehring (U McGill). As a separate note, the pdb files used for the initial *in silico* docking were to the UBR domain published from this group (Matta-Camacho et al., 2010; Muñoz-Escobar et al., 2017). The purified protein domain was investigated for inhibitor and peptide binding using a protein thermal shift assay (Huynh & Partch, 2015). The Gehring group has extensively used the protein thermal shift assay to investigate peptides binding on this domain (Muñoz-Escobar et al., 2017).

As these previous investigations using this technique were at protein concentrations (50  $\mu\text{M}$ ) much higher than our target binding affinities, we have evaluated this method at low protein concentrations. **Figure 4-9.E** reveals the fluorescence of a protein thermal shift assay in the presence of a substrate peptide (9.5 mM) and analogue II (10  $\mu\text{M}$ ) at low protein concentrations (1.5  $\mu\text{M}$ ). While significant noise in the fluorescent signal at this protein concentration is observed, quantification is possible. Titrations reveal an apparent binding affinity of  $\sim 5\mu\text{M}$  for Analogue II which is in good agreement with the cellular inhibition data, **Figure 4-9.D**, considering that buffer optimization for the assay was not performed.

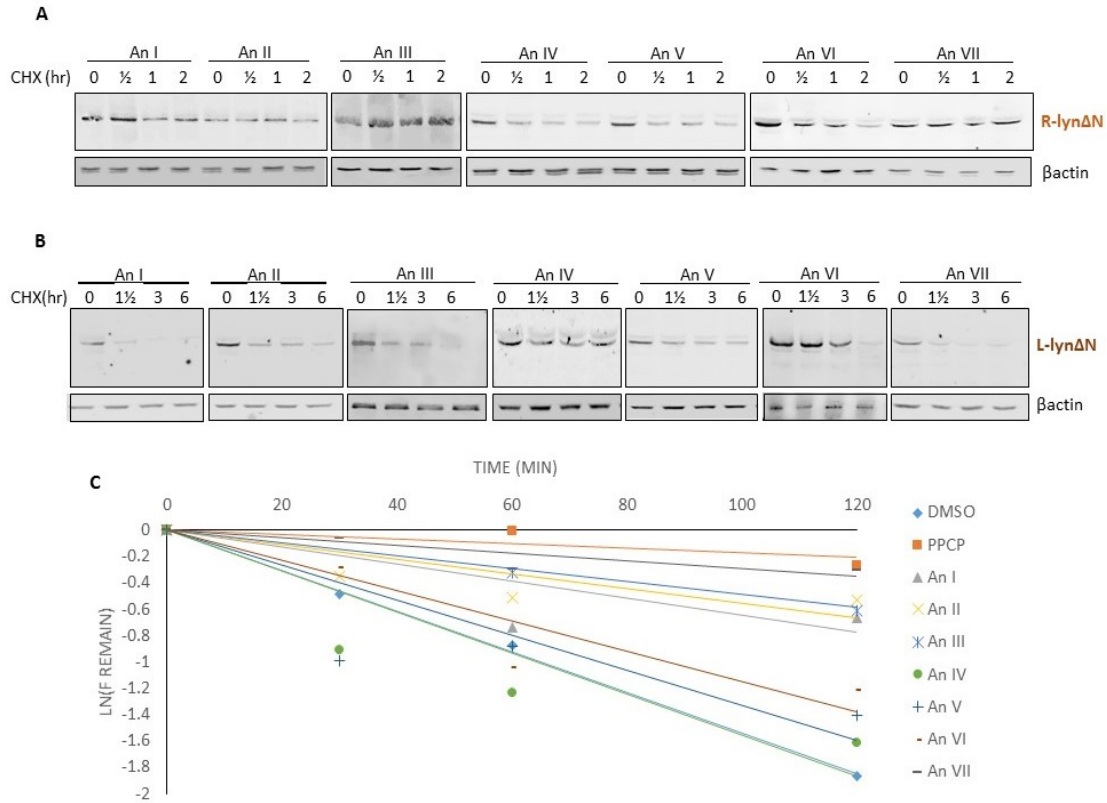
Considering the chemical structures of both analogs I and II, the removal of a carboxyl group from the amino parental chain simplified the structures compared to the PPCP and appears to strengthen the binding interaction with the UBR-box domain impacting the type I protein stability, **Figure 4-9.E**. On the other hand, the addition of a fluorine or a  $\text{SNO}_2\text{H}_2$  on the benzene ring enabled the inhibitory activity shown by the PPCP.

## 2.2 Marine compound demonstrates higher efficacy on protein stability

The analog II is a marine natural product isolated from the Okinawan ascidian, *Didemnum mole*, a colonial tunicate native to the Red Sea and the tropical waters of the Indo-Pacific region (Van der Land, 2008). Currently, little is known about this small molecule, 1,3-diphenethylurea, other than it has an anti-depressant (IWAI, HIRANO, AWAYA, MATSUO, & OMURA, 1978) effect and promotes adipocyte differentiation (Choi et al., 2011).

The findings that the 1,3-diphenethylurea can inhibit the N-end Rule pathway opens a new spectrum of investigation. This compound could be a better fit for future drug development, considering its natural origin and lower effective concentration for protein degradation inhibition. Further, studies are necessary to reveal its toxicity and prospective usage.

This research is the first in the field to demonstrate the selective inhibition of the Arg/N-end Rule Pathway. Three novel compounds, the PPCP, Analogs I and Analog II, demonstrated high specificity in the inhibition of type I N-termini with lower EC50. Nevertheless, these small molecules demonstrated low cellular toxicity when used alone, appearing as great candidates for drug development. The discovery of these novel N-terminal inhibitors expands the understanding of the degradation pathway and could have a valuable therapeutic implication towards distinct malignancies.

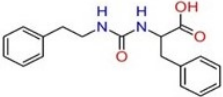
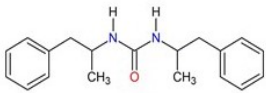
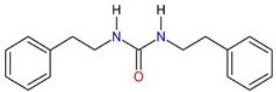
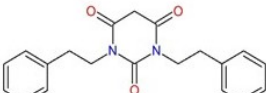
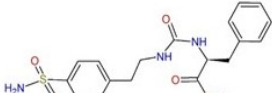
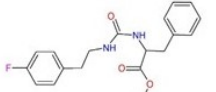
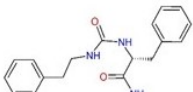
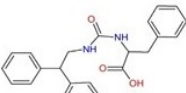


**Figure 4-8. Protein Stability after PPCP and analogs treatment**

**A.** R-lyn $\Delta$ N (type I) stability after 50  $\mu$ M PPCP analogs (I to VII) treatment. Following one-hour incubation time, HeLa cells were lysate after the addition of 100  $\mu$ g/mL CHX at the specific time points and analysed through WB. The blots were incubated with anti-FLAG or anti-actin antibody for detection. **B.** Same procedure in figure A with a lower concentration, 3  $\mu$ M. **C.** Quantification of the degradation of type I N-terminal reporter protein (R-lyn) after treatment with DMSO, PPCP, and Analogs I to VII. The amounts remaining of each different treatment are quantified relative to an actin loading control, where the rates of disappearance are depicted as follows: DMSO ( $\diamond$ ), PPCP ( $\square$ ), Analog I ( $\triangle$ ), Analog II ( $\times$ ), Analog II ( $\text{⋈}$ ), Analog IV ( $\circ$ ), Analog V ( $+$ ), Analog VI ( $-$ ), and Analog VII ( $-$ ).

**Table 4-2. PPCP and analogs chemical characteristics.**

The eight compounds (PPCP, An I, An II, An III, An IV, An V, An VI, and An VII) and the respective structure, empirical formula, chemical name and molecular weight available through the Vitascreen.

	Structure	Empirical Formula	Chemical Name	Molecular Weight
PPCP		C <sub>16</sub> H <sub>20</sub> N <sub>2</sub> O <sub>3</sub>	3-phenyl-2-[[9(2-phenylethyl) carbamoyl] amino] propanoic acid	288.34
An I		C <sub>19</sub> H <sub>24</sub> N <sub>2</sub> O	1,3-bis(1-phenylpropan-2-yl) urea	296.41
An II		C <sub>17</sub> H <sub>20</sub> N <sub>2</sub> O	1,3-bis(2-phenylethyl) urea	268.36
An III		C <sub>20</sub> H <sub>20</sub> N <sub>2</sub> O <sub>3</sub>	1,3-bis(1-phenylethyl) pyrimidine-2,4,6(1H,3H5H)-trione	336.39
An IV		C <sub>24</sub> H <sub>24</sub> N <sub>2</sub> O <sub>3</sub>	N-[[2-(4-sulfamoylphenyl) ethyl] carbomoyl]-L-phenylalanine	388.47
An V		C <sub>19</sub> H <sub>21</sub> FN <sub>2</sub> O <sub>3</sub>	methyl N-[[2-(4-fluorophenyl) ethyl] carbomoyl]-D-phenylalaninate	344.39
An VI		C <sub>18</sub> H <sub>22</sub> N <sub>4</sub> O <sub>2</sub>	1-[(2S)-1-hydrazinyl-1-oxo-3-phenylpropan-2-yl]-3-(2-phenylethyl) urea	326.4
An VII		C <sub>18</sub> H <sub>21</sub> N <sub>3</sub> O <sub>5</sub> S	N-[(2,2-diphenylethyl) carbamoyl]-L-phenylalanine	391.45

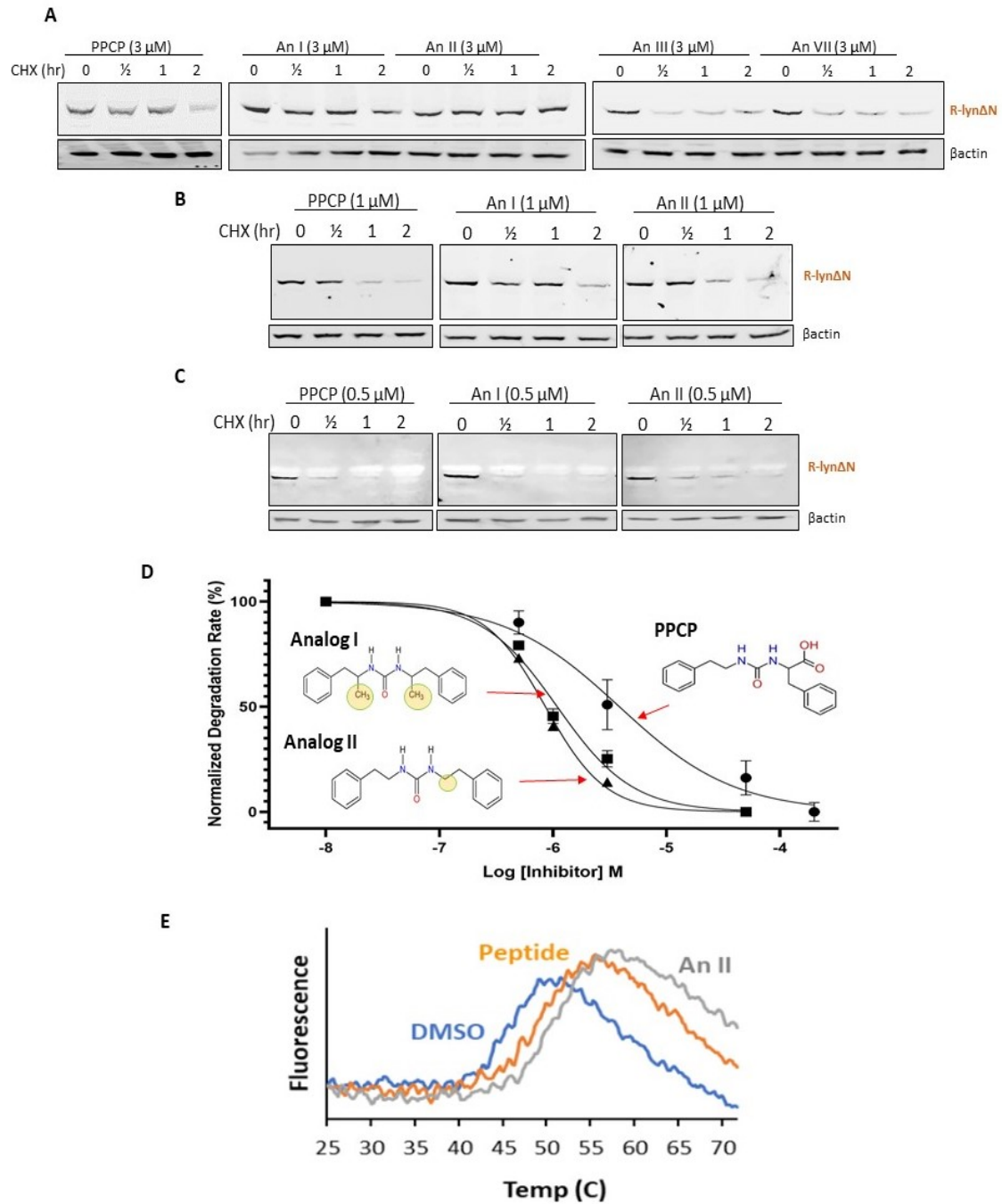


**Figure 4-9. Comparison of protein stability after PPCP and analogs inhibition.**

**A.** Western Blot analysis of R-lyn $\Delta$ N protein fraction after 3  $\mu$ M PPCP and Analogs (I, II, III, or VII) treatment. The blots were incubated with anti-FLAG or anti- $\beta$ actin antibody for detection. **B.** Protein stability after PPCP, An I and An II treatment, same procedure in figure A with a lower concentration (1  $\mu$ M). **C.** Protein stability



after PPCP, An I and An II treatment, same procedure in figure A with a lower concentration (0.5  $\mu\text{M}$ ). **D.** Quantification of the degradation of R-Lyn $\Delta\text{N}$  after treatment with different concentrations of PPCP, An I, or An II. The data was plotted to fit an apparent first order reaction. The data represent the average and S.D. (error bars) from three independent experiments. **E.** Raw fluorescent protein thermal shift analysis for the *in vitro* binding of a peptide (REGK – 9.5 mM), analogue II (10  $\mu\text{M}$ ) and a DMSO control with the purified UBR domain of human UBR1 (1.5  $\mu\text{M}$ ).

## References

- Bachmair, A., Finley, D., & Varshavsky, A. (1986). In vivo half-life of a protein is a function of its amino-terminal residue. *Science*, 234(4773), 179-186.
- Baker, R. T., & Varshavsky, A. (1991). Inhibition of the N-end rule pathway in living cells. *Proceedings of the National Academy of Sciences*, 88(4), 1090-1094.
- Belmokhtar, C. A., Hillion, J., & Sogal-Bendirdjian, E. (2001). Staurosporine induces apoptosis through both caspase-dependent and caspase-independent mechanisms. *Oncogene*, 20(26), 3354.
- Berlett, B. S., & Stadtman, E. R. (1997). Protein oxidation in aging, disease, and oxidative stress. *Journal of Biological Chemistry*, 272(33), 20313-20316.
- Cavaletti, G., Frigeni, B., Lanzani, F., Mattavelli, L., Susani, E., Alberti, P., . . . Bidoli, P. (2010). Chemotherapy-induced peripheral neurotoxicity assessment: A critical revision of the currently available tools. *European Journal of Cancer*, 46(3), 479-494.

- Chen, L., Marechal, V., Moreau, J., Levine, A. J., & Chen, J. (1997). Proteolytic cleavage of the mdm2 oncoprotein during apoptosis. *Journal of Biological Chemistry*, 272(36), 22966-22973.
- Choi, S., Cha, B., Kagami, I., Lee, Y., Sasaki, H., Suenaga, K., . . . Woo, J. (2011). N, N'-diphenethylurea isolated from okinawan ascidian didemnum molle enhances adipocyte differentiation in 3T3-L1 cells. *The Journal of Antibiotics*, 64(3), 277.
- Chou, T. C., & Martin, N. (2005). CompuSyn for drug combinations: PC software and user's guide: A computer program for quantitation of synergism and antagonism in drug combinations, and the determination of IC50 and ED50 and LD50 values. *ComboSyn, Paramus, NJ*,
- Chou, T. (2006). Theoretical basis, experimental design, and computerized simulation of synergism and antagonism in drug combination studies. *Pharmacological Reviews*, 58(3), 621-681.
- Chou, T. (2010). Drug combination studies and their synergy quantification using the chou-talalay method. *Cancer Research*, 70(2), 440-446.
- Ciechanover, A., & Kwon, Y. T. (2015). Degradation of misfolded proteins in neurodegenerative diseases: Therapeutic targets and strategies. *Experimental & Molecular Medicine*, 47(3), e147.
- Conacci-Sorrell, M., Ngouenet, C., & Eisenman, R. N. (2010). Myc-nick: A cytoplasmic cleavage product of myc that promotes  $\alpha$ -tubulin acetylation and cell differentiation. *Cell*, 142(3), 480-493.

- Dang, L., Wen, F., Yang, Y., Liu, D., Wu, K., Qi, Y., . . . Zhang, C. (2014). Proteasome inhibitor MG132 inhibits the proliferation and promotes the cisplatin-induced apoptosis of human esophageal squamous cell carcinoma cells. *International Journal of Molecular Medicine*, 33(5), 1083-1088.
- Datta, R., Kojima, H., Yoshida, K., & Kufe, D. (1997). Caspase-3-mediated cleavage of protein kinase C  $\theta$  in induction of apoptosis. *Journal of Biological Chemistry*, 272(33), 20317-20320.
- David, D. C., Layfield, R., Serpell, L., Narain, Y., Goedert, M., & Spillantini, M. G. (2002). Proteasomal degradation of tau protein. *Journal of Neurochemistry*, 83(1), 176-185.
- Eldeeb, M. A., & Fahlman, R. P. (2014). The anti-apoptotic form of tyrosine kinase lyn that is generated by proteolysis is degraded by the N-end rule pathway. *Oncotarget*, 5(9), 2714.
- Friguet, B., Stadtman, E. R., & Szweda, L. I. (1994). Modification of glucose-6-phosphate dehydrogenase by 4-hydroxy-2-nonenal. formation of cross-linked protein that inhibits the multicatalytic protease. *Journal of Biological Chemistry*, 269(34), 21639-21643.
- Gravitz, L. (2011). First line of defense. *Nature*, 471(7339)
- Haarhuis, J. H., Elbatsh, A. M., & Rowland, B. D. (2014). Cohesin and its regulation: On the logic of X-shaped chromosomes. *Developmental Cell*, 31(1), 7-18.
- Horton, T. M., Drachtman, R. A., Chen, L., Cole, P. D., McCarten, K., Voss, S., . . . Hogan, S. M. (2015). A phase 2 study of bortezomib in combination with

ifosfamide/vinorelbine in paediatric patients and young adults with refractory/recurrent hodgkin lymphoma: A children's oncology group study. *British Journal of Haematology*, 170(1), 118-122.

Hu, R., Sheng, J., Qi, X., Xu, Z., Takahashi, T. T., & Varshavsky, A. (2005). The N-end rule pathway as a nitric oxide sensor controlling the levels of multiple regulators. *Nature*, 437(7061), 981.

Huynh, K., & Partch, C. L. (2015). Analysis of protein stability and ligand interactions by thermal shift assay. *Current Protocols in Protein Science*, 79(1), 28.9. 14.

Irwin, J. J., & Shoichet, B. K. (2005). ZINC– A free database of commercially available compounds for virtual screening. *Journal of Chemical Information and Modeling*, 45(1), 177-182.

IWAI, Y., HIRANO, A., AWAYA, J., MATSUO, S., & OMURA, S. (1978). 1, 3-diphenethylurea from streptomyces sp. no. AM-2498. *The Journal of Antibiotics*, 31(4), 375-376.

Jayat, C., & Ratinaud, M. (1993). Cell cycle analysis by flow cytometry: Principles and applications. *Biology of the Cell*, 78(1-2), 15-25.

Jiang, Y., Choi, W. H., Lee, J. H., Han, D. H., Kim, J. H., Chung, Y., . . . Lee, M. J. (2014). A neurostimulant para-chloroamphetamine inhibits the arginylation branch of the N-end rule pathway. *Scientific Reports*, 4, 6344.

Kasibhatla, S., Amarante-Mendes, G. P., Finucane, D., Brunner, T., Bossy-Wetzel, E., & Green, D. R. (2006). Acridine orange/ethidium bromide (AO/EB)

staining to detect apoptosis. *Cold Spring Harbor Protocols*, 2006(3), pdb.  
prot4493.

Kwon, Y. T., Levy, F., & Varshavsky, A. (1999). Bivalent inhibitor of the N-end rule pathway. *Journal of Biological Chemistry*, 274(25), 18135-18139.

Lee, J. H., Jiang, Y., Kwon, Y. T., & Lee, M. J. (2015a). Pharmacological modulation of the N-end rule pathway and its therapeutic implications. *Trends in Pharmacological Sciences*, 36(11), 782-797.

Lee, J. H., Jiang, Y., Kwon, Y. T., & Lee, M. J. (2015b). Pharmacological modulation of the N-end rule pathway and its therapeutic implications. *Trends in Pharmacological Sciences*, 36(11), 782-797.

Lee, M. J., Kim, D. E., Zakrzewska, A., Yoo, Y. D., Kim, S., Kim, S. T., . . . Oh, U. (2012). Characterization of arginylation branch of N-end rule pathway in G-protein-mediated proliferation and signaling of cardiomyocytes. *Journal of Biological Chemistry*, 287(28), 24043-24052.

Lee, M. J., Tasaki, T., Moroi, K., An, J. Y., Kimura, S., Davydov, I. V., & Kwon, Y. T. (2005). RGS4 and RGS5 are in vivo substrates of the N-end rule pathway. *Proceedings of the National Academy of Sciences*, 102(42), 15030-15035.

Leverrier, S., Vallentin, A., & Joubert, D. (2002). Positive feedback of protein kinase C proteolytic activation during apoptosis. *Biochemical Journal*, 368(3), 905-913.

Liu, K., Liu, P., Liu, R., & Wu, X. (2015). Dual AO/EB staining to detect apoptosis in osteosarcoma cells compared with flow cytometry. *Medical Science Monitor Basic Research*, 21, 15.

- Liu, Y., Liu, C., Chang, Z., Wadas, B., Brower, C. S., Song, Z. H., . . . Wang, L. (2016). Degradation of the separase-cleaved Rec8, a meiotic cohesin subunit, by the N-end rule pathway. *Journal of Biological Chemistry*, , jbc.M116. 714964.
- Manasanch, E. E., & Orlowski, R. Z. (2017). Proteasome inhibitors in cancer therapy. *Nature Reviews Clinical Oncology*, 14(7), 417.
- Matta-Camacho, E., Kozlov, G., Li, F. F., & Gehring, K. (2010). Structural basis of substrate recognition and specificity in the N-end rule pathway. *Nature Structural and Molecular Biology*, 17(10), 1182.
- Muñoz-Escobar, J., Matta-Camacho, E., Cho, C., Kozlov, G., & Gehring, K. (2017). Bound waters mediate binding of diverse substrates to a ubiquitin ligase. *Structure*, 25(5), 729. e3.
- Nasmyth, K., & Haering, C. H. (2009). Cohesin: Its roles and mechanisms. *Annual Review of Genetics*, 43
- Panigrahi, A. K., Zhang, N., Mao, Q., & Pati, D. (2011). Calpain-1 cleaves Rad21 to promote sister chromatid separation. *Molecular and Cellular Biology*, , 11.
- Papanagnou, E., Terpos, E., Kastiris, E., Papassideri, I. S., Tsitsilonis, O. E., Dimopoulos, M. A., & Trougakos, I. P. (2018). Molecular responses to therapeutic proteasome inhibitors in multiple myeloma patients are donor-, cell type-and drug-dependent. *Oncotarget*, 9(25), 17797.
- Piatkov, K. I., Brower, C. S., & Varshavsky, A. (2012). The N-end rule pathway counteracts cell death by destroying proapoptotic protein fragments. *Proceedings of the National Academy of Sciences*, 109(27), E1847.

- Pozarowski, P., & Darzynkiewicz, Z. (2004). Analysis of cell cycle by flow cytometry. *Checkpoint controls and cancer* (pp. 301-311) Springer.
- Rao, H., Uhlmann, F., Nasmyth, K., & Varshavsky, A. (2001). Degradation of a cohesin subunit by the N-end rule pathway is essential for chromosome stability. *Nature*, *410*(6831), 955.
- Richardson, P. G., Briemberg, H., Jagannath, S., Wen, P. Y., Barlogie, B., Berenson, J., . . . Schuster, M. (2006). Frequency, characteristics, and reversibility of peripheral neuropathy during treatment of advanced multiple myeloma with bortezomib. *J Clin Oncol*, *24*(19), 3113-3120.
- RIVETT, A. J. (1986). Regulation of intracellular protein turnover: Covalent modification as a mechanism of marking proteins for degradation. *Current topics in cellular regulation* (pp. 291-337) Elsevier.
- Sooman, L., Gullbo, J., Bergqvist, M., Bergström, S., Lennartsson, J., & Ekman, S. (2017). Synergistic effects of combining proteasome inhibitors with chemotherapeutic drugs in lung cancer cells. *BMC Research Notes*, *10*(1), 544.
- Sriram, S., Lee, J. H., Mai, B. K., Jiang, Y., Kim, Y., Yoo, Y. D., . . . Lee, M. J. (2013). Development and characterization of monomeric N-end rule inhibitors through in vitro model substrates. *Journal of Medicinal Chemistry*, *56*(6), 2540-2546.
- Sterling, T., & Irwin, J. J. (2015). ZINC 15–ligand discovery for everyone. *Journal of Chemical Information and Modeling*, *55*(11), 2324-2337.

- Sun, Y. (2003). Targeting E3 ubiquitin ligases for cancer therapy. *Cancer Biology & Therapy*, 2(6), 623-629.
- Tallarida, R. J. (2000). *Drug synergism and dose-effect data analysis* Chapman and Hall/CRC.
- Tallarida, R. J. (2011). Quantitative methods for assessing drug synergism. *Genes & Cancer*, 2(11), 1003-1008.
- Tasaki, T., Mulder, L. C., Iwamatsu, A., Lee, M. J., Davydov, I. V., Varshavsky, A., . . . Kwon, Y. T. (2005). A family of mammalian E3 ubiquitin ligases that contain the UBR box motif and recognize N-degrons. *Molecular and Cellular Biology*, 25(16), 7120-7136.
- Van der Land, J. (2008). UNESCO-IOC register of marine organisms (URMO). Available at [H Ttp://Www.Marinespecies.Org/Urmo](http://www.marinespecies.org/Urmo),
- Varshavsky, A. (2011). The n-end rule pathway and regulation by proteolysis. *Protein Science*, 20(8), 1298-1345.
- Zhang, N., Jiang, Y., Mao, Q., Demeler, B., Tao, Y. J., & Pati, D. (2013). Characterization of the interaction between the cohesin subunits Rad21 and SA1/2. *PLoS One*, 8(7), e69458.



## CHAPTER 5 . FINAL CONSIDERATIONS

## **1. The N-end rule pathway and its growing level of complexity**

Since its discovery in 1986, by Varshavsky and colleagues, the role of N-end rule pathway in various cellular processes have expanded exponentially. In the first studies, engineered substrates carrying different N-terminal residues were rapidly degraded in *Saccharomyces cerevisiae* cells (Bachmair, Finley, & Varshavsky, 1986a). Shortly after, it was shown that the pathway was also present in mammalian cells, as well as in plants and bacteria (Tobias, Shrader, Rocap, & Varshavsky, 1991; Gonda et al., 1989; Potuschak et al., 1998). Nowadays, it has been demonstrated that not only the extent of the N-end rule pathway role in a great number of species, biological processes and physiological implications but also that the recognition of the substrates and consequent proteasomal degradation is more complex than it was first reported.

## **2. Second position amino acid pivotal role in N-termini recognition**

In Chapter 3, the data demonstrated that the recognition of the N-termini depends not only on the first position, stable or unstable residue but also, on the second amino acid position. This was the first time that a phosphorylated serine on the second position was directly reported as a limiting factor on the substrate enzymatic recognition by the NTAN1 in N-end rule pathway.

Looking from a broader perspective, the phosphorylation of the Ser331 of PKC $\delta$  opens an important prospect on the identification of newly formed fragments by the N-end rule pathway reinforcing the importance of not only its N-termini but also its amino acid sequence, especially for the second position residue. In this

sense, some questions are still being asked such as, if the other amino acid positions are also relevant to the N-end Rule enzymatic recognition? Or even if there are other post-translational modifications relevant to the enzymatic recognition on the N-end rule pathway?

On the other hand, the PKC $\delta$  cleaved fragment ( $\Delta$ N-PKC $\delta$ ) stability could reveal greater importance of this fragment in the cell signalling process, especially in the apoptosis. As mentioned previously, the  $\Delta$ N-PKC $\delta$  is partially active in the nucleus during apoptosis, and function as a feedforward for the complementary PKC $\delta$  and caspase-3 proteolytic activation (Cross et al., 2000; Durrant, Liu, Yang, & Lee, 2004; Ren et al., 2002). Having an extended half-life could represent a crucial role of the PKC $\delta$  cleaved fragment in prolongating the apoptosis.

### **3. The regulation of the protein degradation through the UBR box inhibition**

Despite the advances in the investigation of the N-end rule pathway substrates and enzymatic counterparts, it was only recently that the investigation of the ubiquitin enzymes for pharmacological modulation had achieved important outcomes. Small molecules, such as the synthetic heterovalent compounds (RF-C11), and the Phe-derived monomeric molecules (e.g. para-chloramphetamine – PCA) not to mention the dipeptides (e.g. arg-ala, phe-ala, lys-ala), have been reported as E3 ubiquitin enzymes inhibitors. Nevertheless, all of them have at least one of the following downsides: a high amount of product required, neural toxicity, the need for endopeptidase inhibitor, and the non-selectivity of the substrate.

Nevertheless, the present study represents important attainment with the identification of a small molecule that overcomes the major disadvantages of the

previous N-end rule inhibitors. The 3-phenyl-2-{{[9(2-phenylethyl) carbamoyl] amino} propanoic acid (PPCP) and two of its analogs (I and II), demonstrated high specificity in the inhibition of type I N-termini with an EC50 of 3.8  $\mu$ M, 1.1  $\mu$ M, and 0.8  $\mu$ M, respectively. Additionally, the PPCP and analogs demonstrated low cellular toxicity when used alone appearing as great candidates for drug development, such as a prospective adjuvant of cancer treatment. The combination of a proteasome inhibitor with chemotherapy has already been successfully reported having synergistic effects and proven to be safe for cancer patients (Bachmair, Finley, & Varshavsky, 1986b; Baker & Varshavsky, 1991; Chen et al., 2009; Choi et al., 2010; Gonda et al., 1989; Horton et al., 2015; Jiang et al., 2014; Kwon, Levy, & Varshavsky, 1999; Lee, Jiang, Kwon, & Lee, 2015; Matta-Camacho, Kozlov, Li, & Gehring, 2010; Potuschak et al., 1998; Sooman et al., 2017; Sriram et al., 2013; Tobias, Shrader, Rocap, & Varshavsky, 1991; Zhao, Xia, & Chen, 2012).

As mentioned, the PPCP had no significant cellular toxicity, but when used with a caspase activator it increased cellular apoptosis. This outcome could be better understood in **Figure 5-1**. The proteasomal degradation is responsible to maintain the balance of cell responses and empirical products. As such, once apoptotic fragments start to accumulate the protein balance is obtained through the N-end rule pathway. That also happens in cancer cells when treated with chemotherapeutical drugs. The cancer cells after a certain period offer some resistance to the treatment as per the cellular homeostasis. Nevertheless, this process can be disrupted by the effect of the E3 ligase selective inhibition, with the accumulation of the toxic fragments and consequent cellular death.

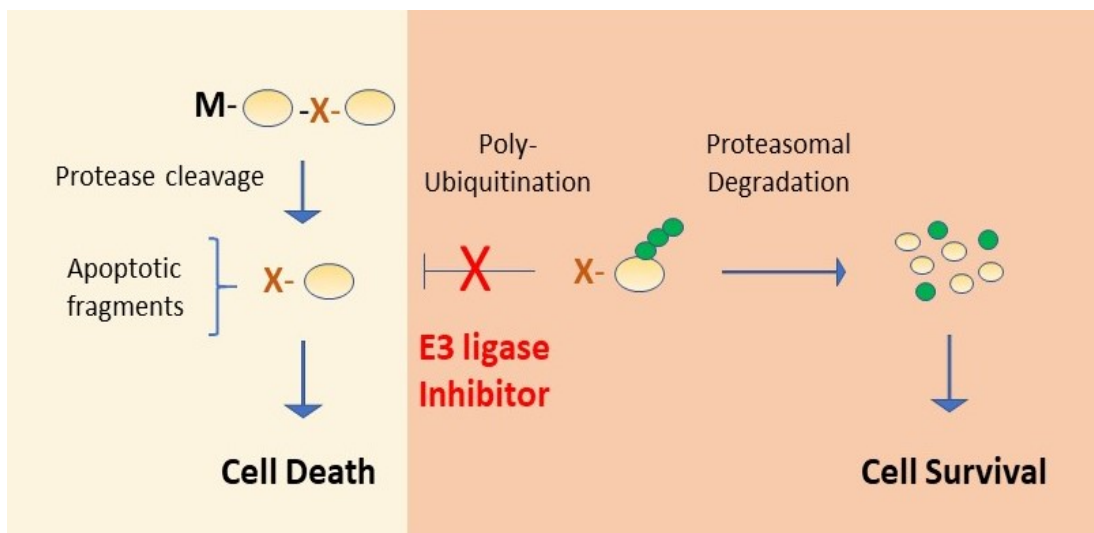


**Figure 5-1. Schematic of the E3 ligase inhibitor activity.**

The figure summarizes the cellular effect, cell death or survival, after the protease cleavage and the availability of the newly formed apoptotic fragments. Following the natural course of the cell signalling it would lead to cell survival, whereas after the inhibition of the proteasomal degradation the accumulation of apoptotic fragments would lead to cellular death.

Most of the known apoptotic fragments are type I N-termini, such as Asp-BCL(XL), Arg-BID, and Arg-BIM(EL) (Lee et al., 2015; Piatkov, Colnaghi, Békés, Varshavsky, & Huang, 2012). The selectivity of the PPCP and analogs to type I N-terminal would target those fragments and prevent some of the toxic effects that a complete N-end rule pathway inhibition would cause.

In summary, this study offers two important breakthroughs in the protein degradation field, one on the N-end rule pathway itself and the other one regarding a new inhibitor of the pathway. There is no doubt that these findings open new perspectives for future investigation, some of them already under development.

#### 4. Future directions

The continuous investigation of the N-end Rule Pathway is extremely important to widening the understanding of its mechanisms and additional roles in mammalian cells physiology. Nevertheless, the present study reveals three remarkable topics that would demand further analysis: the impact of phosphorylation in the NTAN1 substrate recognition and what it represents to cell signaling, the effect of the PPCP and Analogs in the stability of endogenous type I N-terminal substrates, and the development of novel synthetic compounds with lower EC50 for pharmacological modulation.

As it has been suggested by the present study, the change of the electrolytic charge may be the cause of binding inhibition between the substrate and the NTAN1 enzyme. As such, additional investigation would enhance the understanding of the phosphorylation role in the substrate recognition of endogenous fragments including the ones deaminated by NTAQ1. This natural degradation regulator might be involved in several signalling events and its investigation would assist the understanding of the stability and functionality in a diverse number of protease cleaved fragments.

On the other hand, the selective regulation of the N-end Rule by the PPCP and Analogs enters in a new phase of investigation where the novel compounds require further *in vivo* analysis that might evolve into the pharmacological modulation. Despite the positive results in a controlled environment with protein stability and cell toxicity, the *in vivo* tests would allow the compounds to be analyzed towards its drug availability and adverse effects. Nevertheless, the development of a novel

synthetic compound with lower effective concentrations, using the PPCP and analogs as developmental basis, would expand its impact and usage for clinical treatment.

## References

- Bachmair, A., Finley, D., & Varshavsky, A. (1986a). In vivo half-life of a protein is a function of its amino-terminal residue. *Science*, 234(4773), 179-186.
- Bachmair, A., Finley, D., & Varshavsky, A. (1986b). In vivo half-life of a protein is a function of its amino-terminal residue. *Science*, 234(4773), 179-186.
- Baker, R. T., & Varshavsky, A. (1991). Inhibition of the N-end rule pathway in living cells. *Proceedings of the National Academy of Sciences*, 88(4), 1090-1094.
- Chen, J., Lin, H. H., Kim, K., Lin, A., Ou, J. J., & Ann, D. K. (2009). PKC $\delta$  signaling: A dual role in regulating hypoxic stress-induced autophagy and apoptosis. *Autophagy*, 5(2), 244-246.
- Choi, W. S., Jeong, B., Joo, Y. J., Lee, M., Kim, J., Eck, M. J., & Song, H. K. (2010). Structural basis for the recognition of N-end rule substrates by the UBR box of ubiquitin ligases. *Nature Structural and Molecular Biology*, 17(10), 1175.
- Cross, T., Griffiths, G., Deacon, E., Sallis, R., Gough, M., Watters, D., & Lord, J. M. (2000). PKC- $\delta$  is an apoptotic lamin kinase. *Oncogene*, 19(19), 2331.

- Durrant, D., Liu, J., Yang, H., & Lee, R. M. (2004). The bortezomib-induced mitochondrial damage is mediated by accumulation of active protein kinase C- $\delta$ . *Biochemical and Biophysical Research Communications*, 321(4), 905-908.
- Gonda, D. K., Bachmair, A., Wüning, I., Tobias, J. W., Lane, W. S., & Varshavsky, A. (1989). Universality and structure of the N-end rule. *Journal of Biological Chemistry*, 264(28), 16700-16712.
- Horton, T. M., Drachtman, R. A., Chen, L., Cole, P. D., McCarten, K., Voss, S., . . . Hogan, S. M. (2015). A phase 2 study of bortezomib in combination with ifosfamide/vinorelbine in paediatric patients and young adults with refractory/recurrent hodgkin lymphoma: A children's oncology group study. *British Journal of Haematology*, 170(1), 118-122.
- Jiang, Y., Choi, W. H., Lee, J. H., Han, D. H., Kim, J. H., Chung, Y., . . . Lee, M. J. (2014). A neurostimulant para-chloroamphetamine inhibits the arginylation branch of the N-end rule pathway. *Scientific Reports*, 4, 6344.
- Kwon, Y. T., Levy, F., & Varshavsky, A. (1999). Bivalent inhibitor of the N-end rule pathway. *Journal of Biological Chemistry*, 274(25), 18135-18139.
- Lee, J. H., Jiang, Y., Kwon, Y. T., & Lee, M. J. (2015). Pharmacological modulation of the N-end rule pathway and its therapeutic implications. *Trends in Pharmacological Sciences*, 36(11), 782-797.
- Matta-Camacho, E., Kozlov, G., Li, F. F., & Gehring, K. (2010). Structural basis of substrate recognition and specificity in the N-end rule pathway. *Nature Structural & Molecular Biology*, 17(10), 1182.



- Piatkov, K. I., Colnaghi, L., Békés, M., Varshavsky, A., & Huang, T. T. (2012). The auto-generated fragment of the Usp1 deubiquitylase is a physiological substrate of the N-end rule pathway. *Molecular Cell*, *48*(6), 926-933.
- Potuschak, T., Stary, S., Schlögelhofer, P., Becker, F., Nejinskaia, V., & Bachmair, A. (1998). PRT1 of arabidopsis thaliana encodes a component of the plant N-end rule pathway. *Proceedings of the National Academy of Sciences*, *95*(14), 7904-7908.
- Ren, J., Datta, R., Shioya, H., Li, Y., Oki, E., Biedermann, V., . . . Kufe, D. (2002). p73 $\beta$  is regulated by protein kinase c $\delta$  catalytic fragment generated in the apoptotic response to DNA damage. *Journal of Biological Chemistry*, *277*(37), 33758-33765.
- Sooman, L., Gullbo, J., Bergqvist, M., Bergström, S., Lennartsson, J., & Ekman, S. (2017). Synergistic effects of combining proteasome inhibitors with chemotherapeutic drugs in lung cancer cells. *BMC Research Notes*, *10*(1), 544.
- Sriram, S., Lee, J. H., Mai, B. K., Jiang, Y., Kim, Y., Yoo, Y. D., . . . Lee, M. J. (2013). Development and characterization of monomeric N-end rule inhibitors through in vitro model substrates. *Journal of Medicinal Chemistry*, *56*(6), 2540-2546.
- Tobias, J. W., Shrader, T. E., Rocap, G., & Varshavsky, A. (1991). The N-end rule in bacteria. *Science*, *254*(5036), 1374-1377.

Zhao, M., Xia, L., & Chen, G. (2012). Protein kinase c $\delta$  in apoptosis: A brief overview. *Archivum Immunologiae Et Therapiae Experimentalis*, 60(5), 361-372.

## BIBLIOGRAPHY

Agarwalla, P., & Banerjee, R. (2016). N-end rule pathway inhibition assists colon tumor regression via necroptosis. *Molecular Therapy-Oncolytics*, 3

Alagramam, K., Naider, F., & Becker, J. M. (1995). A recognition component of the ubiquitin system is required for peptide transport in *saccharomyces cerevisiae*. *Molecular Microbiology*, 15(2), 225-234.

Bachmair, A., Finley, D., & Varshavsky, A. (1986). In vivo half-life of a protein is a function of its amino-terminal residue. *Science*, 234(4773), 179-186.

Baker, R. T., & Varshavsky, A. (1991). Inhibition of the N-end rule pathway in living cells. *Proceedings of the National Academy of Sciences*, 88(4), 1090-1094.

Balogh, S. A., McDowell, C. S., & Denenberg, V. H. (2002). Behavioral characterization of mice lacking the ubiquitin ligase UBR1 of the N-End rule pathway. *Genes, Brain and Behavior*, 1(4), 223-229.

Bartel, B., Wüning, I., & Varshavsky, A. (1990). The recognition component of the n-end rule pathway. *The EMBO Journal*, 9(10), 3179-3189.

Belmokhtar, C. A., Hillion, J., & Sogal-Bendirdjian, E. (2001). Staurosporine induces apoptosis through both caspase-dependent and caspase-independent mechanisms. *Oncogene*, 20(26), 3354.

- Benes, C. H., Wu, N., Elia, A. E., Dharia, T., Cantley, L. C., & Soltoff, S. P. (2005). The C2 domain of PKCdelta is a phosphotyrosine binding domain. *Cell*, 121(2), 271-280. doi:S0092-8674(05)00164-9 [pii]
- Berlett, B. S., & Stadtman, E. R. (1997). Protein oxidation in aging, disease, and oxidative stress. *Journal of Biological Chemistry*, 272(33), 20313-20316.
- Billecke, C., Finniss, S., Tahash, L., Miller, C., Mikkelsen, T., Farrell, N. P., & Bogler, O. (2006). Polynuclear platinum anticancer drugs are more potent than cisplatin and induce cell cycle arrest in glioma. *Neuro-Oncology*, 8(3), 215-226. doi:15228517-2006-004 [pii]
- Blass, M., Kronfeld, I., Kazimirsky, G., Blumberg, P. M., & Brodie, C. (2002). Tyrosine phosphorylation of protein kinase cδ is essential for its apoptotic effect in response to etoposide. *Molecular and Cellular Biology*, 22(1), 182-195.
- Brower, C. S., & Varshavsky, A. (2009). Ablation of arginylation in the mouse N-end rule pathway: Loss of fat, higher metabolic rate, damaged spermatogenesis, and neurological perturbations. *PloS One*, 4(11), e7757. doi:10.1371/journal.pone.0007757 [doi]
- Brower, C. S., Piatkov, K. I., & Varshavsky, A. (2013). Neurodegeneration-associated protein fragments as short-lived substrates of the N-end rule pathway. *Molecular Cell*, 50(2), 161-171.
- Byrd, C., Turner, G. C., & Varshavsky, A. (1998). The N-end rule pathway controls the import of peptides through degradation of a transcriptional repressor. *The EMBO Journal*, 17(1), 269-277. doi:10.1093/emboj/17.1.269 [doi]

Cao, X., Deng, X., & May, W. S. (2003). Cleavage of bax to p18 bax accelerates stress-induced apoptosis, and a cathepsin-like protease may rapidly degrade p18 bax. *Blood*, 102(7), 2605-2614.

Cavaletti, G., Frigeni, B., Lanzani, F., Mattavelli, L., Susani, E., Alberti, P., . . . Bidoli, P. (2010). Chemotherapy-induced peripheral neurotoxicity assessment: A critical revision of the currently available tools. *European Journal of Cancer*, 46(3), 479-494.

Cha-Molstad, H., Sung, K. S., Hwang, J., Kim, K. A., Yu, J. E., Yoo, Y. D., . . . Kim, J. G. (2015). Amino-terminal arginylation targets endoplasmic reticulum chaperone BiP for autophagy through p62 binding. *Nature Cell Biology*, 17(7), 917.

Chen, J., Lin, H. H., Kim, K., Lin, A., Ou, J. J., & Ann, D. K. (2009). PKC $\delta$  signaling: A dual role in regulating hypoxic stress-induced autophagy and apoptosis. *Autophagy*, 5(2), 244-246.

Chen, L., Hahn, H., Wu, G., Chen, C., Liron, T., Schechtman, D., . . . Bolli, R. (2001). Opposing cardioprotective actions and parallel hypertrophic effects of  $\delta$ PKC and  $\epsilon$ PKC. *Proceedings of the National Academy of Sciences*, 98(20), 11114-11119.

Chen, L., Marechal, V., Moreau, J., Levine, A. J., & Chen, J. (1997). Proteolytic cleavage of the mdm2 oncoprotein during apoptosis. *Journal of Biological Chemistry*, 272(36), 22966-22973.

Chen, S., Wu, X., Wadas, B., Oh, J., & Varshavsky, A. (2017). An N-end rule pathway that recognizes proline and destroys gluconeogenic enzymes. *Science*, 355(6323), eaal3655.

- Cheng, N., He, R., Tian, J., Dinauer, M. C., & Ye, R. D. (2007). A critical role of protein kinase C delta activation loop phosphorylation in formyl-methionyl-leucyl-phenylalanine-induced phosphorylation of p47(phox) and rapid activation of nicotinamide adenine dinucleotide phosphate oxidase. *Journal of Immunology (Baltimore, Md.: 1950)*, 179(11), 7720-7728. doi:179/11/7720 [pii]
- Cho, W., & Stahelin, R. V. (2006). Membrane binding and subcellular targeting of C2 domains. *Biochimica Et Biophysica Acta (BBA)-Molecular and Cell Biology of Lipids*, 1761(8), 838-849.
- Choi, S., Cha, B., Kagami, I., Lee, Y., Sasaki, H., Suenaga, K., . . . Woo, J. (2011). N, N'-diphenethylurea isolated from okinawan ascidian didemnum molle enhances adipocyte differentiation in 3T3-L1 cells. *The Journal of Antibiotics*, 64(3), 277.
- Choi, W. S., Jeong, B., Joo, Y. J., Lee, M., Kim, J., Eck, M. J., & Song, H. K. (2010). Structural basis for the recognition of N-end rule substrates by the UBR box of ubiquitin ligases. *Nature Structural & Molecular Biology*, 17(10), 1175.
- Chou, T. (2006). Theoretical basis, experimental design, and computerized simulation of synergism and antagonism in drug combination studies. *Pharmacological Reviews*, 58(3), 621-681.
- Chou, T. (2010). Drug combination studies and their synergy quantification using the chou-talalay method. *Cancer Research*, 70(2), 440-446.
- Chou, T. C., & Martin, N. (2005). *CompuSyn for drug combinations: PC software and user's guide: A computer program for quantitation of synergism and*

antagonism in drug combinations, and the determination of IC50 and ED50 and LD50 values. ComboSyn, Paramus, NJ,

Ciechanover, A., & Kwon, Y. T. (2015). Degradation of misfolded proteins in neurodegenerative diseases: Therapeutic targets and strategies. *Experimental & Molecular Medicine*, 47(3), e147.

Conacci-Sorrell, M., Ngouenet, C., & Eisenman, R. N. (2010). Myc-nick: A cytoplasmic cleavage product of myc that promotes  $\alpha$ -tubulin acetylation and cell differentiation. *Cell*, 142(3), 480-493.

Cornachione, A. S., Leite, F. S., Wang, J., Leu, N. A., Kalganov, A., Volgin, D., . . . Yates III, J. R. (2014). Arginylation of myosin heavy chain regulates skeletal muscle strength. *Cell Reports*, 8(2), 470-476.

Craft, I. L., Geddes, D., Hyde, C. W., Wise, I. J., & Matthews, D. M. (1968). Absorption and malabsorption of glycine and glycine peptides in man. *Gut*, 9(4), 425-437.

Cross, T., Griffiths, G., Deacon, E., Sallis, R., Gough, M., Watters, D., & Lord, J. M. (2000). PKC- $\delta$  is an apoptotic lamin kinase. *Oncogene*, 19(19), 2331.

Dang, L., Wen, F., Yang, Y., Liu, D., Wu, K., Qi, Y., . . . Zhang, C. (2014). Proteasome inhibitor MG132 inhibits the proliferation and promotes the cisplatin-induced apoptosis of human esophageal squamous cell carcinoma cells. *International Journal of Molecular Medicine*, 33(5), 1083-1088.

Datta, R., Kojima, H., Yoshida, K., & Kufe, D. (1997). Caspase-3-mediated cleavage of protein kinase C  $\theta$  in induction of apoptosis. *Journal of Biological Chemistry*, 272(33), 20317-20320.

- Daub, H., Olsen, J. V., Bairlein, M., Gnad, F., Oppermann, F. S., Körner, R., . . . Mann, M. (2008). Kinase-selective enrichment enables quantitative phosphoproteomics of the kinome across the cell cycle. *Molecular Cell*, 31(3), 438-448.
- David, D. C., Layfield, R., Serpell, L., Narain, Y., Goedert, M., & Spillantini, M. G. (2002). Proteasomal degradation of tau protein. *Journal of Neurochemistry*, 83(1), 176-185.
- Deka, K., Singh, A., Chakraborty, S., Mukhopadhyay, R., & Saha, S. (2016). Protein arginylation regulates cellular stress response by stabilizing HSP70 and HSP40 transcripts. *Cell Death Discovery*, 2, 16074.
- Denning, M. F., Wang, Y., Tibudan, S., Alkan, S., Nickoloff, B. J., & Qin, J. Z. (2002). Caspase activation and disruption of mitochondrial membrane potential during UV radiation-induced apoptosis of human keratinocytes requires activation of protein kinase C. *Cell Death and Differentiation*, 9(1), 40-52. doi:10.1038/sj.cdd.4400929 [doi]
- DeVries, T. A., Neville, M. C., & Reyland, M. E. (2002). Nuclear import of PKC $\delta$  is required for apoptosis: Identification of a novel nuclear import sequence. *The EMBO Journal*, 21(22), 6050-6060.
- DeVries-Seimon, T. A., Ohm, A. M., Humphries, M. J., & Reyland, M. E. (2007). Induction of apoptosis is driven by nuclear retention of protein kinase c $\delta$ . *Journal of Biological Chemistry*, 282(31), 22307-22314.
- Ditzel, M., Wilson, R., Tenev, T., Zachariou, A., Paul, A., Deas, E., & Meier, P. (2003). Degradation of DIAP1 by the N-end rule pathway is essential for regulating apoptosis. *Nature Cell Biology*, 5(5), 467.



- Dizin, E., Ray, H., Suau, F., Voeltzel, T., & Dalla Venezia, N. (2008). Caspase-dependent BRCA1 cleavage facilitates chemotherapy-induced apoptosis. *Apoptosis*, 13(2), 237-246.
- Dougan, D. A., Micevski, D., & Truscott, K. N. (2012). The N-end rule pathway: From recognition by N-recognins, to destruction by AAA+proteases. *Biochimica Et Biophysica Acta*, 1823(1), 83-91.  
doi:10.1016/j.bbamcr.2011.07.002 [doi]
- Durrant, D., Liu, J., Yang, H., & Lee, R. M. (2004). The bortezomib-induced mitochondrial damage is mediated by accumulation of active protein kinase C- $\delta$ . *Biochemical and Biophysical Research Communications*, 321(4), 905-908.
- Durrant, D., Liu, J., Yang, H., & Lee, R. M. (2004). The bortezomib-induced mitochondrial damage is mediated by accumulation of active protein kinase C- $\delta$ . *Biochemical and Biophysical Research Communications*, 321(4), 905-908.
- Dutil, E. M., Toker, A., & Newton, A. C. (2031). Regulation of conventional protein kinase C isozymes by phosphoinositide-dependent kinase 1 (PDK-1). *Current Biology : CB*, 8(25), 1366-1375. doi:S0960-9822(98)00017-7 [pii]
- Eldeeb, M. A., & Fahlman, R. P. (2014). The anti-apoptotic form of tyrosine kinase lyn that is generated by proteolysis is degraded by the N-end rule pathway. *Oncotarget*, 5(9), 2714.
- Eldeeb, M. A., & Fahlman, R. P. (2016). Phosphorylation impacts N-end rule degradation of the proteolytically activated form of BMX kinase. *Journal of Biological Chemistry*, 291(43), 22757-22768.

- Eldeeb, M., & Fahlman, R. (2016). The-N-end rule: The beginning determines the end. *Protein and Peptide Letters*, 23(4), 343-348.
- Eldeeb, M., Fahlman, R., Esmaili, M., & Ragheb, M. (2018). Regulating apoptosis by degradation: The N-end rule-mediated regulation of apoptotic proteolytic fragments in mammalian cells. *International Journal of Molecular Sciences*, 19(11), 3414.
- Erdelyi, H. A., Lahti, R. A., Lopez, M. B., Myers, C. S., Roberts, R. C., Tamminga, C. A., & Vogel, M. W. (2004). Regional expression of RGS4 mRNA in human brain. *The European Journal of Neuroscience*, 19(11), 3125-3128.  
doi:10.1111/j.0953-816X.2004.03364.x [doi]
- Eymin, B., Sordet, O., Droin, N., Munsch, B., Haugg, M., Van de Craen, M., . . . Solary, E. (1999). Caspase-induced proteolysis of the cyclin-dependent kinase inhibitor p27 Kip1 mediates its anti-apoptotic activity. *Oncogene*, 18(34), 4839.
- Friguet, B., Stadtman, E. R., & Szwed, L. I. (1994). Modification of glucose-6-phosphate dehydrogenase by 4-hydroxy-2-nonenal. formation of cross-linked protein that inhibits the multicatalytic protease. *Journal of Biological Chemistry*, 269(34), 21639-21643.
- Fujiwara, H., Tanaka, N., Yamashita, I., & Kitamura, K. (2013). Essential role of UBR11, but not UBR1, as an n-end rule ubiquitin ligase in *Schizosaccharomyces pombe*. *Yeast*, 30(1), 1-11.
- Gallegos, L. L., & Newton, A. C. (2008). Spatiotemporal dynamics of lipid signaling: Protein kinase C as a paradigm. *IUBMB Life*, 60(12), 782-789.

- Gamas, P., Marchetti, S., Puissant, A., Grosso, S., Jacquet, A., Colosetti, P., . . . Auberger, P. (2009). Inhibition of imatinib-mediated apoptosis by the caspase-cleaved form of the tyrosine kinase lyn in chronic myelogenous leukemia cells. *Leukemia*, 23(8), 1500.
- Gan, L., Wang, J., Xu, H., & Yang, X. (2011). Resistance to docetaxel-induced apoptosis in prostate cancer cells by p38/p53/p21 signaling. *The Prostate*, 71(11), 1158-1166.
- Giaime, E., Sunyach, C., Herrant, M., Grosso, S., Auberger, P., McLean, P. J., . . . Da Costa, C. A. (2006). Caspase-3-derived C-terminal product of synphilin-1 displays antiapoptotic function via modulation of the p53-dependent cell death pathway. *Journal of Biological Chemistry*, 281(17), 11515-11522.
- Gonda, D. K., Bachmair, A., Wüning, I., Tobias, J. W., Lane, W. S., & Varshavsky, A. (1989). Universality and structure of the N-end rule. *Journal of Biological Chemistry*, 264(28), 16700-16712.
- Gong, J., Park, M., & Steinberg, S. F. (2017). Cleavage alters the molecular determinants of protein kinase C- $\delta$  catalytic activity. *Molecular and Cellular Biology*, 37(20), 324.
- Gravitz, L. (2011). First line of defense. *Nature*, 471(7339)
- Haarhuis, J. H., Elbatsh, A. M., & Rowland, B. D. (2014). Cohesin and its regulation: On the logic of X-shaped chromosomes. *Developmental Cell*, 31(1), 7-18.
- Hahn, H. S., Yussman, M. G., Toyokawa, T., Marreez, Y., Barrett, T. J., Hilty, K. C., . . . Dorn, G. W. (2002). Ischemic protection and myofibrillar

cardiomyopathy: Dose-dependent effects of in vivo  $\delta$ PKC inhibition.

*Circulation Research*, 91(8), 741-748.

Holm, L., Kriinen, S., Rosenström, P., & Schenkel, A. (2008). Searching protein structure databases with DaliLite v. 3. *Bioinformatics*, 24(23), 2780-2781.

Horton, T. M., Drachtman, R. A., Chen, L., Cole, P. D., McCarten, K., Voss, S., . . . Hogan, S. M. (2015). A phase 2 study of bortezomib in combination with ifosfamide/vinorelbine in paediatric patients and young adults with refractory/recurrent hodgkin lymphoma: A children's oncology group study. *British Journal of Haematology*, 170(1), 118-122.

Hu, R., Sheng, J., Qi, X., Xu, Z., Takahashi, T. T., & Varshavsky, A. (2005). The N-end rule pathway as a nitric oxide sensor controlling the levels of multiple regulators. *Nature*, 437(7061), 981.

Humphries, M. J., Ohm, A. M., Schaack, J., Adwan, T. S., & Reyland, M. E. (2008). Tyrosine phosphorylation regulates nuclear translocation of PKC $\delta$ . *Oncogene*, 27(21), 3045.

Hurley, J. H., Newton, A. C., Parker, P. J., Blumberg, P. M., & Nishizuka, Y. (1997). Taxonomy and function of C1 protein kinase C homology domains. *Protein Science*, 6(2), 477-480.

Huskens, J. (2006). Multivalent interactions at interfaces. *Current Opinion in Chemical Biology*, 10(6), 537-543. doi:S1367-5931(06)00147-5 [pii]

- Huynh, K., & Partch, C. L. (2015). Analysis of protein stability and ligand interactions by thermal shift assay. *Current Protocols in Protein Science*, 79(1), 28.9. 14.
- Hwang, C., Shemorry, A., & Varshavsky, A. (2009). Two proteolytic pathways regulate DNA repair by cotargeting the Mgt1 alkylguanine transferase. *Proceedings of the National Academy of Sciences*, 106(7), 2142-2147.
- Hwang, C., Sukalo, M., Batygin, O., Addor, M., Brunner, H., Aytes, A. P., . . . Zenker, M. (2011). Ubiquitin ligases of the N-end rule pathway: Assessment of mutations in UBR1 that cause the johanson-blizzard syndrome. *PLoS One*, 6(9), e24925.
- Igumenova, T. I. (2015). Dynamics and membrane interactions of protein kinase C. *Biochemistry*, 54(32), 4953-4968.
- Inagaki, K., Chen, L., Ikeno, F., Lee, F. H., Imahashi, K., Bouley, D. M., . . . Mochly-Rosen, D. (2003). Inhibition of  $\delta$ -protein kinase C protects against reperfusion injury of the ischemic heart in vivo. *Circulation*, 108(19), 2304-2307.
- Ingber, D., Fujita, T., Kishimoto, S., Sudo, K., Kanamaru, T., Brem, H., & Folkman, J. (1990). Synthetic analogues of fumagillin that inhibit angiogenesis and suppress tumour growth. *Nature*, 348(6301), 555-557. doi:10.1038/348555a0 [doi]
- Irwin, J. J., & Shoichet, B. K. (2005). ZINC– A free database of commercially available compounds for virtual screening. *Journal of Chemical Information and Modeling*, 45(1), 177-182.

- Iwai, Y., Hirano, A., Awaya, J., Matsuo, S., & Omura, S. (1978). 1, 3-diphenethylurea from streptomyces sp. no. AM-2498. *The Journal of Antibiotics*, 31(4), 375-376.
- Jackson, D. N., & FOSTER, D. A. (2004). The enigmatic protein kinase cδ: Complex roles in cell proliferation and survival. *The FASEB Journal*, 18(6), 627-636.
- Jayat, C., & Ratinaud, M. (1993). Cell cycle analysis by flow cytometry: Principles and applications. *Biology of the Cell*, 78(1-2), 15-25.
- Jiang, Y., Choi, W. H., Lee, J. H., Han, D. H., Kim, J. H., Chung, Y., . . . Lee, M. J. (2014). A neurostimulant para-chloroamphetamine inhibits the arginylation branch of the N-end rule pathway. *Scientific Reports*, 4, 6344.
- Jiang, Y., Lee, J., Lee, J. H., Lee, J. W., Kim, J. H., Choi, W. H., . . . Kwon, Y. T. (2016). The arginylation branch of the N-end rule pathway positively regulates cellular autophagic flux and clearance of proteotoxic proteins. *Autophagy*, 12(11), 2197-2212.
- Jiang, Y., Pore, S. K., Lee, J. H., Sriram, S., Mai, B. K., Han, D. H., . . . Banerjee, R. (2013). Characterization of mammalian N-degrons and development of heterovalent inhibitors of the N-end rule pathway. *Chemical Science*, 4(8), 3339-3346.
- Jordan, M., Schallhorn, A., & Wurm, F. M. (1996). Transfecting mammalian cells: Optimization of critical parameters affecting calcium-phosphate precipitate formation. *Nucleic Acids Research*, 24(4), 596-601.

- Kajimoto, T., Shirai, Y., Sakai, N., Yamamoto, T., Matsuzaki, H., Kikkawa, U., & Saito, N. (2004). Ceramide-induced apoptosis by translocation, phosphorylation, and activation of protein kinase cδ in the golgi complex. *Journal of Biological Chemistry*, 279(13), 12668-12676.
- Kao, S., Wang, W., Chen, C., Chang, Y., Wu, Y., Wang, Y., . . . Hong, T. (2015). Analysis of protein stability by the cycloheximide chase assay. *Bio-Protocol*, 5(1)
- Kasibhatla, S., Amarante-Mendes, G. P., Finucane, D., Brunner, T., Bossy-Wetzell, E., & Green, D. R. (2006). Acridine orange/ethidium bromide (AO/EB) staining to detect apoptosis. *Cold Spring Harbor Protocols*, 2006(3), pdb.prot4493.
- Kaul, S., Anantharam, V., Yang, Y., Choi, C. J., Kanthasamy, A., & Kanthasamy, A. G. (2005). Tyrosine phosphorylation regulates the proteolytic activation of protein kinase cδ in dopaminergic neuronal cells. *Journal of Biological Chemistry*, 280(31), 28721-28730.
- Kawaguchi, J., Maejima, K., Kuroiwa, H., & Taki, M. (2013). Kinetic analysis of the leucyl/phenylalanyl-tRNA-protein transferase with acceptor peptides possessing different n-terminal penultimate residues. *FEBS Open Bio*, 3(1), 252-255.
- Keränen, L. M., Dutil, E. M., & Newton, A. C. (1995). Protein kinase C is regulated in vivo by three functionally distinct phosphorylations. *Current Biology : CB*, 5(12), 1394-1403. doi:S0960-9822(95)00277-6 [pii]

- Kikkawa, U., Matsuzaki, H., & Yamamoto, T. (2002). Protein kinase c $\delta$  (PKC $\delta$ ): Activation mechanisms and functions. *The Journal of Biochemistry*, 132(6), 831-839.
- Kiley, S. C., Clark, K. J., Duddy, S. K., Welch, D. R., & Jaken, S. (1999). Increased protein kinase c $\delta$  in mammary tumor cells: Relationship to transformation and metastatic progression. *Oncogene*, 18(48), 6748.
- Kiley, S. C., Parker, P. J., Fabbro, D., & Jaken, S. (1992). Selective redistribution of protein kinase C isozymes by thapsigargin and staurosporine. *Carcinogenesis*, 13(11), 1997-2001.
- Kim, K. H., & Sederstrom, J. M. (2015). Assaying cell cycle status using flow cytometry. *Current Protocols in Molecular Biology*, , 28.6. 11.
- Konishi, H., Tanaka, M., Takemura, Y., Matsuzaki, H., Ono, Y., Kikkawa, U., & Nishizuka, Y. (1997). Activation of protein kinase C by tyrosine phosphorylation in response to H<sub>2</sub>O<sub>2</sub>. *Proceedings of the National Academy of Sciences*, 94(21), 11233-11237.
- Kronfeld, I., Kazimirsky, G., Lorenzo, P. S., Garfield, S. H., Blumberg, P. M., & Brodie, C. (2000). Phosphorylation of protein kinase c $\delta$  on distinct tyrosine residues regulates specific cellular functions. *Journal of Biological Chemistry*, 275(45), 35491-35498.
- Kumar, A., Birnbaum, M. D., Patel, D. M., Morgan, W. M., Singh, J., Barrientos, A., & Zhang, F. (2016). Posttranslational arginylation enzyme Ate1 affects DNA mutagenesis by regulating stress response. *Cell Death & Disease*, 7(9), e2378.



- Kwon, Y. T., Levy, F., & Varshavsky, A. (1999). Bivalent inhibitor of the N-end rule pathway. *Journal of Biological Chemistry*, 274(25), 18135-18139.
- Kwon, Y. T., Xia, Z., Davydov, I. V., Lecker, S. H., & Varshavsky, A. (2001). Construction and analysis of mouse strains lacking the ubiquitin ligase UBR1 (E3a) of the N-end rule pathway. *Molecular and Cellular Biology*, 21(23), 8007-8021.
- Le Good, J. A., Ziegler, W. H., Parekh, D. B., Alessi, D. R., Cohen, P., & Parker, P. J. (1998). Protein kinase C isotypes controlled by phosphoinositide 3-kinase through the protein kinase PDK1. *Science*, 281(5385), 2042-2045.
- Lee, J. H., Jiang, Y., Kwon, Y. T., & Lee, M. J. (2015). Pharmacological modulation of the N-end rule pathway and its therapeutic implications. *Trends in Pharmacological Sciences*, 36(11), 782-797.
- Lee, M. J., Kim, D. E., Zakrzewska, A., Yoo, Y. D., Kim, S., Kim, S. T., . . . Oh, U. (2012). Characterization of arginylation branch of N-end rule pathway in G-protein-mediated proliferation and signaling of cardiomyocytes. *Journal of Biological Chemistry*, 287(28), 24043-24052.
- Lee, M. J., Pal, K., Tasaki, T., Roy, S., Jiang, Y., An, J. Y., . . . Kwon, Y. T. (2008). Synthetic heterovalent inhibitors targeting recognition E3 components of the N-end rule pathway. *Proceedings of the National Academy of Sciences*, 105(1), 100-105.
- Lee, M. J., Tasaki, T., Moroi, K., An, J. Y., Kimura, S., Davydov, I. V., & Kwon, Y. T. (2005). RGS4 and RGS5 are in vivo substrates of the N-end rule pathway. *Proceedings of the National Academy of Sciences*, 102(42), 15030-15035.

- Leibersperger, H., Gschwendt, M., Gernold, M., & Marks, F. (1991). Immunological demonstration of a calcium-unresponsive protein kinase C of the delta-type in different species and murine tissues. predominance in epidermis. *Journal of Biological Chemistry*, 266(22), 14778-14784.
- Leitges, M., Mayr, M., Braun, U., Mayr, U., Li, C., Pfister, G., . . . Xu, Q. (2001). Exacerbated vein graft arteriosclerosis in protein kinase c $\delta$ -null mice. *The Journal of Clinical Investigation*, 108(10), 1505-1512.
- Leverrier, S., Vallentin, A., & Joubert, D. (2002). Positive feedback of protein kinase C proteolytic activation during apoptosis. *Biochemical Journal*, 368(3), 905-913.
- Li, W., Zhang, J., Bottaro, D. P., Li, W., & Pierce, J. H. (1997). Identification of serine 643 of protein kinase C- $\delta$  as an important autophosphorylation site for its enzymatic activity. *Journal of Biological Chemistry*, 272(39), 24550-24555.
- Liu, K., Liu, P., Liu, R., & Wu, X. (2015). Dual AO/EB staining to detect apoptosis in osteosarcoma cells compared with flow cytometry. *Medical Science Monitor Basic Research*, 21, 15.
- Liu, Y., Belkina, N. V., Graham, C., & Shaw, S. (2006). Independence of protein kinase C- $\delta$  activity from activation loop phosphorylation structural basis and altered functions in cells. *Journal of Biological Chemistry*, 281(17), 12102-12111.
- Liu, Y., Liu, C., Chang, Z., Wadas, B., Brower, C. S., Song, Z. H., . . . Wang, L. (2016). Degradation of the separase-cleaved Rec8, a meiotic cohesin

- subunit, by the N-end rule pathway. *Journal of Biological Chemistry*, , jbc. M116. 714964.
- Lu, W., Lee, H., Xiang, C., Finniss, S., & Brodie, C. (2007). The phosphorylation of tyrosine 332 is necessary for the caspase 3-dependent cleavage of PKC $\delta$  and the regulation of cell apoptosis. *Cellular Signalling*, 19(10), 2165-2173.
- Malavez, Y., Gonzalez-Mejia, M. E., & Doseff, A. I. (2009). PRKCD (protein kinase C, delta). *Atlas of Genetics and Cytogenetics in Oncology and Haematology*,
- Manasanch, E. E., & Orlowski, R. Z. (2017). Proteasome inhibitors in cancer therapy. *Nature Reviews Clinical Oncology*, 14(7), 417.
- Matta-Camacho, E., Kozlov, G., Li, F. F., & Gehring, K. (2010). Structural basis of substrate recognition and specificity in the N-end rule pathway. *Nature Structural & Molecular Biology*, 17(10), 1182.
- Mayr, M., Metzler, B., Chung, Y., McGregor, E., Mayr, U., Troy, H., . . . Griffiths, J. R. (2004). Ischemic preconditioning exaggerates cardiac damage in PKC- $\delta$  null mice. *American Journal of Physiology-Heart and Circulatory Physiology*, 287(2), H956.
- Mecklenbräuker, I., Saijo, K., Zheng, N., Leitges, M., & Tarakhovsky, A. (2002). Protein kinase c $\delta$  controls self-antigen-induced B-cell tolerance. *Nature*, 416(6883), 860.
- Mediavilla-Varela, M., Pacheco, F. J., Almaguel, F., Perez, J., Sahakian, E., Daniels, T. R., . . . Lilly, M. B. (2009). Docetaxel-induced prostate cancer cell death involves concomitant activation of caspase and lysosomal pathways and is attenuated by LEDGF/p75. *Molecular Cancer*, 8(1), 68.

- Menyhárt, O., Harami-Papp, H., Sukumar, S., Schäfer, R., Magnani, L., de Barrios, O., & Győrffy, B. (2016). Guidelines for the selection of functional assays to evaluate the hallmarks of cancer. *Biochimica Et Biophysica Acta (BBA)-Reviews on Cancer*, 1866(2), 300-319.
- Metzger, M. B., Hristova, V. A., & Weissman, A. M. (2012). HECT and RING finger families of E3 ubiquitin ligases at a glance. *J Cell Sci*, 125(3), 531-537.
- Morales, K. A., Lasagna, M., Gribenko, A. V., Yoon, Y., Reinhart, G. D., Lee, J. C., . . . Igumenova, T. I. (2011). Pb<sup>2+</sup> as modulator of protein-membrane interactions. *Journal of the American Chemical Society*, 133(27), 10599-10611. doi:10.1021/ja2032772 [doi]
- Morreale, F. E., & Walden, H. (2016). Types of ubiquitin ligases. *Cell*, 165(1), 248. e1.
- Mosmann, T. (1983). Rapid colorimetric assay for cellular growth and survival: Application to proliferation and cytotoxicity assays. *Journal of Immunological Methods*, 65(1-2), 55-63.
- Motulsky, H. J. (2007). Prism 5 statistics guide, 2007. GraphPad Software, 31(1), 39-42.
- Muñoz-Escobar, J., Matta-Camacho, E., Cho, C., Kozlov, G., & Gehring, K. (2017). Bound waters mediate binding of diverse substrates to a ubiquitin ligase. *Structure*, 25(5), 729. e3.
- Murray, D., & Honig, B. (2002). Electrostatic control of the membrane targeting of C2 domains. *Molecular Cell*, 9(1), 145-154. doi:S1097-2765(01)00426-9 [pii]

- Nasmyth, K., & Haering, C. H. (2009). Cohesin: Its roles and mechanisms. *Annual Review of Genetics*, 43
- Newey, H., & Smyth, D. H. (1960). Intracellular hydrolysis of dipeptides during intestinal absorption. *The Journal of Physiology*, 152, 367-380.
- Newton, A. C. (2001). Protein kinase C: Structural and spatial regulation by phosphorylation, cofactors, and macromolecular interactions. *Chemical Reviews*, 101(8), 2353-2364.
- Okhrimenko, H., Lu, W., Xiang, C., Ju, D., Blumberg, P. M., Gomel, R., . . . Brodie, C. (2005). Roles of tyrosine phosphorylation and cleavage of protein kinase cδ in its protective effect against tumor necrosis factor-related apoptosis inducing ligand-induced apoptosis. *Journal of Biological Chemistry*, 280(25), 23643-23652.
- Ouyang, Y., Kwon, Y. T., An, J. Y., Eller, D., Tsai, S., Diaz-Perez, S., . . . Marahrens, Y. (2006). Loss of UBR2, an E3 ubiquitin ligase, leads to chromosome fragility and impaired homologous recombinational repair. *Mutation Research/Fundamental and Molecular Mechanisms of Mutagenesis*, 596(1-2), 64-75.
- Page, K., Li, J., Zhou, L., Iasvoyskaia, S., Corbit, K. C., Soh, J., . . . Hershenson, M. B. (2003). Regulation of airway epithelial cell NF-κB-dependent gene expression by protein kinase cδ. *The Journal of Immunology*, 170(11), 5681-5689.
- Panigrahi, A. K., Zhang, N., Mao, Q., & Pati, D. (2011). Calpain-1 cleaves Rad21 to promote sister chromatid separation. *Molecular and Cellular Biology*, , 11.

- Papanagnou, E., Terpos, E., Kastiris, E., Papassideri, I. S., Tsitsilonis, O. E., Dimopoulos, M. A., & Trougakos, I. P. (2018). Molecular responses to therapeutic proteasome inhibitors in multiple myeloma patients are donor-, cell type-and drug-dependent. *Oncotarget*, 9(25), 17797.
- Parekh, D. B., Ziegler, W., & Parker, P. J. (2000). Multiple pathways control protein kinase C phosphorylation. *The EMBO Journal*, 19(4), 496-503.
- Park, I. C., Park, M. J., Hwang, C. S., Rhee, C. H., Whang, D. Y., Jang, J. J., . . . Lee, S. H. (2000). Mitomycin C induces apoptosis in a caspases-dependent and fas/CD95-independent manner in human gastric adenocarcinoma cells. *Cancer Letters*, 158(2), 125-132. doi:S0304383500004894 [pii]
- Park, S., Kim, J., Seok, O., Cho, H., Wadas, B., Kim, S., . . . Hwang, C. (2015). Control of mammalian G protein signaling by N-terminal acetylation and the N-end rule pathway. *Science*, 347(6227), 1249-1252.
- Persaud, S. D., Hoang, V., Huang, J., & Basu, A. (2005). Involvement of proteolytic activation of PKCdelta in cisplatin-induced apoptosis in human small cell lung cancer H69 cells. *International Journal of Oncology*, 27(1), 149-154.
- Piatkov, K. I., Brower, C. S., & Varshavsky, A. (2012). The N-end rule pathway counteracts cell death by destroying proapoptotic protein fragments. *Proceedings of the National Academy of Sciences*, 109(27), E1847.
- Piatkov, K. I., Colnaghi, L., Békés, M., Varshavsky, A., & Huang, T. T. (2012). The auto-generated fragment of the Usp1 deubiquitylase is a physiological substrate of the N-end rule pathway. *Molecular Cell*, 48(6), 926-933.

- Piatkov, K. I., Oh, J., Liu, Y., & Varshavsky, A. (2014). Calpain-generated natural protein fragments as short-lived substrates of the N-end rule pathway. *Proceedings of the National Academy of Sciences*, , 201401639.
- Potuschak, T., Stary, S., Schlögelhofer, P., Becker, F., Nejnskaia, V., & Bachmair, A. (1998). PRT1 of arabidopsis thaliana encodes a component of the plant N-end rule pathway. *Proceedings of the National Academy of Sciences*, 95(14), 7904-7908.
- Pozarowski, P., & Darzynkiewicz, Z. (2004). Analysis of cell cycle by flow cytometry. *Checkpoint controls and cancer* (pp. 301-311) Springer.
- Qi, X., & Mochly-Rosen, D. (2008). The PKC $\delta$ -abl complex communicates ER stress to the mitochondria—an essential step in subsequent apoptosis. *J Cell Sci*, 121(6), 804-813.
- Rao, H., Uhlmann, F., Nasmyth, K., & Varshavsky, A. (2001). Degradation of a cohesin subunit by the N-end rule pathway is essential for chromosome stability. *Nature*, 410(6831), 955.
- Ren, J., Datta, R., Shioya, H., Li, Y., Oki, E., Biedermann, V., . . . Kufe, D. (2002). p73 $\beta$  is regulated by protein kinase c $\delta$  catalytic fragment generated in the apoptotic response to DNA damage. *Journal of Biological Chemistry*, 277(37), 33758-33765.
- Reyland, M. E. (2007). No title. *Protein Kinase C $\delta$  and Apoptosis*.
- Reyland, M. E., Anderson, S. M., Matassa, A. A., Barzen, K. A., & Quissell, D. O. (1999). Protein kinase C  $\delta$  is essential for etoposide-induced apoptosis in

salivary gland acinar cells. *Journal of Biological Chemistry*, 274(27), 19115-19123.

Richardson, P. G., Briemberg, H., Jagannath, S., Wen, P. Y., Barlogie, B., Berenson, J., . . . Schuster, M. (2006). Frequency, characteristics, and reversibility of peripheral neuropathy during treatment of advanced multiple myeloma with bortezomib. *J Clin Oncol*, 24(19), 3113-3120.

Rivett, A. J. (1986). Regulation of intracellular protein turnover: Covalent modification as a mechanism of marking proteins for degradation. *Current topics in cellular regulation* (pp. 291-337) Elsevier.

Roffey, J., Rosse, C., Linch, M., Hibbert, A., McDonald, N. Q., & Parker, P. J. (2009). Protein kinase C intervention—the state of play. *Current Opinion in Cell Biology*, 21(2), 268-279.

Rybin, V. O., Guo, J., Sabri, A., Elouardighi, H., Schaefer, E., & Steinberg, S. F. (2004). Stimulus-specific differences in protein kinase c $\delta$  localization and activation mechanisms in cardiomyocytes. *Journal of Biological Chemistry*, 279(18), 19350-19361.

Safran, M., Chalifa-Caspi, V., Shmueli, O., Olender, T., Lapidot, M., Rosen, N., . . . Feldmesser, E. (2003). Human gene-centric databases at the weizmann institute of science: GeneCards, UDB, CroW 21 and HORDE. *Nucleic Acids Research*, 31(1), 142-146.

Saha, S., Mundia, M. M., Zhang, F., Demers, R. W., Korobova, F., Svitkina, T., . . . Kashina, A. (2010). Arginylation regulates intracellular actin polymer level by modulating actin properties and binding of capping and severing proteins. *Molecular Biology of the Cell*, 21(8), 1350-1361.



- Saha, S., Wang, J., Buckley, B., Wang, Q., Lilly, B., Chernov, M., & Kashina, A. (2012). Small molecule inhibitors of arginyltransferase regulate arginylation-dependent protein degradation, cell motility, and angiogenesis. *Biochemical Pharmacology*, 83(7), 866-873. doi:10.1016/j.bcp.2012.01.012 [doi]
- Shao, X., Davletov, B. A., Sutton, R. B., Südhof, T. C., & Rizo, J. (1996). Bipartite Ca<sup>2+</sup>-binding motif in C2 domains of synaptotagmin and protein kinase C. *Science*, 273(5272), 248-251.
- Silk, D. B., Grimble, G. K., & Rees, R. G. (1985). Protein digestion and amino acid and peptide absorption. *The Proceedings of the Nutrition Society*, 44(1), 63-72. doi:S0029665185000167 [pii]
- Singh, R. K., Kumar, S., Gautam, P. K., Tomar, M. S., Verma, P. K., Singh, S. P., & Acharya, A. (2017). Protein kinase C- $\alpha$  and the regulation of diverse cell responses. *Biomolecular Concepts*, 8(3-4), 143-153.
- Sooman, L., Gullbo, J., Bergqvist, M., Bergström, S., Lennartsson, J., & Ekman, S. (2017). Synergistic effects of combining proteasome inhibitors with chemotherapeutic drugs in lung cancer cells. *BMC Research Notes*, 10(1), 544.
- Sriram, S., Lee, J. H., Mai, B. K., Jiang, Y., Kim, Y., Yoo, Y. D., . . . Lee, M. J. (2013). Development and characterization of monomeric N-end rule inhibitors through in vitro model substrates. *Journal of Medicinal Chemistry*, 56(6), 2540-2546.
- Stahelin, R. V., Kong, K. F., Raha, S., Tian, W., Melowic, H. R., Ward, K. E., . . . Cho, W. (2012). Protein kinase ctheta C2 domain is a phosphotyrosine binding module that plays a key role in its activation. *The Journal of*

Biological Chemistry, 287(36), 30518-30528. doi:10.1074/jbc.M112.391557  
[doi]

Steinberg, S. F. (2004). Distinctive activation mechanisms and functions for protein kinase c $\delta$ . *Biochemical Journal*, 384(3), 449-459.

Steinberg, S. F. (2008). Structural basis of protein kinase C isoform function. *Physiological Reviews*, 88(4), 1341-1378.

Stempka, L., Girod, A., Müller, H., Rincke, G., Marks, F., Gschwendt, M., & Bossemeyer, D. (1997). Phosphorylation of protein kinase c $\delta$  (PKC $\delta$ ) at threonine 505 is not a prerequisite for enzymatic activity EXPRESSION OF RAT PKC $\delta$  AND AN ALANINE 505 MUTANT IN BACTERIA IN A FUNCTIONAL FORM. *Journal of Biological Chemistry*, 272(10), 6805-6811.

Stempka, L., Schnölzer, M., Radke, S., Rincke, G., Marks, F., & Gschwendt, M. (1999). Requirements of protein kinase c $\delta$  for catalytic function ROLE OF GLUTAMIC ACID 500 AND AUTOPHOSPHORYLATION ON SERINE 643. *Journal of Biological Chemistry*, 274(13), 8886-8892.

Sterling, T., & Irwin, J. J. (2015). ZINC 15–ligand discovery for everyone. *Journal of Chemical Information and Modeling*, 55(11), 2324-2337.

Sun, S., Wu, Q., Song, J., & Sun, S. (2018). Protein kinase C  $\delta$ -dependent regulation of ubiquitin-proteasome system function in breast cancer. *Cancer Biomarkers*, 21(1), 1-9.

Sun, Y. (2003). Targeting E3 ubiquitin ligases for cancer therapy. *Cancer Biology & Therapy*, 2(6), 623-629.

- Tallarida, R. J. (2000). Drug synergism and dose-effect data analysis Chapman and Hall/CRC.
- Tallarida, R. J. (2011). Quantitative methods for assessing drug synergism. *Genes & Cancer*, 2(11), 1003-1008.
- Tasaki, T., Mulder, L. C., Iwamatsu, A., Lee, M. J., Davydov, I. V., Varshavsky, A., . . . Kwon, Y. T. (2005). A family of mammalian E3 ubiquitin ligases that contain the UBR box motif and recognize N-degrons. *Molecular and Cellular Biology*, 25(16), 7120-7136.
- Tobias, J. W., Shrader, T. E., Rocap, G., & Varshavsky, A. (1991). The N-end rule in bacteria. *Science*, 254(5036), 1374-1377.
- Turner, G. C., Du, F., & Varshavsky, A. (2000). Peptides accelerate their uptake by activating a ubiquitin-dependent proteolytic pathway. *Nature*, 405(6786), 579-583. doi:10.1038/35014629 [doi]
- Utz, P. J., & Anderson, P. (2000). Life and death decisions: Regulation of apoptosis by proteolysis of signaling molecules. *Cell Death and Differentiation*, 7(7), 589.
- Van der Land, J. (2008). UNESCO-IOC register of marine organisms (URMO). Available at [H Ttp://Www.Marinespecies.Org/Urmo](http://www.marinespecies.org/Urmo),
- Varshavsky, A. (2011). The n-end rule pathway and regulation by proteolysis. *Protein Science*, 20(8), 1298-1345.
- Varshavsky, A. (2017). The ubiquitin system, autophagy, and regulated protein degradation. *Annual Review of Biochemistry*, 86, 123-128.

- Verdaguer, N., Corbalan-Garcia, S., Ochoa, W. F., Fita, I., & Gómez-Fernández, J. C. (1999). Ca<sup>2+</sup> bridges the C2 membrane-binding domain of protein kinase  $\alpha$  directly to phosphatidylserine. *The EMBO Journal*, 18(22), 6329-6338.
- Wadas, B., Piatkov, K. I., Brower, C. S., & Varshavsky, A. (2016). Analyzing N-terminal arginylation through the use of peptide arrays and degradation assays. *Journal of Biological Chemistry*, 291(40), 20976-20992.
- Weaver, B. P., Weaver, Y. M., Mitani, S., & Han, M. (2017). Coupled caspase and N-end rule ligase activities allow recognition and degradation of pluripotency factor LIN-28 during non-apoptotic development. *Developmental Cell*, 41(6), 673. e6.
- Xu, Z., Payoe, R., & Fahlman, R. P. (2012). The C-terminal proteolytic fragment of the breast cancer susceptibility type 1 protein (BRCA1) is degraded by the N-end rule pathway. *Journal of Biological Chemistry*, 287(10), 7495-7502.
- Yamano, K., & Youle, R. J. (2013). PINK1 is degraded through the N-end rule pathway. *Autophagy*, 9(11), 1758-1769.
- Yang, Q., Langston, J. C., Tang, Y., Kiani, M. F., & Kilpatrick, L. E. (2019). The role of tyrosine phosphorylation of protein kinase C delta in infection and inflammation. *International Journal of Molecular Sciences*, 20(6), 1498.
- Yang, Y., Shu, C., Li, P., & Igumenova, T. I. (2018). Structural basis of protein kinase  $\alpha$  regulation by the C-terminal tail. *Biophysical Journal*, 114(7), 1590-1603.

- Yin, S. Q., Wang, J. J., Zhang, C. M., & Liu, Z. P. (2012). The development of MetAP-2 inhibitors in cancer treatment. *Current Medicinal Chemistry*, 19(7), 1021-1035. doi:BSP/CMC/E-Pub/2012/089 [pii]
- Zenker, M., Mayerle, J., Lerch, M. M., Tagariello, A., Zerres, K., Durie, P. R., . . . Rehder, H. (2005). Deficiency of UBR1, a ubiquitin ligase of the N-end rule pathway, causes pancreatic dysfunction, malformations and mental retardation (johanson-blizzard syndrome). *Nature Genetics*, 37(12), 1345.
- Zhang, F., Patel, D. M., Colavita, K., Rodionova, I., Buckley, B., Scott, D. A., . . . Chernov, M. (2015). Arginylation regulates purine nucleotide biosynthesis by enhancing the activity of phosphoribosyl pyrophosphate synthase. *Nature Communications*, 6, 7517.
- Zhang, N., Jiang, Y., Mao, Q., Demeler, B., Tao, Y. J., & Pati, D. (2013). Characterization of the interaction between the cohesin subunits Rad21 and SA1/2. *PLoS One*, 8(7), e69458.
- Zhao, M., Xia, L., & Chen, G. (2012). Protein kinase cδ in apoptosis: A brief overview. *Archivum Immunologiae Et Therapiae Experimentalis*, 60(5), 361-372.
- Ziegler, W. H., Parekh, D. B., Le Good, J. A., WHeLan, R., Kelly, J. J., Frech, M., . . . Parker, P. J. (1999). Rapamycin-sensitive phosphorylation of PKC on a carboxy-terminal site by an atypical PKC complex. *Current Biology*, 9(10), 522-529.

| APPENDIX

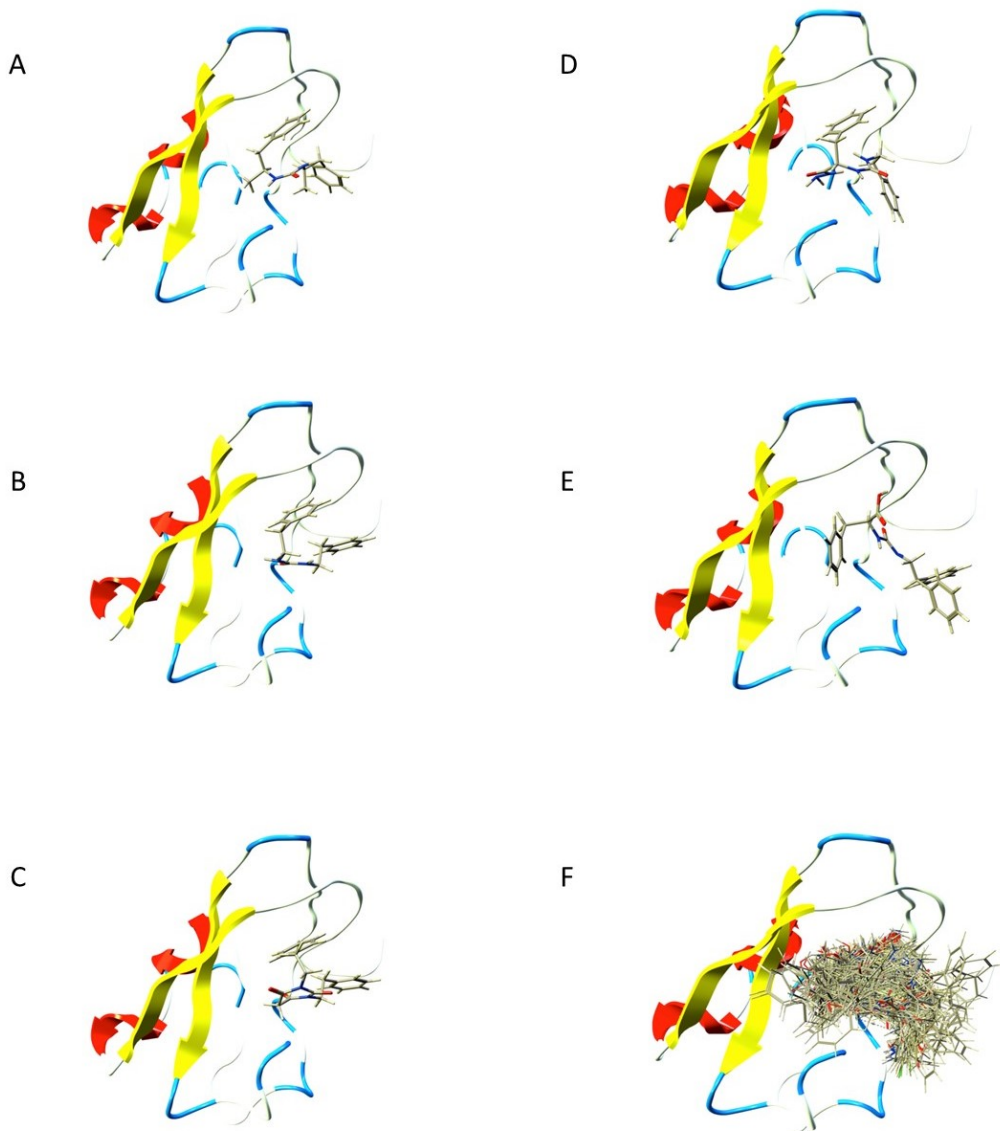


**Figure A - 1. Docking result of top scoring Analogs**

Docking model of Analogs, as determined by *in silico* screening, bound to the UBR domain of UBR1. **A.** Analog I. **B.** Analog II. **C.** Analog III. **D.** Analog VI **E.** Analog VII. **F.** Top ten conformers of all Compounds.

**Table A - 1 Cell counting after Gy irradiation 1-hour post inhibitor treatment.**

<b>Treatment</b>	<b>Plate 1</b>	<b>Plate 2</b>	<b>Plate 3</b>	<b>Average</b>	<b># cells</b>	<b>Eff. Corr.</b>	<b>% cells</b>
control	106	149	137	130,6667	200	130,6667	99,99997
2 Gy	69	110	106	95	200	130,6667	72,70406
4 Gy	113	94	95	100,6667	400	261,334	38,52031
6 Gy	71	38	51	53,33333	800	522,668	10,20406
8 Gy	26	16	27	23	2000	1300,666	1,768325
13.33 uM	76	73	95	81,33333	200	130,6667	62,24488
13.33 uM +2 Gy	43	51	36	43,33333	200	130,6667	33,16326
13.33 uM + 4 Gy	14	30	33	25,66667	400	261,334	9,821404
13.33 uM + 6Gy	14	9	9	10,66667	800	522,668	2,040811
13.33 uM + 8Gy	4	5	6	5	2000	1300,666	0,384418





**Table A - 2. Trypan Blue cell viability test in Jurkat cell line**


		Time (hrs)				
		0	24	48	96	144
<b>DMSO</b>	cell/m	1,96E+	5,43E+	1,26E+	2,64E+	3,01E+
	L	05	05	06	06	06
	%	95%	98%	94%	92%	91%
<b>PPCP(100uM) +Phe-NH2 (200uM)</b>	cell/m	3,42E+	7,59E+	1,18E+	1,78E+	2,20E+
	L	05	05	06	06	06
	%	90%	95%	91%	90%	80%
<b>Phe-NH2 (200uM)</b>	cell/m	3,42E+	6,94E+	1,45E+	2,10E+	2,06E+
	L	05	05	06	06	06
	%	91%	98%	96%	91%	79%
<b>PPCP(100uM)</b>	cell/m	3,12E+	6,28E+	9,30E+	1,04E+	1,21E+
	L	05	05	05	06	06
	%	89%	95%	94%	90%	70%
<b>PPCP(50uM)</b>	cell/m	5,38E+	9,78E+	1,26E+	1,37E+	1,99E+
	L	05	05	06	06	06
	%	92%	96%	95%	90%	79%
<b>PPCP(25uM)</b>	cell/m	2,82E+	6,03E+	1,07E+	1,65E+	2,04E+
	L	05	05	06	06	06
	%	93%	90%	93%	88%	81%
<b>PPCP(6uM)</b>	cell/m	3,47E+	6,44E+	1,07E+	1,79E+	1,72E+
	L	05	05	06	06	06
	%	80%	97%	93%	90%	79%
<b>PPCP(3uM)</b>	cell/m	1,46E+	4,12E+	9,08E+	1,38E+	1,78E+
	L	05	05	05	06	06
	%	82%	95%	96%	91%	71%
<b>PPCP(0.7uM)</b>	cell/m	2,31E+	5,27E+	8,04E+	1,49E+	2,13E+
	L	05	05	05	06	06
	%	81%	89%	95%	90%	81%
<b>PPCP(0.3uM)</b>	cell/m	2,56E+	7,25E+	9,89E+	1,95E+	2,36E+
	L	05	05	05	06	06
	%	80%	99%	95%	90%	83%

## Ub-PKCδ-FLAG sequence

ancagagctctctggcnnnagagaacccactgcttactggcttatcgaaattaatacgac  
X E L S G X X R T H C L L A Y R N - Y D  
tcactatagggagaccaagctggctagcgtttaacttaagcttggccatggagatcttc  
S L - G D P S W L A F K L K L A M E I F  
gtgaagaccctgaccggcaagaccatcactctggaggtggagcccagtgacaccatcgaa  
V K T L T G K T I T L E V E P S D T I E  
aatgtgaaagccaagatccaagataaagaaggcatccccccgaccagcagaggctcatc  
N V K A K I Q D K E G I P P D Q Q R L I  
tttgcaggcaagcagctggaagatggccgcactctttccgactacaacatccagaaagag  
F A G K Q L E D G R T L S D Y N I Q K E  
tcgaccctgcacctggtcctgcgccctgaggggtggaaacagtgggacctacggcaagatc  
S T L H L V L R L R G G N S G T Y G K I  
tgggagggcagcagcaagtgcaacatcaacaacttcatcttcacaaggtcctgggcaa  
W E G S S K C N I N N F I F H K V L G K  
ggcagcttcgggaaggtgctgcttggagagctgaagggcagaggagaataactttgccat  
G S F G K V L L G E L K G R G E Y F A I  
aaggccctcaagaaggatgtggtcctgatcgacgacgacgtggagtgcaccatggttgag  
K A L K K D V V L I D D D V E C T M V E  
aagcgggtgctgacacttgccgcagagaatccctttctcaccacctcatctgcaccttc  
K R V L T L A A E N P F L T H L I C T F  
cagaccaaggaccacctgttctttgtgatggagtctcctcaacgggggggacctgatgtac  
Q T K D H L F F V M E F L N G G D L M Y  
cacatccaggacaaaggccgctttgaactctaccgtgccacgttttatgccgctganata  
H I Q D K G R F E L Y R A T F Y A A X I  
atgtgtggactgcagtttctacacagcaagggcatcatttacagggncctcaaactggac  
M C G L Q F L H S K G I I Y R X L K L D  
natgtgctgctggaccggntggncacatcnagattgncnactttgggnngtgcaaan  
X V L L D R X X H I X I X X F G X C K X  
aacatattnnngananncnngncnagcacnttctgcngcaccngactatatcgccccng  
N I X X X X X X S X F C X T X T I S P X  
annn  
X X

 Ubiquitin

 First position residue of the cleaved fragment

 Second position residue of the cleaved fragment